

AD-A048 966

AIR FORCE INST OF TECH WRIGHT-PATTERSON AFB OHIO SCH--ETC F/G 19/4  
MAGNUS EFFECTS ON BALLISTIC TRAJECTORIES.(U)

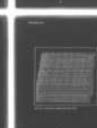
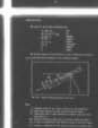
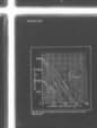
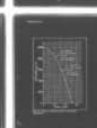
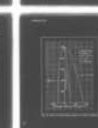
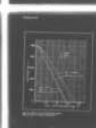
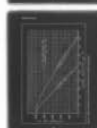
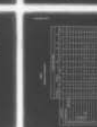
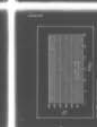
UNCLASSIFIED

AFIT/GA/AA-77D-8

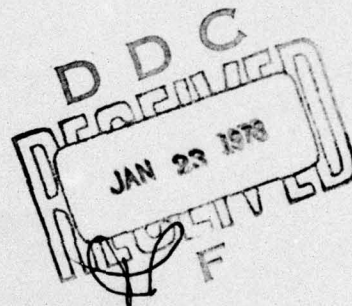
NL

1 of 2

AD-A048 966



12



MAGNUS EFFECTS ON  
BALLISTIC TRAJECTORIES  
THESIS

AFIT/GA/AA-77D-8

James D. Schneider  
Major USAF



6  
MAGNUS EFFECTS ON  
BALLISTIC TRAJECTORIES.

9  
Master's THESIS

Presented to the Faculty of the School of Engineering  
of the Air Force Institute of Technology  
Air University

in Partial Fulfillment of the  
Requirements for the Degree of  
Master of Science

14 AFIT/GA/AA-77D-8 by

10 James D. Schneider  
Major

B.S.  
USAF

12 118p. Graduate Astronautical Engineering

11 December 1977

ACCESSION for	
NTIS	White Section <input checked="" type="checkbox"/>
DDC	Buff Section <input type="checkbox"/>
UNANNOUNCED	<input type="checkbox"/>
JUSTIFICATION	
BY	
DISTRIBUTION/AVAILABILITY STATEMENT	
Dist.	Avail
A	1

Approved for public release, distribution unlimited.

1473  
012 225

LB

Preface

Most of my time during the past six months has been spent preparing for, working at, and finally completing this project. As time progressed, I managed to develop at least a measure of proficiency in working with the six degree of freedom equations of motion, was introduced to the utility of aerodynamic coefficients, and gained considerable experience working with a computer simulation. This learning experience, unlike most of my rote textbook encounters, was found to be satisfying, rewarding, and real. I also found the professional people I came in contact with during the project to be knowledgeable, motivated engineers willing to share their time and talent. My association with my advisor, Dr. D.W. Breuer of the Aeronautics and Astronautics department, Air Force Institute of Technology; Major Ed Mirmak, Air Force Avionics Laboratory who proposed the project; and Captain Bill Miklos, Flight Dynamics Laboratory who provided the computer program, made the project not only possible but enjoyable. An enormous amount of expertise was available to me through these people as well as from those who have previously documented their efforts in this field. This project represents the conclusion to a personal challenge of the first degree with its own reward at the time of completion. If any part of it is ever useful to anyone else, then all the effort is even more worthwhile.



Contents

Preface .....	11
List of Figures .....	v
List of Tables .....	viii
List of Symbols .....	1x
Abstract .....	xi
I. Introduction .....	1
Purpose .....	1
Background .....	1
Assumptions .....	2
II. Mathematical Theory .....	4
Reference Frame Transformation Matrix .....	4
Equation of Motion .....	5
Differential Equations of Motion in Rotational Parameters .....	9
III. Method of Problem Solution .....	12
The Computer Program .....	12
Projectile Model Description.....	13
Aerodynamic Coefficients .....	14
Approach to the Investigation .....	23
IV. Results of the Simulations .....	28
Effect of Magnus Coefficients .....	28
Effect of Initial Pitch Motion .....	30
Effect of Spin Rate .....	41
Other Observations .....	44
V. Conclusions .....	51



Contents

Bibliography .....	53
Appendix A .....	54
Appendix B .....	57
Appendix C .....	67
Appendix D .....	69
Appendix E .....	83
Appendix F .....	85
Appendix G .....	99
Vita .....	105

List of Figures

Figure		Page
1	Reference Frames .....	4
2	Rotational and Linear Velocity Axes .....	6
3	Projectile Model .....	13
4	Periodic Change in $C_{l_0}$ .....	15
5	Typical Theoretical vs Experimental Data Curves .....	16
6	Definition of Cross-Spin/Velocity Terms .....	17
7	Force Coefficient vs Mach Number .....	21
8	Change in Magnus Force Coefficient .....	22
9	Magnus Lift .....	24
10	Magnus Moment .....	25
11	Effect of Magnus & Side Force Coefficients on Lateral Displacement .....	29
12	Effect of Pitch Motion and Magnus Coefficients on Lateral Displacement .....	33
13	Projectile Nose Track after Release .....	35
14	Initial Rate of Lateral Displacement .....	36
15	Effect of Initial Side Velocity on Lateral Progression .....	38
16	Lateral Displacement vs Yaw Oscillation .....	40
17	Effect of Spin Rate on Lateral Displacement .....	43
18	Effect of Release Velocity and Altitude on Velocity Progression .....	45
19	Effect of Release Velocity on Total Projectile Acceleration .	47
20	Effect of Initial Pitch Motion on Lateral Deflection .....	48



21	Effect of Release Velocity on Altitude Progression .....	49
22	Effect of Release Velocity and Altitude on Lateral Displacement .....	50
B-1a thru g	Computer Input Cards .....	57 - 61
B-2	Flight Path/Perturbation Angle Input .....	62
B-3	Scale Factor Inputs .....	64
E-1	Local Level Reference Frame .....	83



List of Tables

Table	Page
I Differential Equations of Motion .....	11
II Force and Moment Coefficients .....	18
III Aerodynamic Coefficients .....	19
IV Magnus Force Aerodynamic Coefficient Array .....	23
V Parameters Investigated .....	27
VI Effect of Magnus Coefficients.....	31
VII Effect of Spin Rate .....	42
A-I Wind Tunnel Spin Up Data .....	55
A-II Wind Tunnel Spin Down Data .....	56
B-I Aerodynamic Coefficient Array .....	65
B-II Computer Input Array .....	66
C-I Sample Computer Readout .....	68

List of Symbols

## Aerodynamic coefficients

(See Table 3)

$C_L, C_M, C_N$	Moment coefficient about body X, Y, Z axes
$C_x, C_y, C_z$	Force coefficient along inertial axes
$C_X, C_Y, C_Z$	Force coefficient along body axes
$d$	Maximum projectile diameter
$\vec{F}$	Net force vector
$F_X, F_Y, F_Z$	Components of $\vec{F}$ along body axes
$g$	Gravitational acceleration
$\vec{h}$	Net angular momentum vector
$h_X, h_Y, h_Z$	Components of $\vec{h}$ along body axes
$I_X, I_Y, I_Z$	Moment of inertia about body axes
$m$	Mass of projectile
$\vec{M}$	Net moment vector
$M_X, M_Y, M_Z$	Components of $\vec{M}$ about body axes
$p, q, r$	Rate of rotation about body X, Y, Z
$Q$	Dynamic pressure
$q''$	Magnitude of cross-spin vector
$S$	Cross-sectional area of projectile
$t$	Time
$t_E$	Simulation termination time
$v_a$	Speed with respect to air mass
$\vec{V}$	Net velocity vector
$u, v, w$	Components of $\vec{V}$ along body XYZ axes respectively
$y_{min}$	Simulation termination altitude
$w$	Wedge angle
$x, y, z$	Axes of inertial reference frame



$X, Y, Z$	Axes of body fixed reference frame
$x''$	Position of inertial $x$ after second rotation 0
$z'$	New position of inertial $z$ axis after rotation
$\alpha$	Angle of attack
$\beta$	Side slip angle
$\Delta t$	Numerical integration step size
$\phi'$	Angle from cross-velocity vector to $Z$ fin
$\phi''$	Angle from cross-spin vector to $Y$ fin
$\psi, \theta, \phi$	Rotation about inertial $y, z', x''$ axes
$\lambda$	Rotational parameter
$\eta$	Number of fins
$\rho$	Air density
$\omega^{bi}$	Rotation between body and inertial reference frames

Note for hand printed equations:  $X, Y, Z = X, Y, Z$

$x, y, z = x, y, z$



## ABSTRACT

A six degree of freedom computer simulation was used to investigate the lateral progression of a free-fall ballistic trajectory due to spin rate, Magnus aerodynamic coefficients and initial projectile pitching motion. The increased spin rate extends the projectile impact point both downrange and cross range due to a slight increase in time of flight generated by a predominately positive angle of attack. The Magnus force, Magnus moment and side force coefficients, under normal release conditions, presents only a minor influence and can be omitted from the simulation without altering the trajectory appreciably. If the release altitude is sufficiently high, however, the small influence of these coefficients could propagate to a correctable magnitude. Projectile oscillations encountered at release can increase the lateral progression of the trajectory significantly, especially for high speed deliveries. Oscillations induced by an initial pitch rate of the projectile generates considerably more lateral deviation than an initial pitch displacement of equivalent maximum amplitude. This increased lateral displacement causes a corresponding decrease in range impact. Other observations concerning the performance of a projectile following a ballistic trajectory are included as support material in the last section of the study.

## MAGNUS EFFECTS ON BALLISTIC TRAJECTORIES

### I. Introduction

#### Purpose

This study uses computer simulations to investigate three factors that effect a free-fall ballistic trajectory. The first objective is to determine the relative influence of Magnus force, Magnus moment, and side force coefficients. The next area of interest is the effect of oscillatory motion induced by initial pitch rate motion compared to initial pitch displacement of the projectile. The third set of simulations determines how spin rate induced by the projectile fins alters the trajectory.

The development of the equations of motion used in the computer program is included in this study, followed by a discussion of the aerodynamic coefficients. The results of the simulations are presented in the last section.

#### Background

A ballistic projectile is designed to spin so that a predictable trajectory is generated. Without spin, aerodynamic lift created by non-symmetrical shape resulting from manufacturing imperfections would cause the projectile to fly away from the expected ballistic trajectory. Spin is also required for stability considerations. If the projectile has insufficient angular momentum, it will eventually begin precessing and, if the spin rate is in the neighborhood of the natural pitch frequency, it



may develop catastrophic yaw. Conversely, with excessive angular momentum, the projectile spin axis tends to become gyroscopically oriented with respect to inertial space and will not track properly throughout the trajectory. Conventional bombs are therefore designed so that a spin rate is achieved that will maintain satisfactory stability within either limit of spin rate (Ref 4:64 & 12:29). This spin, while desirable and necessary for a predictable trajectory, induces lateral errors which are attributable to Magnus lift and a gyroscopically induced lateral angle of attack. These effects are additive and can cause the bomb to progressively deviate laterally.

#### Assumptions

The set of equations that completely describe the trajectory of a spinning ballistic projectile are fully coupled, non-linear expressions that are developed in dynamics texts (such as Ref 4:99). The solutions to this set of equations requires extensive digital computer capability even with the following simplifying assumptions:

1. The earth curvature, variation in terrain, and earth rotation are neglected. For normal conventional weapon delivery airspeeds and altitudes, no significant error is introduced since the range and time of flight of the projectile is sufficiently small. This assumption eliminates the earth reference and allows the advantage of direct transformations between the body and inertial reference frames (See Fig 1). This greatly decreases the required computer time with no appreciable loss in accuracy.
2. The gravitational field is considered uniform over the entire trajectory.
3. The coriolis acceleration is neglected even though it can have



a small but discernable effect on the projectile impact point. For this investigation, the change in trajectory is of primary interest, not the precise trajectory itself. Coriolis acceleration is addressed in Appendix E but is not written into the computer program.

4. A standard atmosphere is assumed adequate for normal release altitudes. The ARDC 1959 Model Atmosphere was used and no winds were included in the simulation.

## II. Mathematical Theory

### Reference Frame Transformation Matrix

The orthogonal reference frame used in this development is the body fixed reference frame (XYZ) moving with respect to the inertial frame (xyz). The origin of the body frame is located at the center of gravity of the projectile.

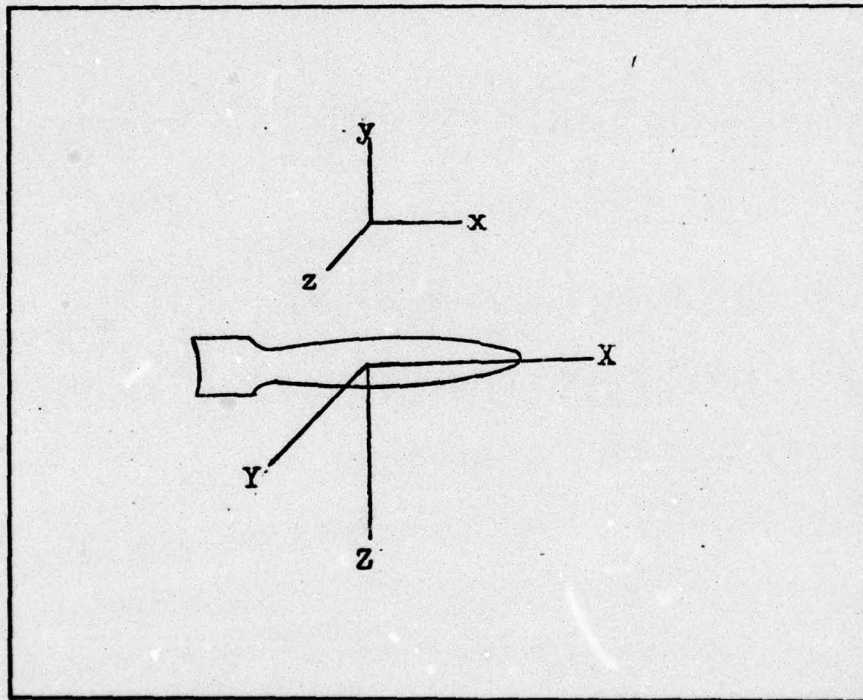


Fig. 1. Reference Frames

To facilitate the direction cosine matrix development, the body reference frame is rotated  $90^\circ$  in the negative direction about the X axis to align the YZ axes with the corresponding yz axes. The following sequence of Euler angles is then used to generate the direction cosine matrix (Ref 2:8): yaw rotation  $\psi$  about the y axis, pitch rotation  $\theta$  about the new z' axis, then roll rotation  $\phi$  about the new x" axes.



The resulting matrix is:

$$\begin{bmatrix} 1 & 0 & 0 \\ 0 & c\phi & s\phi \\ 0 & -s\phi & c\phi \end{bmatrix} \begin{bmatrix} c\theta & s\theta & 0 \\ -s\theta & c\theta & 0 \\ 0 & 0 & 1 \end{bmatrix} \begin{bmatrix} c\psi & 0 & s\psi \\ 0 & 1 & 0 \\ -s\psi & 0 & c\psi \end{bmatrix} \quad (1)$$

which expands to a single Euler angle transformation so that the set of equations describing the velocity vector is (Ref 7:10):

$$\begin{bmatrix} \dot{x} \\ \dot{y} \\ \dot{z} \end{bmatrix} = \begin{bmatrix} c\psi c\theta & s\theta & c\theta s\psi \\ -s\theta s\psi - c\phi c\psi s\theta & c\phi c\theta & s\phi c\psi - c\phi s\psi s\theta \\ -c\phi s\psi + s\phi c\psi s\theta & -s\phi c\theta & c\phi c\psi + s\phi s\psi s\theta \end{bmatrix}^T \begin{bmatrix} u \\ v \\ w \end{bmatrix} \quad (2)$$

Where  $\dot{x}$ ,  $\dot{y}$ ,  $\dot{z}$  are the velocity components in the inertial reference frame and  $u$ ,  $v$ ,  $w$  are the velocities along the body frame (Fig 2).  $S$ ,  $C$  denotes sine and cosine respectively.

#### Equations of Motion

The relationship between vector derivatives in any two reference frames (where  $\bar{Z}$  denotes any vector) can be expressed as (Ref 6:109):

$$\frac{d\bar{Z}}{dt}{}^i = \frac{d\bar{Z}}{dt}{}^b + \bar{\omega}^{bi} \times \bar{Z} \quad (3)$$

Then, for a velocity vector  $\bar{V}$

$$\frac{d\bar{V}}{dt}{}^i = \frac{d\bar{V}}{dt}{}^b + \bar{\omega}^{bi} \times \bar{V} \quad (4)$$

Consequently,  $F = ma = m\dot{V}$  can be expressed in the reference frame of interest as

$$\bar{F} = m\dot{\bar{V}} + m\bar{\omega} \times \bar{V} \quad (5)$$

The rotational parameters  $p$ ,  $q$ , and  $r$  are defined as the angular velocities about the  $X$ ,  $Y$ ,  $Z$  body axes respectively and  $u$ ,  $v$  and  $w$  are the linear velocity components along the  $X$ ,  $Y$ ,  $Z$  axes:

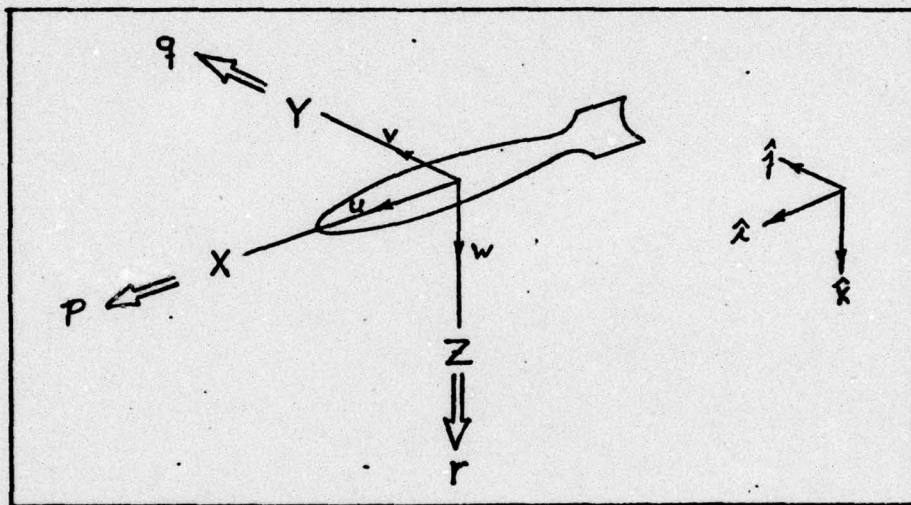


Fig. 2. Rotational and Linear Velocity Axes

The scalar components of equation 5 can be expressed in the body frame as (Ref 4:99):

$$\begin{aligned} F_x &= m(\dot{u} + qw - rv) \\ F_y &= m(\dot{v} + ru - pw) \\ F_z &= m(\dot{w} + pv - qu) \end{aligned} \quad (6)$$



or, equivalently,

$$m \begin{bmatrix} \dot{U} \\ \dot{V} \\ \dot{W} \end{bmatrix} = \begin{bmatrix} F_X \\ F_Y \\ F_Z \end{bmatrix} - m \begin{bmatrix} qW - rV \\ rU - pW \\ pV - qU \end{bmatrix} \quad (7)$$

where the components of  $\bar{F}$  are expressed as the combination of aerodynamic and weight forces.

$$\begin{bmatrix} F_X \\ F_Y \\ F_Z \end{bmatrix} = QS \begin{bmatrix} C_X \\ C_Y \\ C_Z \end{bmatrix} - mg \begin{bmatrix} s\theta \\ c\phi c\theta \\ -s\phi c\theta \end{bmatrix} \quad (8)$$

where  $Q = \frac{1}{2} \rho v_a^2$  = dynamic pressure

$S$  = cross sectional area

$C_X, C_Y, C_Z$  = aerodynamic force coefficients

This set of equations (Ref 2:11) describe the three translational degrees of freedom of a projectile as it proceeds along its path. Three additional equations are needed to account for the spin, pitch and yaw motion that will be encountered.

The expression relating the derivative of the angular momentum vector between the body and inertial frame, from Eq 2, is

$$\dot{\bar{h}}^i = \dot{\bar{h}}^b + \bar{\omega}^{bi} \times \bar{h} \quad (9)$$

where

$$\begin{bmatrix} h_x \\ h_y \\ h_z \end{bmatrix} = \begin{bmatrix} I_x p \\ I_y q \\ I_z r \end{bmatrix} \quad (10)$$

The rate of change of angular momentum expressed in the body frame, for constant mass projectiles, is

$$\begin{bmatrix} \dot{h}_x \\ \dot{h}_y \\ \dot{h}_z \end{bmatrix}_b = \begin{bmatrix} I_x \dot{p} \\ I_y \dot{q} \\ I_z \dot{r} \end{bmatrix} \quad (11)$$

The origin of the body frame of reference is located at the center of gravity of the projectile which eliminates the products of inertia since the body frame is located on principal axes and the moment of inertia about the y & z axes are equal. The scalar components of Eq 9 can therefore be written as

$$\begin{aligned} \dot{h}_x^i &= M_x = I_x \dot{p} + qr[I_z - I_y] \\ \dot{h}_y^i &= M_y = I_y \dot{q} + pr[I_x - I_z] \\ \dot{h}_z^i &= M_z = I_z \dot{r} + pq[I_y - I_x] \end{aligned} \quad (12)$$

Since  $I_y = I_z$  for a projectile with rotational mass symmetry, this set is equivalently presented as (Ref 2:11):

$$\begin{bmatrix} I_x \dot{p} \\ I_y \dot{q} \\ I_z \dot{r} \end{bmatrix}_b = \begin{bmatrix} M_x \\ M_y \\ M_z \end{bmatrix} - (I_y - I_x) p \begin{bmatrix} 0 \\ -r \\ q \end{bmatrix} \quad (13)$$

where the M vector is the moment produced by aerodynamic forces expressed as a function of the aerodynamic moment coefficients  $C_L$ ,  $C_M$ ,  $C_N$

(Ref 2:12):



$$\begin{bmatrix} M_x \\ M_y \\ M_z \end{bmatrix} = Q S d \begin{bmatrix} C_L \\ C_H \\ C_N \end{bmatrix} \quad (14)$$

where  $d$  is the diameter of the projectile.

Eqs 7 and 13 completely describe the motion of a six degree-of-freedom ballistic projectile and form the basis of the six degree-of-freedom computer program used in this investigation.

#### Differential Equations of Motion in Rotational Parameters

Euler angles provide an effective description of body orientation in space and the heading, pitch and roll angles are easily visualized. The transformation matrix of nine direction cosine elements, however, requires considerable computer time to process the numerous trigonometric functions. Also, singularities in the differential equations arise when the pitch angle of  $\pm 90^\circ$  is reached, as well as inducing unacceptable truncation error when integrating in the neighborhood of the singularity point. The use of Euler rotational parameters (sometimes referred to as quaternions) provide a computational device that avoids the singularity limitation of Euler angles. This system uses four parameters to fix the position of a body in space: three direction cosine angles to specify the orientation of the spin axis, and another rotational parameter to specify the amount of spin about that axis. Instead of working with nine direction cosine elements and six constraint equations from the Euler set, the problem is now reduced to expressions for the rate of change of the four quaternion parameters ( $\dot{\lambda}_1, \dot{\lambda}_2, \dot{\lambda}_3, \& \dot{\lambda}_0$ ) and a single constraint equation  $\lambda_1^2 + \lambda_2^2 + \lambda_3^2 + \lambda_0^2 = 1$ . The computer time required to solve this set is reduced but still remains ex-

tensive. The rotational parameter equivalent of the direction cosine matrix of equation 2 is (Ref 2:7):

$$\begin{bmatrix} 2(\lambda_0^2 + \lambda_1^2) - 1 & 2(\lambda_1\lambda_2 + \lambda_0\lambda_3) & 2(\lambda_1\lambda_3 - \lambda_0\lambda_2) \\ 2(\lambda_1\lambda_3 - \lambda_0\lambda_2) & 2(\lambda_0^2 + \lambda_2^2) - 1 & 2(\lambda_2\lambda_3 + \lambda_0\lambda_1) \\ 2(\lambda_1\lambda_3 + \lambda_0\lambda_2) & 2(\lambda_2\lambda_3 - \lambda_0\lambda_1) & 2(\lambda_0^2 + \lambda_3^2) - 1 \end{bmatrix} \quad (15)$$

where

$$\begin{aligned} \lambda_0 &= C \frac{\phi}{2} C \frac{\theta}{2} C \frac{\psi}{2} + S \frac{\phi}{2} S \frac{\theta}{2} S \frac{\psi}{2} \\ \lambda_1 &= C \frac{\phi}{2} S \frac{\theta}{2} S \frac{\psi}{2} + S \frac{\phi}{2} C \frac{\theta}{2} C \frac{\psi}{2} \\ \lambda_2 &= C \frac{\phi}{2} C \frac{\theta}{2} S \frac{\psi}{2} + S \frac{\phi}{2} S \frac{\theta}{2} C \frac{\psi}{2} \\ \lambda_3 &= C \frac{\phi}{2} S \frac{\theta}{2} C \frac{\psi}{2} + S \frac{\phi}{2} C \frac{\theta}{2} S \frac{\psi}{2} \end{aligned} \quad (16)$$

The rate of change of these parameters are given by (Ref 2:10):

$$\begin{bmatrix} \dot{\lambda}_0 \\ \dot{\lambda}_1 \\ \dot{\lambda}_2 \\ \dot{\lambda}_3 \end{bmatrix} = -\frac{1}{2} \begin{bmatrix} 0 & p & q & r \\ -p & 0 & -r & q \\ -q & r & 0 & -p \\ -r & -q & p & 0 \end{bmatrix} \begin{bmatrix} \lambda_0 \\ \lambda_1 \\ \lambda_2 \\ \lambda_3 \end{bmatrix} \quad (17)$$

The algebra required to develop equations 15 and 16 is quite extensive as shown in Appendix D. The derivation of equation 17 is found in Appendix B of reference 2, page 11.

The differential equations of motion are now in the programmed form and are summarized in Table I.



Table I

Differential Equations of Motion

The kinematic relationships are:

$$\begin{bmatrix} \dot{x} \\ \dot{y} \\ \dot{z} \end{bmatrix} = \begin{bmatrix} 2(\lambda_0^2 + \lambda_1^2) - 1 & 2(\lambda_1\lambda_2 + \lambda_0\lambda_3) & 2(\lambda_1\lambda_3 - \lambda_0\lambda_2) \\ 2(\lambda_1\lambda_2 - \lambda_0\lambda_3) & 2(\lambda_0^2 + \lambda_2^2) - 1 & 2(\lambda_2\lambda_3 + \lambda_0\lambda_1) \\ 2(\lambda_1\lambda_3 + \lambda_0\lambda_2) & 2(\lambda_2\lambda_3 - \lambda_0\lambda_1) & 2(\lambda_0^2 + \lambda_3^2) - 1 \end{bmatrix}^T \begin{bmatrix} u \\ v \\ w \end{bmatrix} \quad (18)$$

$$\begin{bmatrix} \dot{\lambda}_0 \\ \dot{\lambda}_1 \\ \dot{\lambda}_2 \\ \dot{\lambda}_3 \end{bmatrix} = -\frac{1}{2} \begin{bmatrix} 0 & p & q & r \\ -p & 0 & -r & q \\ -q & r & 0 & -p \\ -r & -q & p & 0 \end{bmatrix} \begin{bmatrix} \lambda_0 \\ \lambda_1 \\ \lambda_2 \\ \lambda_3 \end{bmatrix} \quad (19)$$

The dynamic relationships are:

$$m \begin{bmatrix} \dot{u} \\ \dot{v} \\ \dot{w} \end{bmatrix} = \begin{bmatrix} F_x \\ F_y \\ F_z \end{bmatrix} - m \begin{bmatrix} qw - rv \\ ru - pw \\ pv - qu \end{bmatrix} \quad (20)$$

$$\begin{bmatrix} I_x \dot{p} \\ I_y \dot{q} \\ I_z \dot{r} \end{bmatrix} = \begin{bmatrix} M_x \\ M_y \\ M_z \end{bmatrix} - (I_y - I_x) p \begin{bmatrix} 0 \\ -r \\ q \end{bmatrix} \quad (21)$$

where  $\bar{F}$  and  $\bar{M}$  are described in Eqs 8 and 14.

### III. Method of Problem Solution

#### The Computer Program

Solution of the set of coupled, non-linear differential equations listed in Table I requires extensive computer capability. The program used in this study was originally coded for the Naval Ordnance Research Computer and has been updated as more advanced generations of computers became operational. The Fortran IV program used for this study was developed by Charles W. Ingram and R.S. Eikenberry using Cohen & Werners' work (Ref 2) as a point of departure. It was written originally for stability analysis applications rather than precision trajectory prediction. The six degree of freedom computer program numerically integrates the set of kinematic and dynamic Euler equations of Table I in the body reference frame and outputs in the inertial reference frame. The accuracy of the program is limited primarily by the quality of the aerodynamic coefficients that are input. The complete program is listed in Appendix F.

Both the Runge-Kutta numerical integration step size (value of A-(20) Table B-2) and the output time increment can be adjusted by the user as a means of tailoring the computer time and cost against the accuracy required. If high projectile spin rates are encountered, coarse step sizes on the order of .01 second could result in erroneous outputs due to insufficient data points to properly resolve the integration problem. The time step should be small enough to provide at least ten integration steps during one revolution of the highest spin rate expected. A step size of .002 second is used for most simulations in this report. Since extensive core memory and computer time is required to pro-



cess this program, it is written for only a single trajectory per run. A core memory of 100,000 was adequate for all trajectories used in this study. (An integration step size of .001 second requires in excess of 200 seconds of computer time for a 10,000 ft drop.)

Discussion of the computer program input and output is included in Appendices B and C.

### Projectile Model Description

The standard Mark 82 warhead with an experimental tail section was the projectile model used to determine the aerodynamic coefficients. The cylindrical aft section has four slotted fins, each fitted with a trailing edge wedge to provide the roll driving moment. The designation of the configuration is FFSW (fin, fixed, slotted, wedge). This particular projectile was selected because of the similarity to existing conventional weapons and, significantly, most of the aerodynamic coefficients were available (Ref 14).

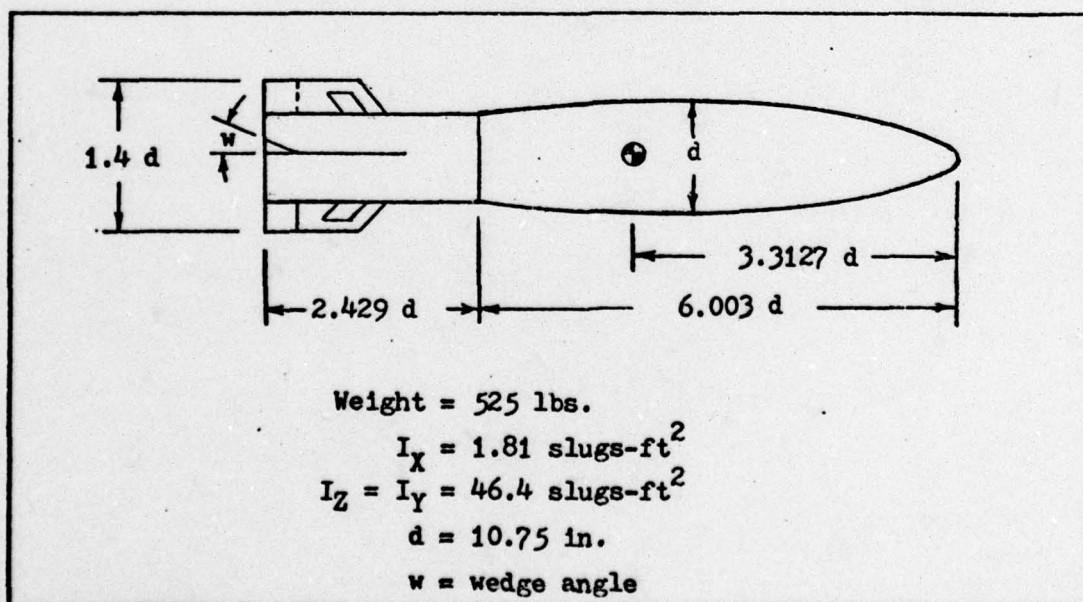


Fig. 3. Projectile Model

The cylindrical tail section provides both a higher drag coefficient and a housing for an inflatable high drag device that may be installed; the slotted fins increase the probability of a well-behaved roll rate throughout the trajectory (Ref 3:1).

A wedge angle of ten degrees is used for most of the simulations in this study. This wedge angle provides sufficient roll acceleration to overcome adverse dynamics encountered during release. The steady state spin rate produced is fast enough to investigate the influence of Magnus coefficients without inducing the type of instabilities that can occur when the spin rate exceeds approximately ten times the nutation frequency (Ref 8; Sec 3,5).

#### Aerodynamic Coefficients

Values of the aerodynamic coefficients used in equations 8 and 14 must be adequately determined by wind tunnel testing of the projectile model before satisfactory trajectory simulations are possible. The aerodynamic force and moment coefficients can, for most applications, be reduced to the expressions listed in Table II. These expressions include cross-velocity terms in both the force and moment coefficients, but cross spin terms are included only in moment coefficients about pitch and yaw axes. (See Fig 6 for definitions of cross-velocity and cross spin terms.) Table III describes the terms which make up the total aerodynamic force and moment coefficients. These mathematical expressions were determined in Cohen and Werners' work (Ref 2:15-19).

In order to illustrate the utility of the aerodynamic coefficient terms, the expression for induced roll moment is used as an example (See Table III):



$$C_{l_0} + C_{l_7} \sin \eta \phi' + C_{l_8} \cos \eta \phi' \quad (22)$$

where

$\phi'$  = Angle to cross velocity vector (See Fig 6)

$C_{l_0}$  = Initial curve shift (See Fig 5)

$C_{l_7}, C_{l_8}$  = Amplitude of curve

$\eta$  = Number of fins

The  $C_{l_0}$  term is the residual rolling moment that remains after the projectile has been aligned in the wind tunnel at the angle of attack of interest with no fin deflection; that is, an index of rolling moment due to body shape.

The next set of terms,  $C_{l_7} \sin \eta \phi' + C_{l_8} \cos \eta \phi'$ , is the mathematical format required to describe the data curve obtained from the wind tunnel measurements. This application can best be appreciated by the illustration of a spinning projectile at various stages of roll moving away at an angle of attack sufficient to cause a vortex to trail along the top of the missile as in Figure 4.

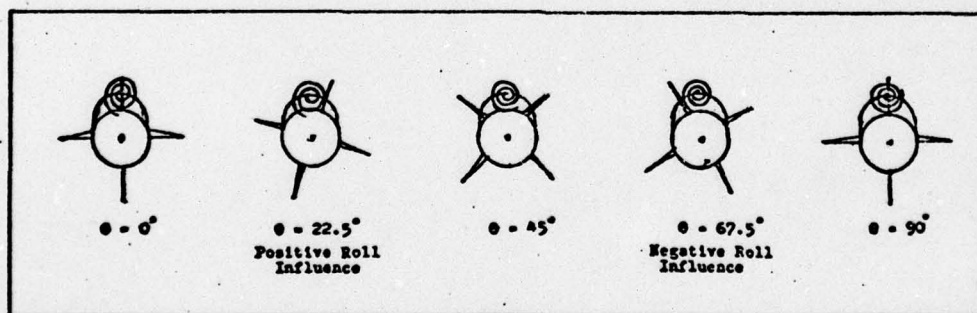


Fig. 4. Periodic Change in Aerodynamic Coefficient  $C_{l_0}$

At the beginning of the sequence, the trailing vortex is cut symmetrically by the fin, so no net roll influence is imposed by the dynamic pressure change on the fin due to the vortex. After 22.5 degrees of

roll, the vortex is in a position to exert a maximum rolling influence. At the  $45^\circ$  angle, a condition of symmetry is again encountered. For this type of oscillating characteristic,  $C_l$  could be graphed for the entire sequence as the solid curve of Fig 5. The graph obtained from the actual wind tunnel data for the coefficient of interest, however, is generally skewed from the theoretical curve as indicated by the dotted curve.

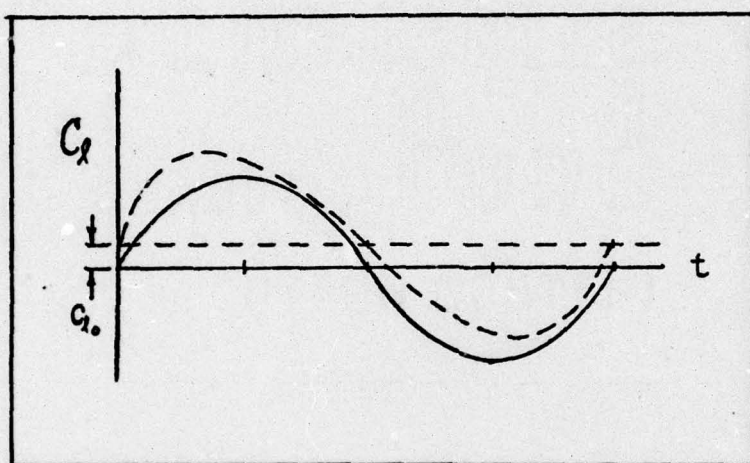


Fig. 5. Theoretical vs Experimental Data Curves

The three terms,  $C_{l_0} + C_{l_7} \sin \eta \phi' + C_{l_8} \cos \eta \phi'$ , are therefore used in whatever combination of magnitudes and sinusoidals that produce the best simulation of the actual wind tunnel data. The relative magnitude of  $C_{l_0}$  versus the amplitude of the sinusoidals often makes one or the other of the terms negligible.

The remaining trigonometric expressions in Table II not defined in Table III are attributable to transformations between reference frames.

Most of the aerodynamic coefficient arrays used in this computer program had been previously determined through a joint effort between the Naval Surface Weapons Center, Dahlgren Laboratory, and the Aero-



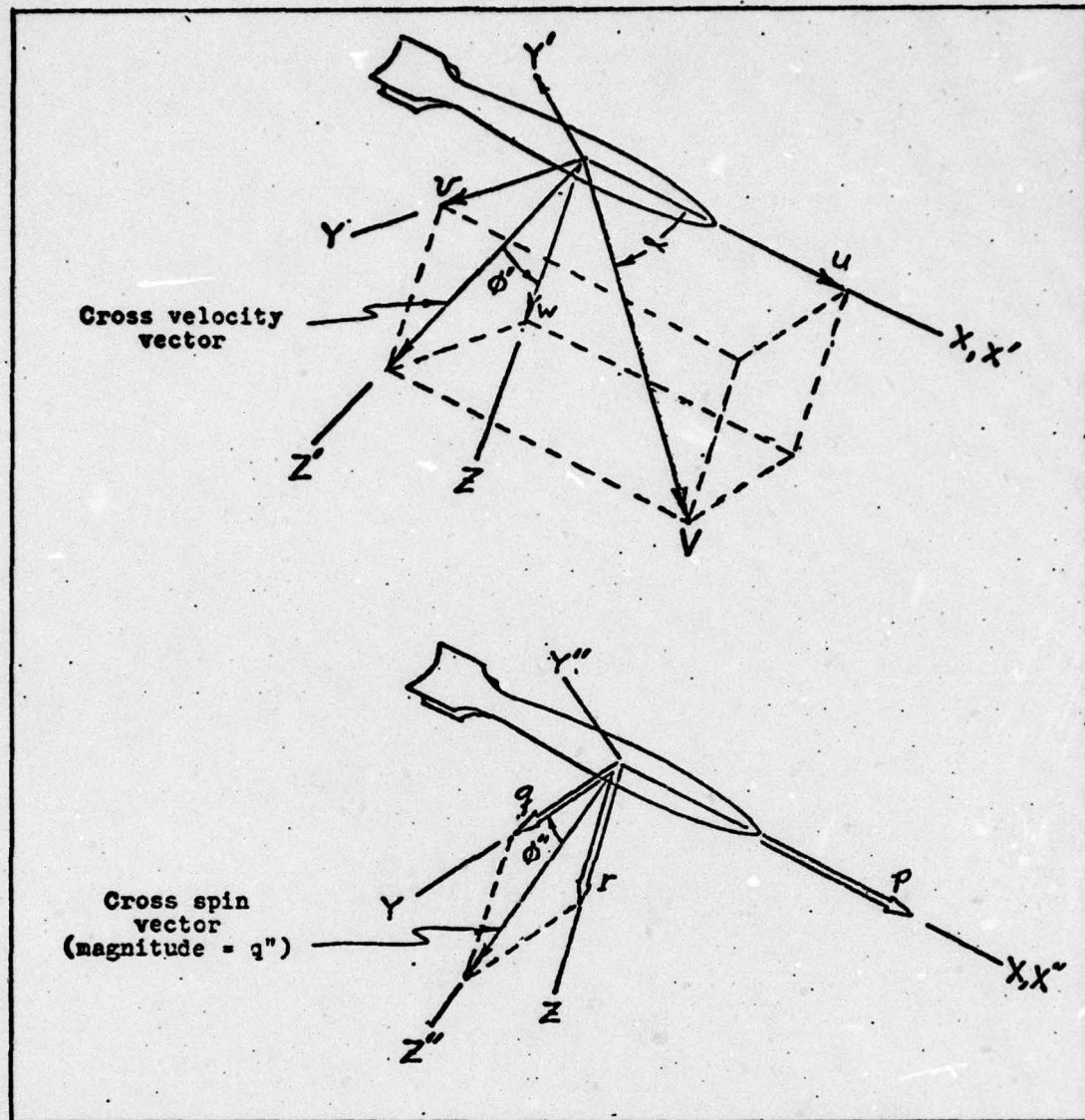


Fig. 6 . Definition of Cross-Spin/Velocity Terms.

where (Ref 2)

$$q'' = \sqrt{q^2 + r^2} \quad , \text{ magnitude of cross-spin (rad/sec)}$$

$$\alpha = \arctan \sqrt{\frac{v^2 + w^2}{u}} \quad , \text{ magnitude of yaw or angle of attack (deg)}$$

$$\phi' = \arctan \frac{v}{w} \quad (\text{angle about X-axis from cross-velocity vector of the center of gravity of missile to Z fin}) (\text{deg})$$

$$\phi'' = \arctan \frac{(-r)}{q} \quad \text{angle about the X-axis from cross-spin vector to Y fin} (\text{deg})$$

$$C_X = C_x$$

$$C_Y = [C_{y_0} + C_{y_7} \sin \eta \phi' + C_{y_8} \cos \eta \phi' + \frac{Pd}{2V_a} C_{y_p}] \cos \phi' + [C_{z_0} + C_{z_7} \sin \eta \phi' + C_{z_8} \cos \eta \phi'] \sin \phi' + C_y(\epsilon)$$

$$C_Z = [C_{y_0} + C_{y_7} \sin \eta \phi' + C_{y_8} \cos \eta \phi' + \frac{Pd}{2V_a} C_{y_p}] (-\sin \phi') + [C_{z_0} + C_{z_7} \sin \eta \phi' + C_{z_8} \cos \eta \phi'] \cos \phi' + C_z(\epsilon)$$

$$C_L = C_{l_0} + C_{l_1}(\delta \omega) + C_{l_7} \sin \eta \phi' + C_{l_8} \cos \eta \phi' + \frac{Pd}{2V_a} C_{l_p} + \alpha (C_{l_1} \bar{\alpha}_0 + C_{l_1} \bar{\alpha}_1 \sin \phi' + C_{l_1} \bar{\alpha}_2 \cos \phi')$$

$$C_M = [C_{m_0} + C_{m_7} \sin \eta \phi' + C_{m_8} \cos \eta \phi'] \cos \phi' + [C_{n_0} + C_{n_7} \sin \eta \phi' + C_{n_8} \cos \eta \phi' + \frac{Pd}{2V_a} C_{n_p}] \sin \phi' \\ + [C_{mq_0} + C_{mq_7} \sin \eta \phi'' + C_{mq_8} \cos \eta \phi''] \frac{q'' d}{2V_a} \cos \phi'' + C_m(\epsilon)$$

$$C_N = [C_{m_0} + C_{m_7} \sin \eta \phi' + C_{m_8} \cos \eta \phi'] (-\sin \phi') + [C_{n_0} + C_{n_7} \sin \eta \phi' + C_{n_8} \cos \eta \phi' + \frac{Pd}{2V_a} C_{n_p}] \cos \phi' \\ + [C_{mq_0} + C_{mq_7} \sin \eta \phi'' + C_{mq_8} \cos \eta \phi''] \frac{q'' d}{2V_a} (-\sin \phi'') + C_n(\epsilon)$$

TABLE II

Force And Moment Coefficients (Adapted from Ref 2)



TABLE III

Aerodynamic Coefficients  
(Adapted from Ref 2)

<u>Description of Coefficient</u>	<u>Array Symbol *</u>
$C_x$	Axial force
CX	
$C_{y0} + C_{y7} \sin \eta \phi' + C_{y8} \cos \eta \phi'$	Induced side force
CY7	
$C_{yp}$	Magnus force
CYP	
$C_{z0} + C_{z7} \sin \eta \phi' + C_{z8} \cos \eta \phi'$	Normal force
CZ	
$C_y (\phi)$	Trim force along Y-axis
N/A	
$C_z (\phi)$	Trim force along Z-axis
N/A	
$C_{l0} + C_{l7} \sin \eta \phi' + C_{l8} \cos \eta \phi'$	Induced roll moment
CLGA	
$C_l (\delta w)$	roll moment due to fin cant
CLDW	
$C_{lp}$	Roll damping moment
CLP	
$C_{m0} + C_{m7} \sin \eta \phi' + C_{m8} \cos \eta \phi'$	Restoring moment
CM	
$[C_{mq0} + C_{mq7} \sin \eta \phi' + C_{mq8} \cos \eta \phi'] \frac{q'' d}{2 V_a}$	Damping moment
CMQ	
$C_{n0} + C_{n7} \sin \eta \phi' + C_{n8} \cos \eta \phi'$	Induced side moment
CNGA	
$C_{np}$	Magnus moment
CNP	
$C_m (\phi)$	Trim moment about y-axis
CMDE	
$C_n (\phi)$	Trim moment about z-axis
N/A	
$\xi (C_{le} \alpha_0 + C_{le} \alpha_1 \sin \phi' + C_{le} \alpha_2 \cos \phi')$	Roll moment due to eccentric tail
N/A	

\* See Appendix G

space Research Laboratory, Wright-Patterson Air Force Base and were available for this project (See Appendix G). The Magnus force coefficient, however, was not available and had to be determined so that its effect on lateral error could be studied. The Magnus force coefficient is determined from the definition

$$C_{yp} = \frac{\partial C_y}{\partial (pd/2V)} \quad (23)$$

where  $p$  = spin rate,  $d$  = projectile diameter,  $V$  = wind tunnel velocity.

This relation states that the slope of a line fit through a plot of  $C_y$  versus  $pd/2V$  should yield the nominal value of  $C_{yp}$  for a specific angle of attack and Mach number. Tables A-I and A-II show the wind tunnel data taken at Mach 0.8 at an angle of attack of 1.87 degrees.  $C_y$  was plotted against  $pd/2V$  and then a "best fit" line was drawn through the data points (Fig 8). Greater weight was given to the lower values  $pd/2V$  so that the cluster of data points in the neighborhood of the steady state spin condition would not overly influence the slope. No attempt was made to force the line through the origin. As long as the axis intercept remains small, the error in the wind tunnel measuring instruments will dominate. The primary objective is to provide a best estimate of the most representative slope of the plot. The slope of the resulting line produced the nominal value of  $C_{yp}$  that was entered as a single element in the CYP array corresponding to Mach = 0.8 and  $\alpha = 2$  (Ref Table IV). The remaining 71 elements of the 8 x 9 matrix were determined in the same manner. Note that the Mach = 0.4 values are used to fill the Mach = 0 row. This is done because, at lower Mach numbers, the compressibility effects diminish and the coefficient remains nearly constant. Fig 7 shows a typical force coefficient progression.



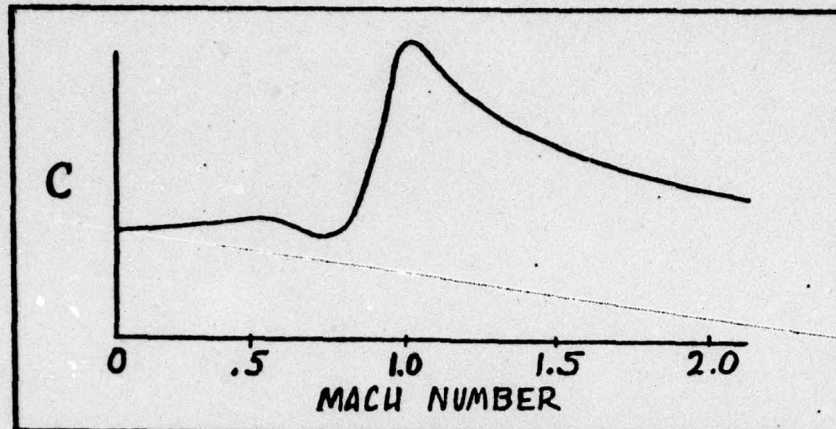


Fig. 7. Force Coefficient vs Mach Number

The  $\alpha = 50^\circ$  column contains unreliable data but is used only to provide a value for the program to interpolate against in the event  $\alpha = 25^\circ$  is exceeded. The computer program is written so that interpolation is accomplished for any intermediate value of angle of attack and Mach. The angles of attack used in this study were well below 25 degrees so this ill-defined edge of the array was not encountered.

#### Approach to the Investigation

The primary objective of this study is to investigate the relative contributions of the Magnus coefficients to lateral deflection of a spinning projectile following a ballistic trajectory. The general approach is to isolate the effect of the Magnus force coefficient  $C_{y_p}$ , the induced side coefficient  $C_{y_\gamma}$ , and the Magnus moment coefficient  $C_{n_p}$  on the trajectories initiated from identical release conditions. Each coefficient is studied individually, and in pairs; then compared to the performance of all three coefficients together. The initial conditions include a range of airspeed, altitudes and attitude perturbations.

The Magnus force coefficient,  $C_{y_p}$ , is of interest because it is

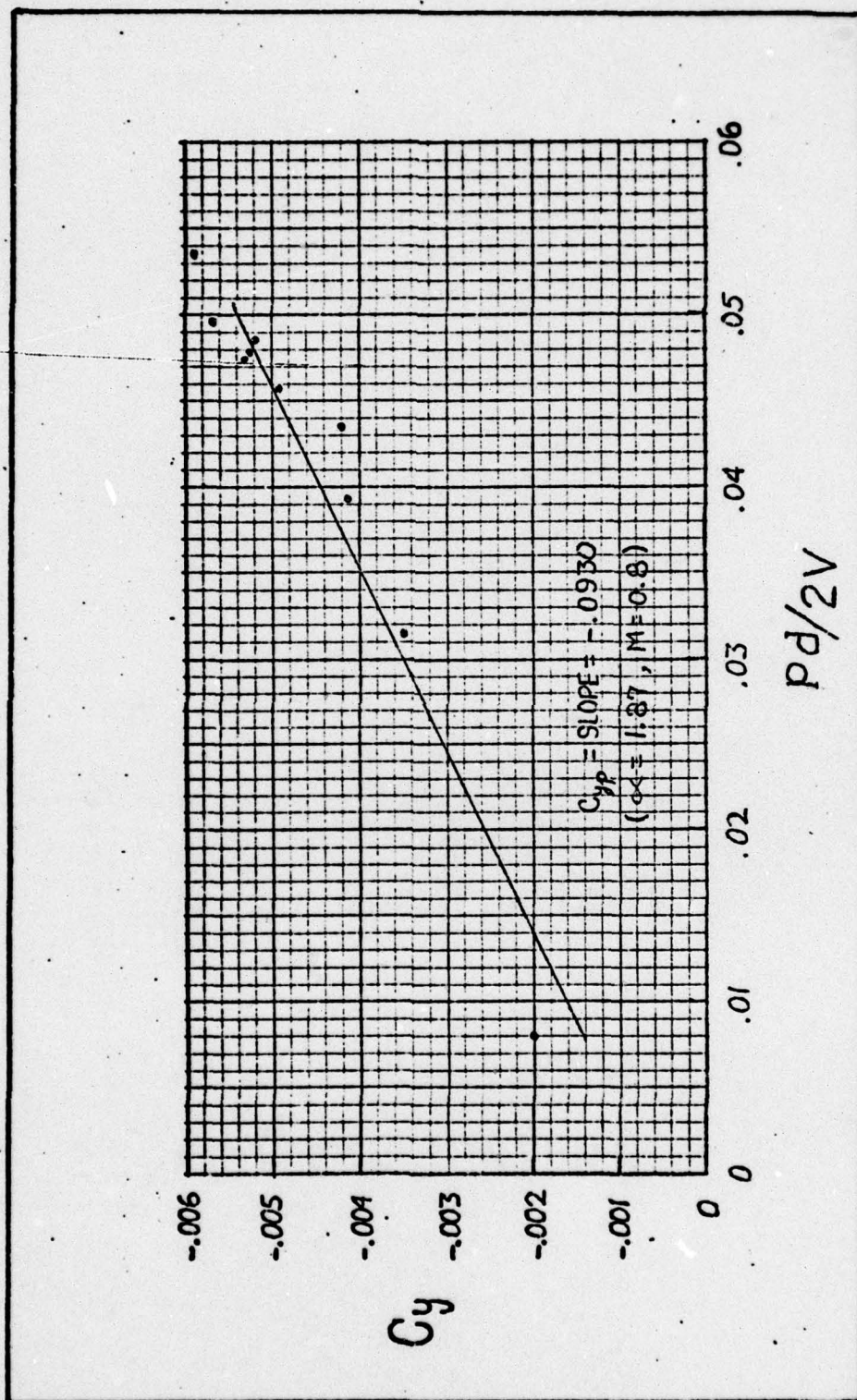


Fig. 8. Change in Magnus Force Coefficient



TABLE IV  
Magnus Force Aerodynamic Coefficient Array.  
(Extracted from Appendix G)

CVP	C (°)												
	AL=MA	0.0000	2.0000	4.0000	6.0000	8.0000	10.0000	15.0000	20.0000	25.0000	30.0000	90.0000	
MACH	0.0000		-0.0300	-0.1350	-0.5350	-0.7750	-2.1030	-5.9100	-12.5000	-12.5000	-12.5000	-12.5000	
MACH	.4000		0.0000	-0.0300	-0.1350	-0.5350	-0.7750	-2.1030	-5.9100	-12.5000	-12.5000	-12.5000	
MACH	.8000		0.0000	-0.0930	-0.1750	-0.4100	-0.6600	-1.1650	-2.9900	-6.1500	-6.1500	-6.1500	
MACH	.9000		0.0000	-0.1050	-0.1850	-0.3500	-0.6000	-1.1000	-2.0000	-5.0000	-5.0000	-5.0000	
MACH	1.0000		0.0000	-0.0700	-0.1650	-0.2950	-0.3300	-0.7000	-2.3720	-3.4500	-3.4500	-3.4500	
MACH	1.1000		0.0000	-0.0800	-0.1600	-0.3120	-0.2540	-0.6000	-2.4630	-3.4000	-3.4000	-3.4000	
MACH	1.2000		0.0000	-0.0800	-0.1800	-0.3100	-0.2650	-0.6750	-1.7700	-2.3300	-2.3300	-2.3300	
MACH	2.0000		0.0000	-0.0800	-0.1800	-0.3100	-0.2650	-0.6750	-1.7700	-2.3300	-2.3300	-2.3300	

the source of Magnus lift that is generated by a spinning body subject to a relative wind component acting perpendicular to the body spin axis. This force will therefore be generated anytime the spinning projectile is falling with an angle of attack. The direction of the lateral Magnus lifting force is determined by the direction of spin and the cross-velocity component  $w$ . The spin rate,  $p$ , causes a velocity differential to be produced as shown in Fig. 9. A corresponding pressure differential is generated which produces lift in the lateral direction.

The side force coefficient,  $C_{y7}$ , contributes to the deflection of a projectile by influencing side lift due to a lateral angle of attack.

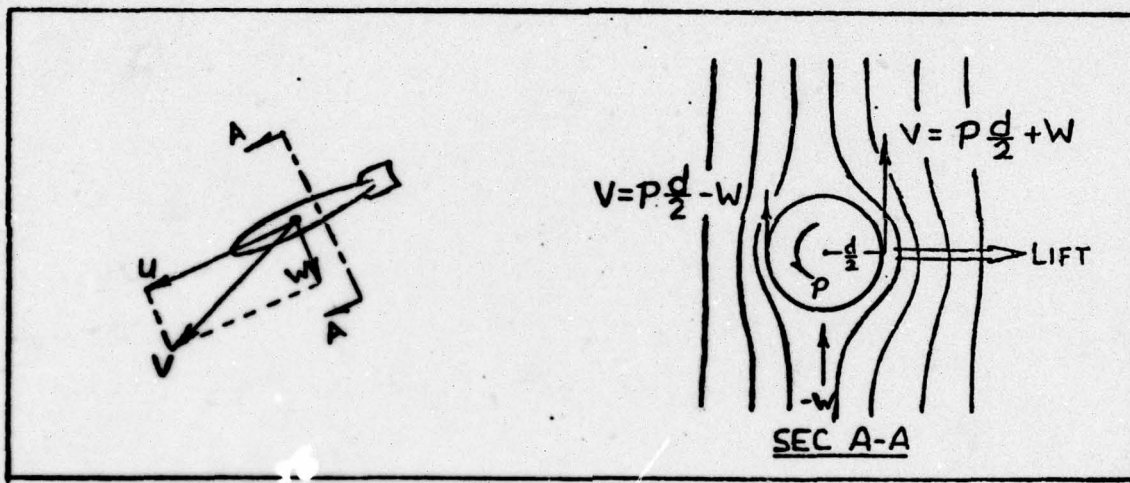


Fig. 9. Magnus Lift

The Magnus moment coefficient,  $C_{np}$ , can directly effect lateral progression of a projectile following a ballistic trajectory. Magnus moment is generated when the projectile, at a sufficiently high angle of attack, trails a wake vortex that blanks out the rolling lift of the fin passing through it. This causes a change in roll torque and a fin force imbalance that produces a yaw moment on the projectile (Fig 10). The value of the aerodynamic coefficient is a measure of the sensitivity of the projectile to this effect.



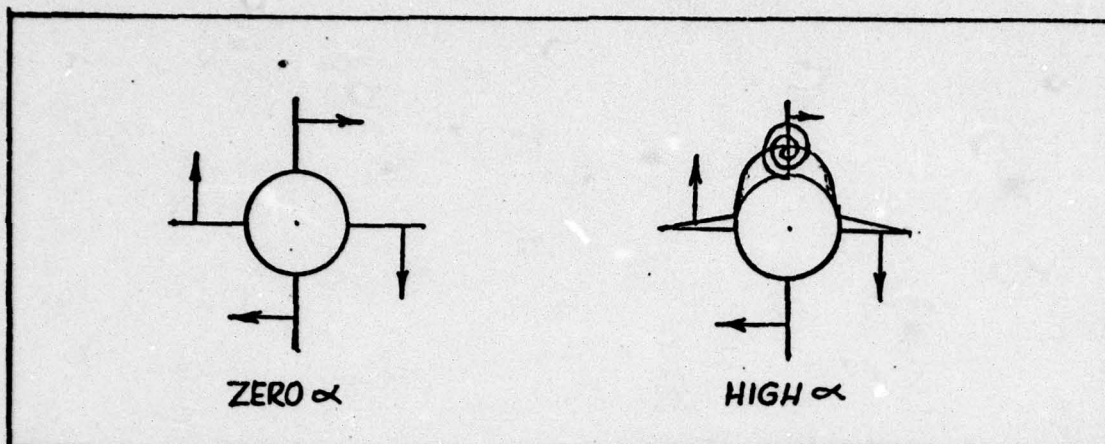


Fig. 10. Magnus Moment

The release velocities used as initial conditions are 600 ft/sec for a lower limit (approximately 350 knots) and 1000 ft/sec for the high speed delivery. The lower limit was selected as a representative velocity for a slow delivery. The 1000 ft/sec velocity remains in the subsonic region and provides adequate velocity spread for comparisons. A velocity of 1200 ft/sec was used, in some cases, to investigate the effect of a supersonic delivery (Mach 1.1 at 10,000 ft).

The 10,000 foot altitude was selected for most of the simulations. This altitude provides sufficient time of flight to identify any significant trajectory trends and does not require prohibitive computer time to process. An altitude of 20,000 feet was used when a lower air density trajectory was desired for comparison.

All releases are from a level flight path. The projectile is, however, perturbed initially under three conditions: zero perturbation, a nose-down rate motion, and a nose-down displacement. The zero perturbation condition simulates a projectile perfectly aligned with the velocity vector at release. The pitch rate motion of  $q = -.5$  radians/sec is used to investigate the effect of motion that could be induced

by the bomb ejection mechanism. The initial angle of attack of  $\alpha_0 = -7.75$  degrees, the third condition, is approximately the same maximum amplitude achieved by the preceding initial motion, but obtained in a different manner.

Spin rate of the projectile directly influences Magnus lift and, consequently, lateral progression of the trajectory. Wedge angles of 5, 10, and 15 degrees were used in the simulations to investigate the relative influence of the different wedges.

The parameters studied under various initial conditions are listed in an overview in Table V.



TABLE V  
Parameters Investigated

Parameters	Initial Conditions											
	Altitude		Velocity				$\alpha_0$		$q_0$		$v_0$	
	10K	20K	600	1000	1200		0	-7.75	0	-0.5	0	+5.
All Coefficients	x	x	x	x	x		x	x	x	x	x	x
$C_{np}$ (Omitted)	x		x									
$C_{yp}$	x		x									
$C_{y\gamma}$	x		x									
$C_{yp}, C_{np}$	x		x									
$C_{yp}, C_{y\gamma}$	x		x									
$C_{np}, C_{y\gamma}$	x		x									
$C_{yp}, C_{np}, C_{y\gamma}$	x		x	x	x		x	x	x	x		
$C_Z$	x		x					x		x		
$5^\circ$	x		x	x								
$10^\circ$	x	x	x	x	x			x		x		
$15^\circ$	x		x	x								
$z$	x	x	x	x	x		x	x	x	x	x	x
$t$	x		x	x				x				

#### IV. Results of the Simulations

##### Effect of Magnus Coefficients

The first simulations were run to determine the relative influence of the Magnus coefficients. Initial release conditions of level flight at an altitude of 10,000 feet and 600 feet per second, using all twelve available aerodynamic coefficient arrays produced the result shown in Fig. 11. The ground zero impact point for the trajectory using all coefficients was 57.73 feet to the left of the inertial x-y plane containing the release point. With three coefficients removed that influence lateral displacement ( $C_{np}$ ,  $C_{y7}$ ,  $C_{yp}$ ), the impact point was changed to 56.58 feet. This total spread of only 1.15 feet, generated over a relatively long trajectory, is lost in the accuracy limitations of the aerodynamic coefficients and the simplifying assumptions used in the equation of motion development. This small, Magnus induced lateral motion is initiated early and propagates slowly throughout the trajectory.

A second set of simulations were run at a velocity of 1200 ft/sec to determine if higher velocity would cause these coefficients to generate a more significant change in the trajectories. The net difference in the trajectories with and without the three coefficients remains on the order of only a few feet.

There are a number of possible explanations why the Magnus influence is so small. Magnus lift depends on both the relative velocity component acting on the projectile due to angle of attack and the spin rate of the projectile. For normal weapon deliveries, the angle of attack is relatively small on release and dampens toward zero early in the fall. During the time the angle of attack is at a maximum, shortly after release, high spin rate has not yet developed. After the projectile



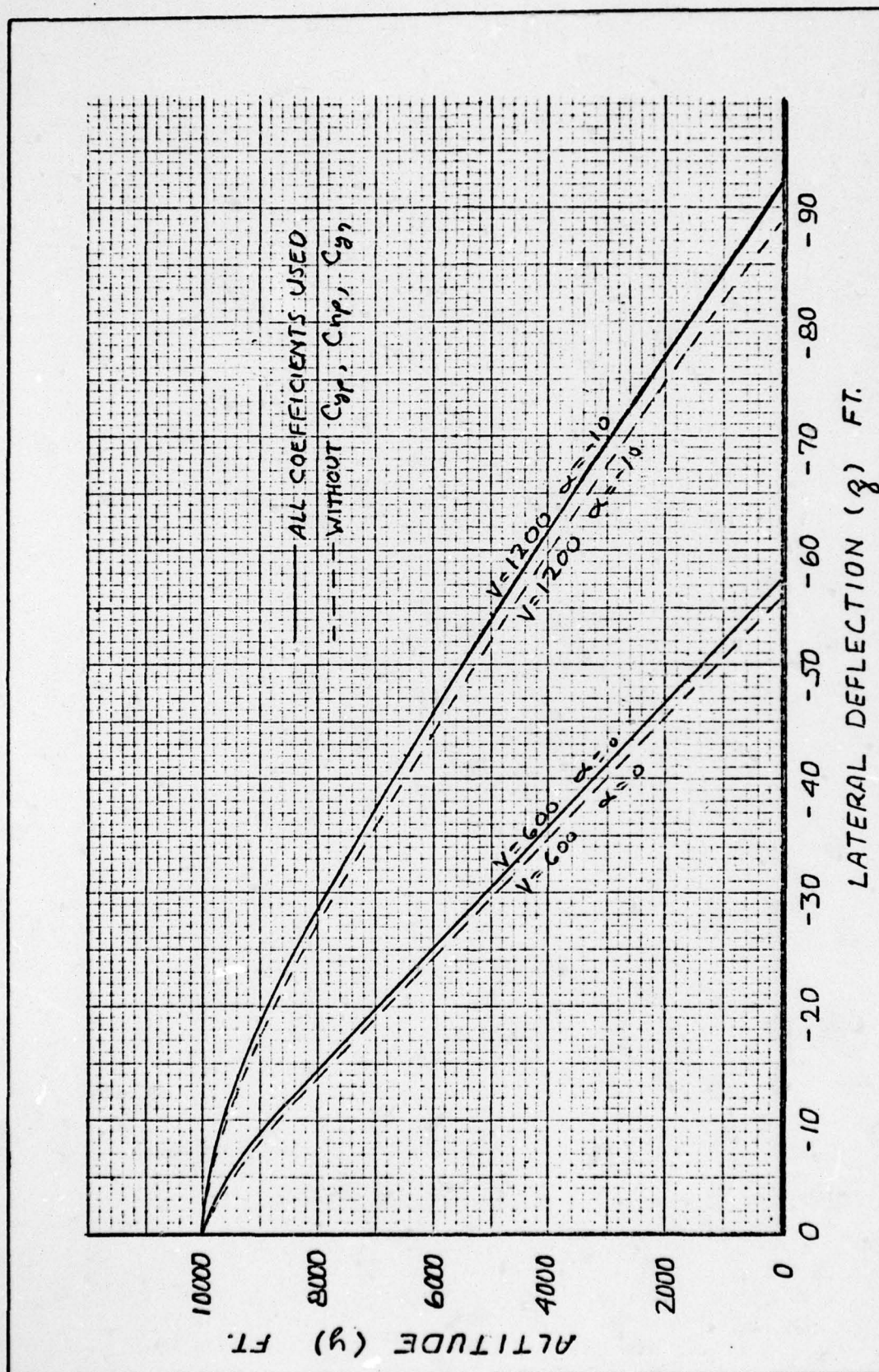


Fig. 11. Effect of Magnus &amp; Side Force Coefficients on Lateral Displacement

has fallen long enough to generate a high spin rate, the angle of attack is negligible. The Magnus side force due to body lift is negligible because the lateral angle of attack is small. The Magnus moment is also small since there is no significant wake generated at small angles of attack to produce a lift differential in the fins.

If oscillatory motion is encountered during release, the projectile angle of attack alternates from positive to negative. The Magnus lift will therefore alternate from positive to negative and average the net influence to zero.

#### Effect of Initial Pitch Motion

To simulate an initial release condition more realistic than perfect alignment of the projectile with the velocity vector, an initial angle of attack of  $-7.75$  degrees was used as an perturbation. The same release initial conditions were used as before and simulations were run first using all coefficients, and then with  $C_{yp}$ ,  $C_{np}$ ,  $C_{y7}$  removed. There was essentially no difference in the resulting trajectories for  $\alpha_0 = -7.75$  degrees compared to  $\alpha_0 = 0$  as shown in Table VI).

An initial pitch rotation of the projectile at release, as might be induced by an ejector mechanism, was then implemented by entering a value of  $q_0 = -.5$  rad/sec. This initial rotation produced the same maximum amplitude of oscillation as the  $\alpha_0 = -7.75^\circ$  case, but a considerable difference in the resulting impact point of the projectile was generated. The increased lateral displacement caused a corresponding decrease in range which is consistent with the principle of conservation of energy. The oscillation induced by an initial angular displacement produced a trajectory that impacted at 14,165 feet downrange and 57.73 feet cross



TABLE VI (a)  
Effect of Magnus Coefficients

Velocity = 600 ft/sec  
Altitude = 10,000 ft  
Wedge angle =  $10^\circ$   
Level flight release

Initial Pitch Motion								t
Altitude = 10,000 ft Wedge angle = 10° Level flight release	Aerodynamic Coefficient	$q_o = 0$ $\alpha_o = 0^\circ$		$q_o = 0$ $\alpha_o = -7.75^\circ$		$q_o = -.5$ $\alpha_o = 0^\circ$		time of flight
		X	Z	X	Z	X	Z	
		Sec						
All coefficients		14165.16	-57.73	14179.60	-56.44	14124.86	-73.02	25.725
Less $C_{yp}$		14165.48	-57.64					25.727
Less $C_{y\gamma}$		14166.83	-56.54	14178.94	-55.86			25.729
Less $C_{np}$		14178.31	-56.60					25.729
Less $C_{yp}$ & $C_{y\gamma}$		14167.15	-56.45					25.729
Less $C_{yp}$ & $C_{np}$		14165.98	-57.73					25.726
Less $C_{y\gamma}$ & $C_{np}$		14167.34	-56.66					25.728
Less $C_{yp}$ , $C_{y\gamma}$ & $C_{np}$		14167.67	-56.58	14179.45	-55.82	14124.47	-67.68	25.728
Less $C_z$ , $C_{yp}$ , $C_{y\gamma}$ & $C_{np}$				14191.70	+ 2.53	14188.68	+ 3.46	
Less $C_z$				14191.06	+ 1.79			

X = Range (Ft)

Z = Lateral displacement (Ft)

TABLE VI (b)  
Effect of Magnus Coefficients

Velocity = 600 ft/sec  
Altitude = 10,000 ft  
Wedge angle =  $10^\circ$   
Level flight release

Aerodynamic Coefficient	Initial Pitch Motion					
	$q_o = 0$ $\alpha_o = 0^\circ$		$q_o = 0$ $\alpha_o = -7.75^\circ$		$q_o = -0.5$ $\alpha_o = 0^\circ$	
	$V_f$	$P_f$	$V_f$	$P_f$	$V_f$	$P_f$
All coefficients	889.06	62.9	889.37	62.9	888.55	62.8
Less $C_{yp}$	889.06	62.9				
Less $C_{y\gamma}$	889.05	62.9	889.36	62.9		
Less $C_{np}$	889.37	62.9				
Less $C_{yp}$ & $C_{y\gamma}$	889.05	62.9				
Less $C_{yp}$ & $C_{np}$	889.10	62.9				
Less $C_{y\gamma}$ & $C_{np}$	889.10	62.9				
Less $C_{yp}$ , $C_{y\gamma}$ & $C_{np}$	889.10	62.9	889.38	62.9	888.63	62.8
Less $C_z$ , $C_{yp}$ , $C_{y\gamma}$ & $C_{np}$			889.76	63.0	889.66	63.0
Less $C_z$			889.76	63.0		

Impact velocity  $V_f$  in ft/sec

Impact spin rate  $P_f$  in rad/sec



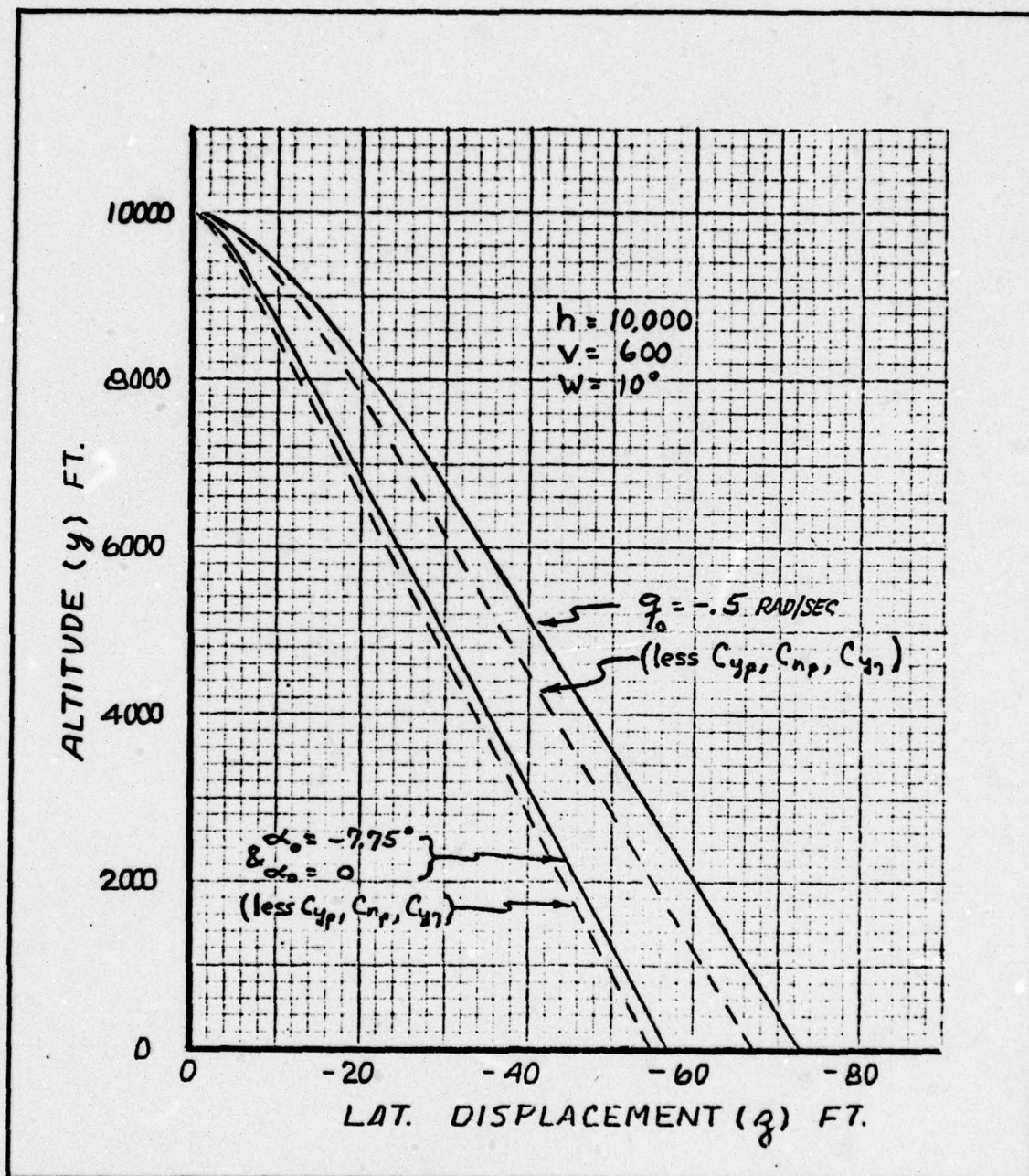


Fig. 12. Effect of Pitch Motion and Magnus Coefficients on Lateral Displacement

range to the left. The rate induced oscillation, with the same release conditions, impacted at 14,179 feet downrange and 73.02 feet cross range (See Table VI and Fig 12).

To investigate the cause of the difference in trajectory, the nose track, viewing the projectile from behind, was plotted for the two different inputs in Fig. 13. The beta versus alpha plot represents a close approximation of the nose track of the projectile early in the trajectory before the body reference frame and the projectile velocity vector rotate a significant amount with respect to the inertial frame. The motion of the projectile nose for the two conditions is quite different. Fig 13a represents single arm coning motion caused by nutation. No precession is evident and the damping is relatively constant. The nose track in Fig 13b shows less coning and displays two arm motion with both nutation and precession. This oscillation dampens faster in pitch than in yaw. The direction of nutation is opposite to the projectile spin rate while the precession is in the same direction. Figs 13c, d, e, f were plotted to identify any parameters that could cause the difference in trajectories. These plots show that the difference in spin rate build-up and velocity progression is very small. A slight phase shift in yaw oscillation is apparent, and the initial slopes of the  $\beta$  versus  $t$  plots are noticeably different. The last plot shows a significantly different behavior in the angle of attack oscillations between the two initial conditions.

The lateral displacement for both initial conditions is plotted against time in Fig. 14 to further define the projectile motion shortly after release. The linearized average slope of these plots produces a measure of the initial lateral average velocity. The slope for the



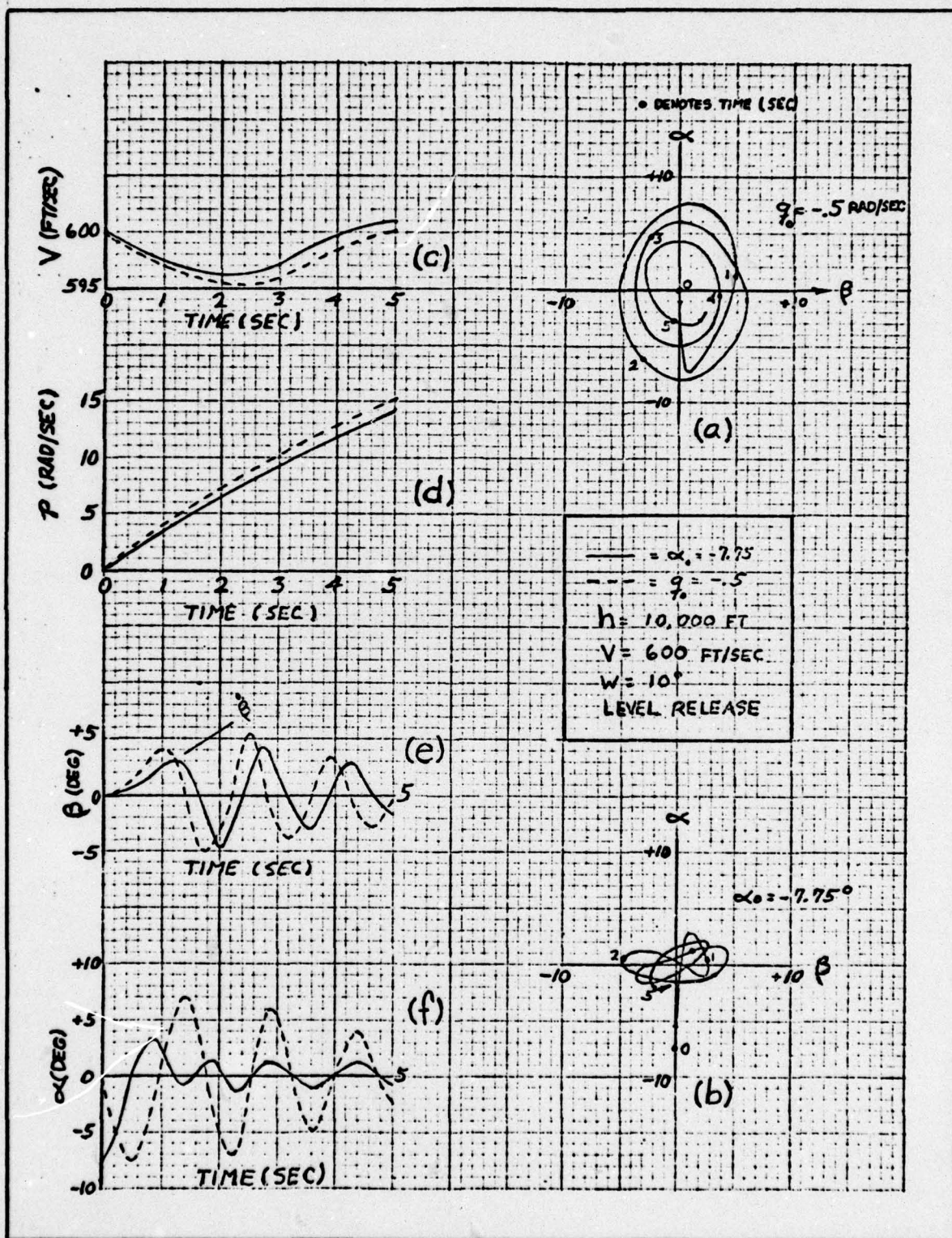


Fig. 13. Projectile Nose Track After Release

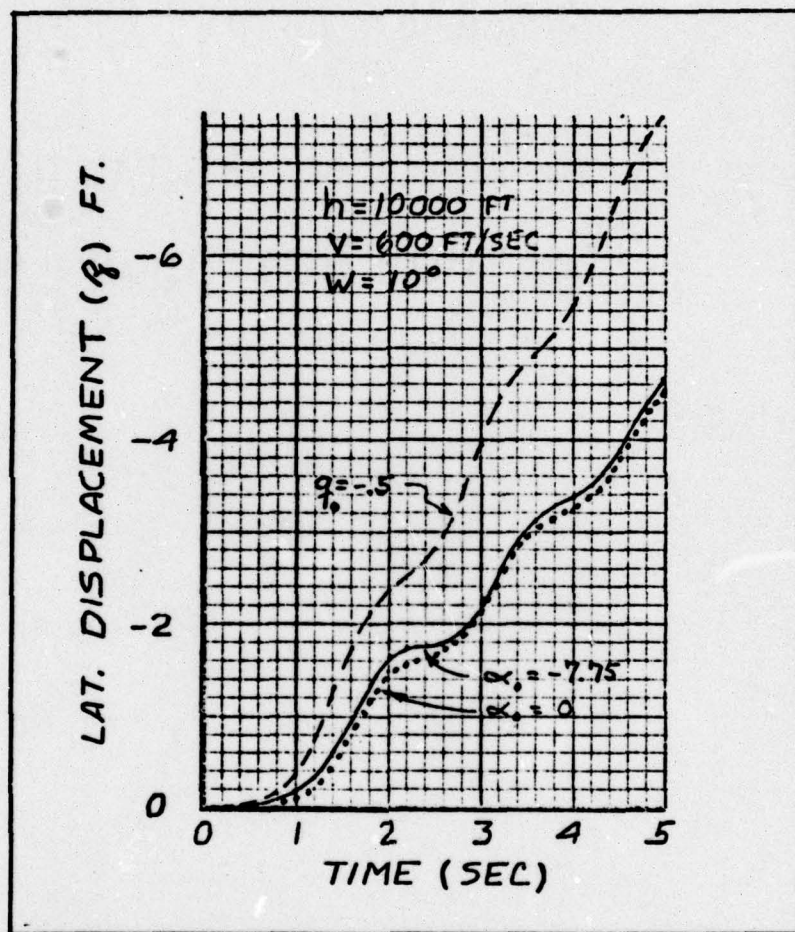


Fig. 14. Initial Rate of Lateral Displacement



$\alpha = -7.75^\circ$  initial condition is approximately 1 ft/sec; for  $q = -.5$  rad/sec, the slope is close to 1.5 ft/sec. These values of slope are significantly different and can be modeled as an initial lateral velocity of the projectile at release. The initial lateral velocity,  $v_0$ , can be input into the simulation to determine its effect. Fig. 15 shows the lateral progression of the trajectories resulting from an initial side velocity of -5, 0, +5 ft/sec. The remaining initial release conditions were the same for all three trajectories. As the plots show, the magnitude of  $v_0$  directly influences the overall trajectory. An equation for this lateral initial velocity is given by (Ref 1:53-68):

$$v_z = -\left(\frac{C_{Z_a} A q}{M}\right)\left(\frac{T}{1 - \omega^2 T^2}\right)(2\beta + T\dot{\beta}) \quad (24)$$

where  $C_{Z_a}$  = the normal force coefficient (acting in plane containing the relative wind).

$A$  = frontal area of the projectile.

$q$  = dynamic pressure.

$M$  = mass

$T$  = time constant for oscillation damping.

$\omega$  = frequency of oscillation.

$\beta$  = yaw angle of attack.

$\dot{\beta}$  = yaw rate.

If the influence of the displacement term is considered small with respect to the rate term, the expression reduces to:

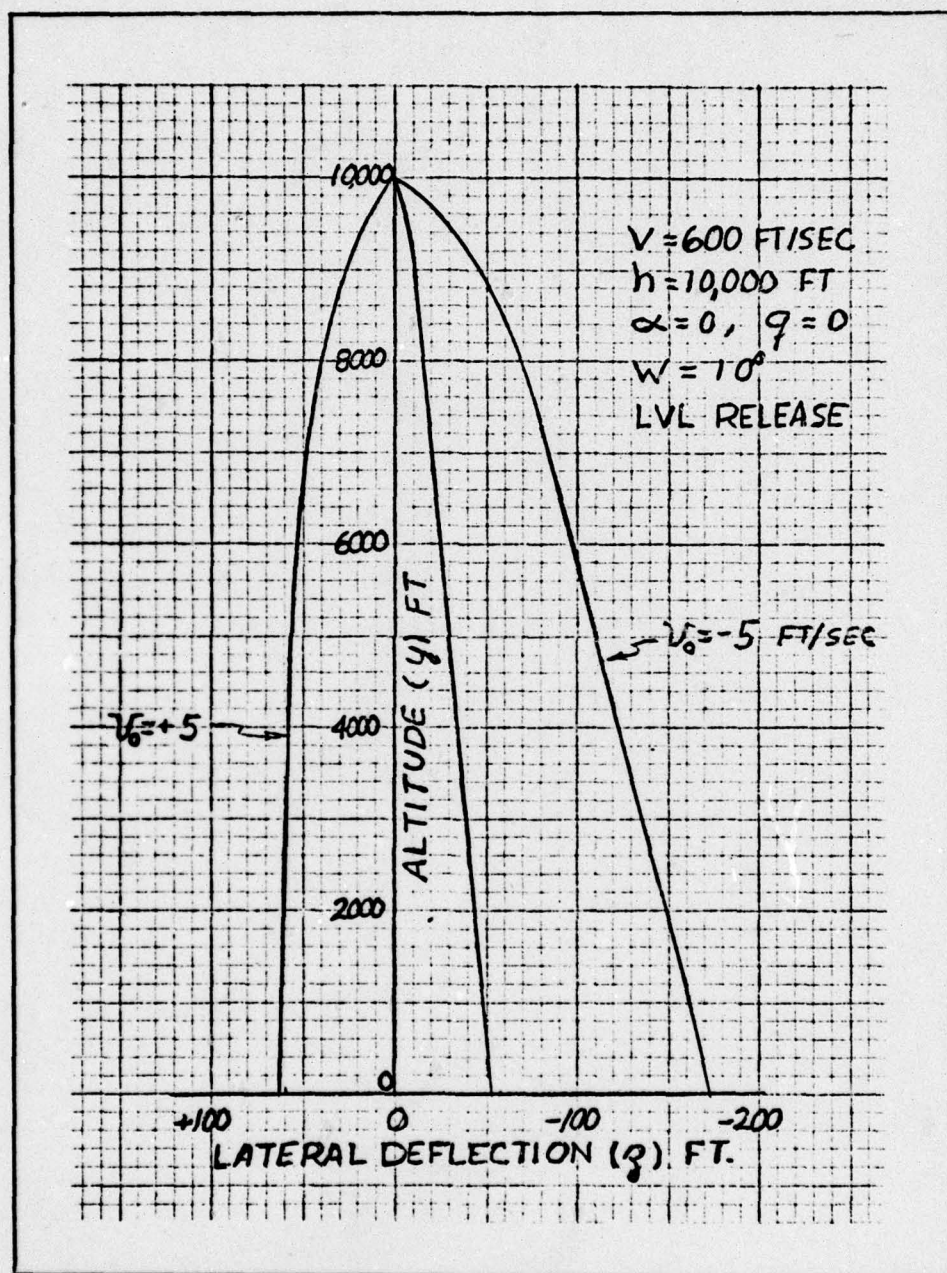


Fig. 15. Effect of Initial Side Velocity on Lateral Progression



$$V_z = - \frac{C_{Z\alpha}}{C_{M\alpha}} \frac{I}{M d} \quad (25)$$

where  $C_{M\alpha}$  = moment coefficient (with respect to total angle of attack).

$I$  = transverse moment of inertia.

$d$  = max diameter of projectile.

and the following relation has been used:

$$\frac{T^2}{1 + \omega^2 T^2} = \frac{I}{C_{M\alpha} \Lambda q d} \quad (26)$$

Equation 25 shows that the lateral velocity induced by oscillation of the projectile is sensitive to the normal force coefficient  $C_Z$ , the moment coefficient  $C_M$ , and the yaw rate  $\dot{\beta}$ .

The magnitude of the side velocity predicted by this closed form approximation is given by (Ref 1:65)

$$V_z = \frac{\dot{\beta}}{\omega} (.362) \text{ ft/sec/degree} \quad (27)$$

where the constant, 0.362, is the result of equation 24 (displacement term neglected) using a velocity of 750 ft/sec, an altitude of 5000 ft, and coefficients of a projectile similar to that in this investigation (coefficients used in this derivation are determined with respect to the total angle of attack instead of  $\text{pd}/2V$ ). These same initial conditions were used in a six degree of freedom simulation and the lateral displacement and yaw oscillations were plotted in Fig. 16. From these plots, a representative yaw rate and frequency of oscillation were

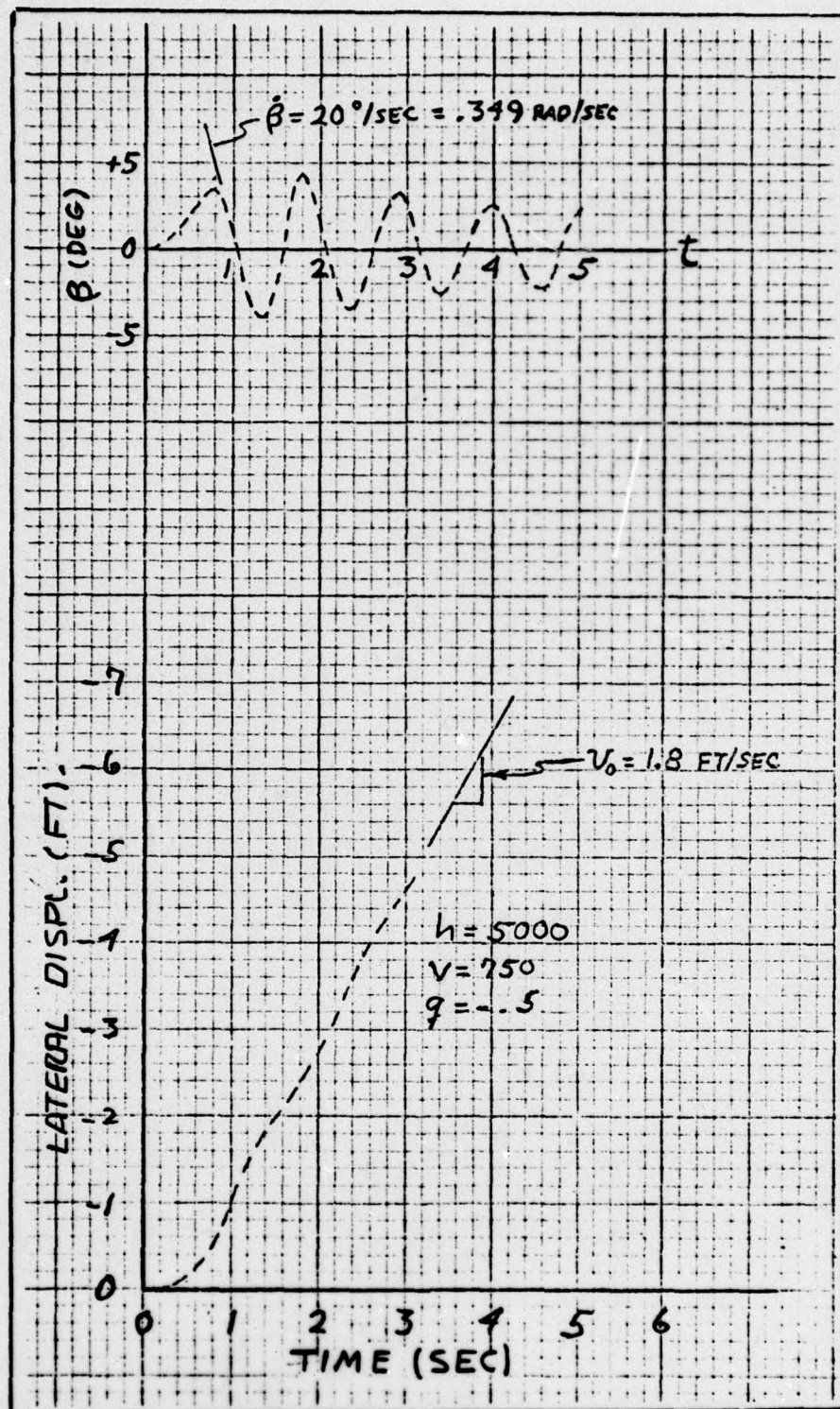


Fig. 16. Lateral Displacement and Yaw Oscillations



estimated as 0.349 radians/sec and 5.34 radians/sec respectively. The closed form approximation (Eqn 27) then produces a value of  $V_z = 1.36$  feet per second.

The plot of lateral displacement versus time indicates the initial lateral velocity, according to the simulation, is approximately 1.8 feet per second. This is on the order of 25% difference between the six degree of freedom simulation results and the closed form expression. This difference can be attributed to the more extensive simplifying assumptions used to make the closed form expression possible.

#### Effect of Spin Rate

The effect of spin rate induced by various wedge angles is investigated at different airspeeds and release perturbations (Table VII). The spin rate, induced by the wedge angle of fifteen degrees, produces the most nominally linear lateral deviation throughout the entire trajectory. This pattern holds for both velocities investigated (Fig 17).

Table VII also reveals that increasing the spin rate of the projectile causes the trajectory to impact longer and wider. This apparent contradiction to the principle of conservation of energy was initially thought to be an error caused by using an integration step size that was too large. A step size of .002 second, however, is adequate for the spin rates encountered.

Another possible explanation is that the projectile developed gyroscopic rigidity and was starting to fly at a net angle of attack rather than averaging to zero angle of attack in its oscillations. This concept is supported by the simulation readout which shows the angle of attack of the projectile with a five degree wedge angle oscillates on the

TABLE VII  
Effect of Spin Rate

Alt = 10,000 ft, level flt release, all coefficients included.

Wedge	V = 600 $\alpha = 0$ q = 0					V = 600 $\alpha = -10$ q = 0				
	X	Z	V <sub>f</sub>	P <sub>f</sub>	t <sub>f</sub>	X	Z	V <sub>f</sub>	P <sub>f</sub>	t <sub>f</sub>
5°	14159	-37.4	888.5	31.4	25.72	14165	-38.9	888.6	31.4	25.70
10°	14165	-57.7	889.1	62.9	25.72	14174	-59.1	889.2	62.9	25.71
15°	14185	-65.6	889.4	94.4	25.73	14199	-66.1	889.6	94.4	25.72
	V = 1000 $\alpha = 0$ q = 0					V = 1000 $\alpha = -10$ q = 0				
	X	Z	V <sub>f</sub>	P <sub>f</sub>	t <sub>f</sub>	X	Z	V <sub>f</sub>	P <sub>f</sub>	t <sub>f</sub>
5°	22668	-30.7	1029.6	38.0	26.11	22669	-41.1	1029.3	38.3	26.10
10°	22716	-79.7	1030.3	76.1	26.13	22718	-79.6	1030.5	76.1	26.12
15°	22746	-87.2	1030.6	114.2	26.14	22738	-93.2	1030.7	114.1	26.13

X = Range (ft)

Z = Lat displacement (ft/sec)

P<sub>f</sub> = Impact spin rate (rad/sec)

t<sub>f</sub> = Time to impact



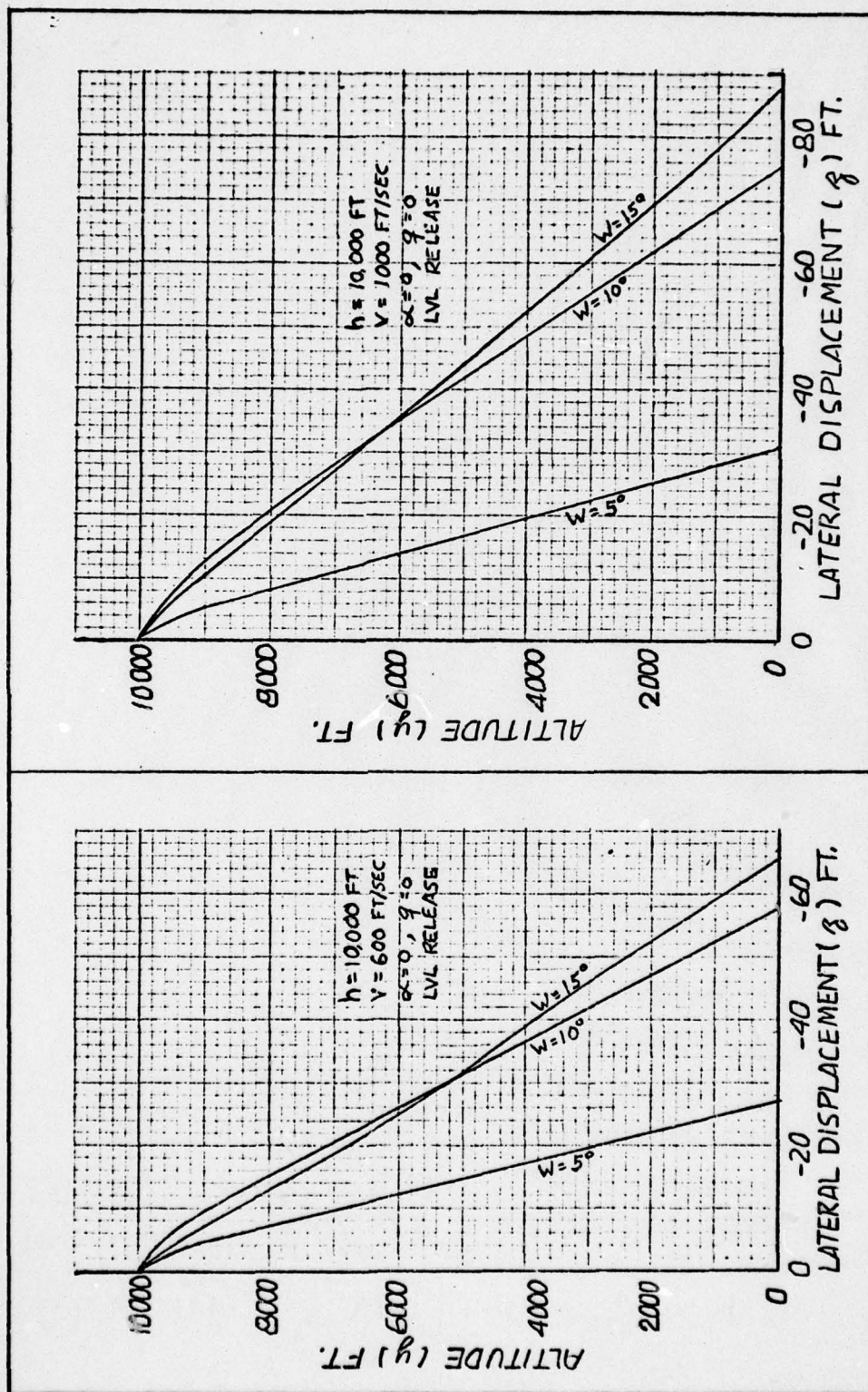


Fig. 17. Effect of Spin Rate on Lateral Displacement

order of  $\pm 0.1$  degree in the latter half of the trajectory. The fifteen degree wedge readout, however, shows only about half the magnitude of oscillation but the oscillations are predominantly positive in the last half of the trajectory. In fact, the angle of attack does not go negative at all during the final ten seconds of flight. Also, Table VII indicates the total time of flight of the projectile spinning at the faster rates is increased very slightly (on the order of 0.02 second). The downrange velocity just prior to impact is approximately 750 ft/sec which produces an opportunity for the projectile to impact 15 feet longer in the extra 0.02 second. This is compatible with the data shown in Table VII.

#### Other Observations

Fig. 18 shows the aerodynamic coefficients,  $C_{y7}$ ,  $C_{yp}$  &  $C_{np}$ , have no discernable effect on the projectile velocity. The velocity progression graphs remained the same regardless of whether or not these coefficients were included in the simulation.

The wedge angle did not change the velocity progression significantly. Simulations modeling spin rates as 5, 10, or  $15^\circ$  wedge angle indicates the velocity progression is not influenced by spin rate. This observation is subject to the projectile spin rate remaining low enough to preclude instability.

The higher dynamic pressure encountered during release at high airspeeds causes a significantly greater velocity change of the projectile after release. The magnitude of the difference in the release and steady state velocity of the projectile governs how the velocity will progress throughout the trajectory. The projectile shows significant velocity change throughout the trajectory when released from a low speed condition.



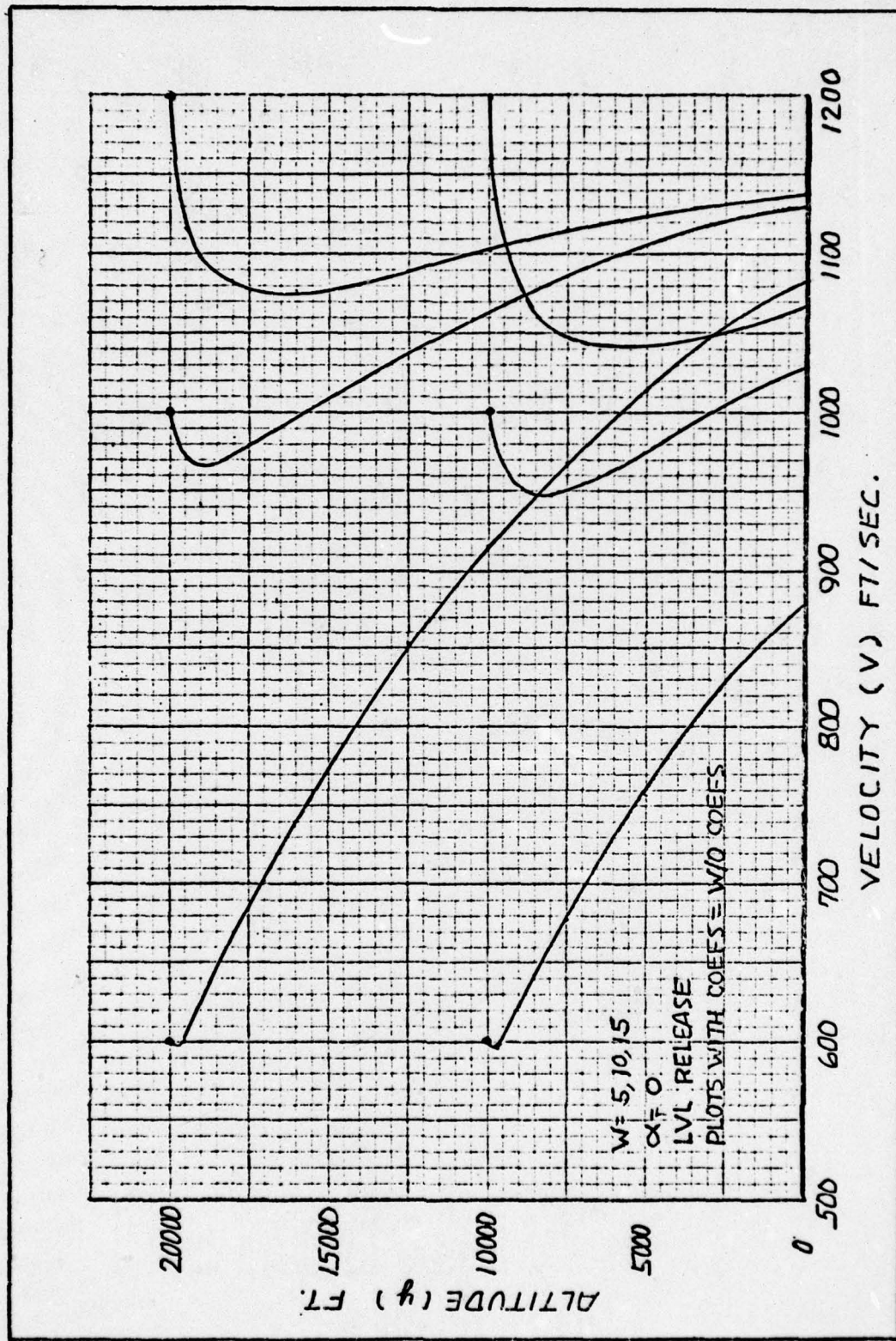


Fig. 18. Effect of Release Velocity and Altitude on Velocity Progression

The projectile shows much less acceleration when released from a high dynamic pressure condition.

Figure 19 investigates projectile acceleration from release to impact. The slope of the velocity vs time curve shows that maximum deceleration is proportional to the drag force encountered at release and, as a result, velocity loss is greater at high release velocities. The time required for transition from deceleration to acceleration also increases with higher release velocities. The same plots apply for each of the projectile fin wedge angles investigated. Also, there are no significant changes in the graphs for an initial angle of attack of  $\alpha_0 = 0$  versus  $\alpha_0 = -10$ .

Fig. 20 shows the lateral displacement progression of a projectile subjected to two different release perturbations ( $\alpha_0 = -10^\circ$  and  $q_0 = -.5$  rad/sec) at two different release velocities. The slope of a pair of the curves is nearly identical at any given time but the magnitude of the lateral displacement attained in the same given time can be significantly different at the lower airspeed.

Fig. 21 shows that the rate of altitude loss does not change significantly with initial release airspeeds. For the 10,000 ft drop, time of flight through a standard atmosphere is increased on the order of one second compared to the time of flight through a vacuum.

The effect of release velocity and altitude is shown as a composite in Fig. 22. The set of trajectories initiated at 10,000 ft is essentially a duplication of Fig. 11 and is included with the 20,000 ft set to give an indication of the effect of air density on the lateral deflection.



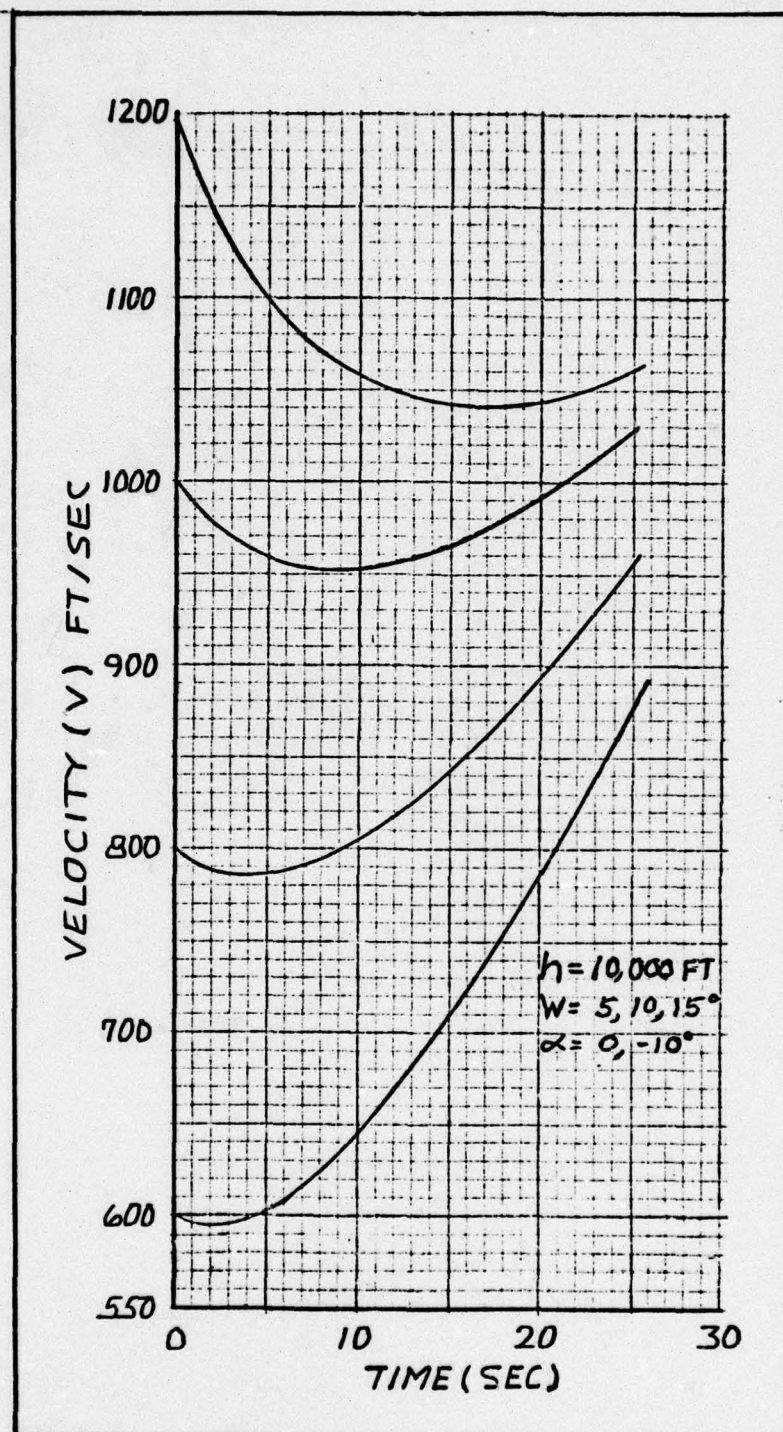


Fig. 19. Effect of Release Velocity on Total Projectile Acceleration

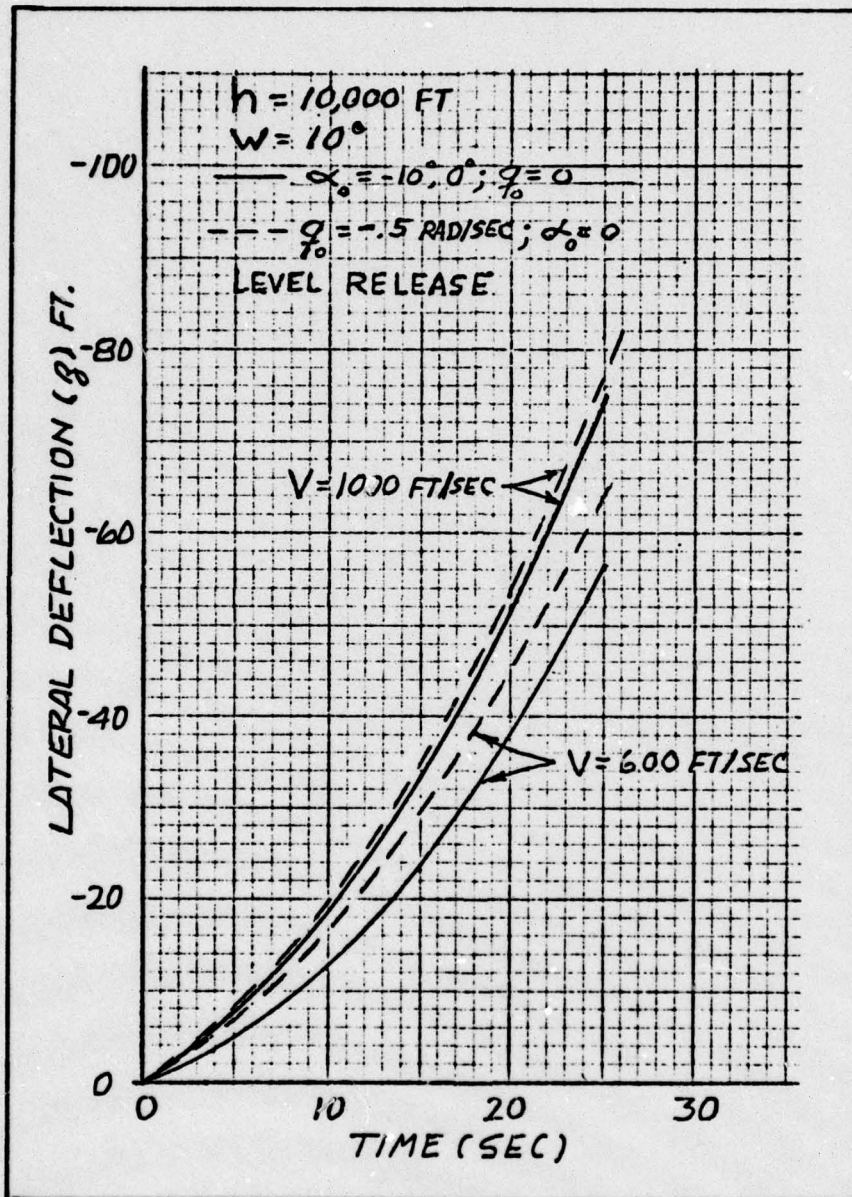


Fig. 20. Effect of Initial Pitch Motion on Lateral Deflection



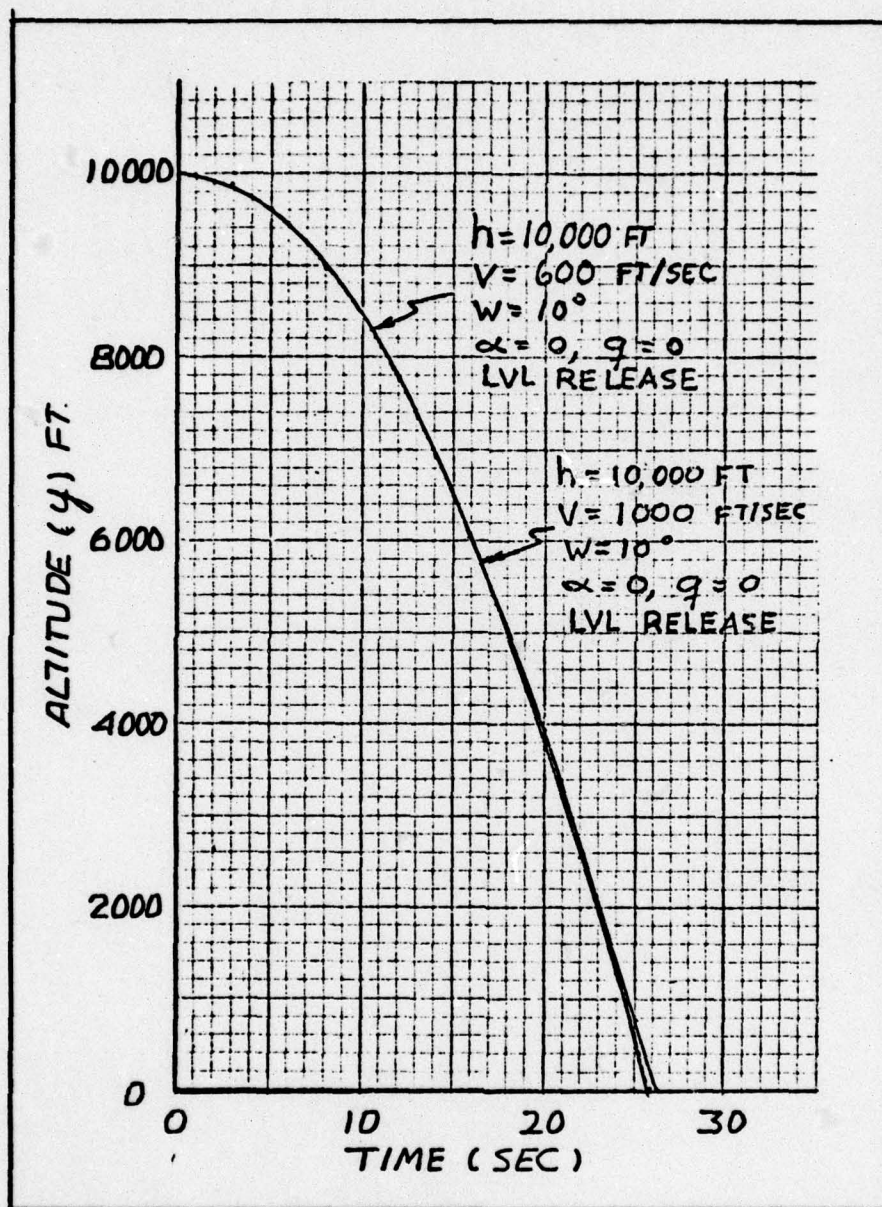


Fig. 21. Effect of Release Velocity on Altitude Progression

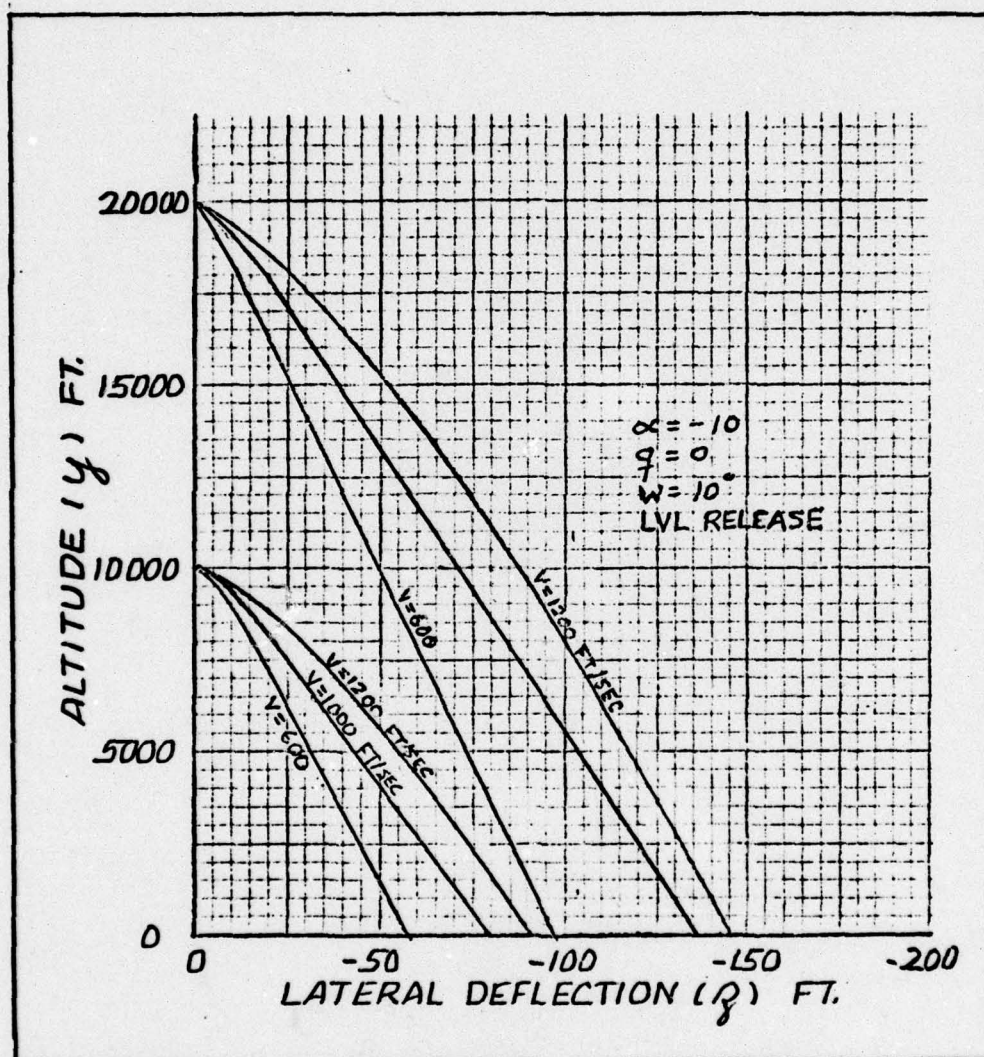


Fig. 22. Effect of Release Velocity and Altitude on Lateral Displacement



## V. Conclusions

The Magnus force, Magnus moment, and side force coefficients, for a projectile of the type modeled in the simulations, and for normal release conditions, exert only a very small influence on the impact point. The cross range displacement attributable to these coefficients, for a trajectory initiated at 10,000 feet, are on the order of only a few feet. The influence on the downrange component of the trajectory is also very small. These coefficients could be influential under conditions of high angle of attack and high spin rates which, for normal releases, are not present simultaneously. When the projectile oscillation and the corresponding angle of attack is maximum following release, the spin rate has not yet developed. As the projectile progresses along the trajectory, the spin rate builds up but the oscillations dampen to a very small value. Also, the oscillations alternate about the velocity vector of the center of gravity of the projectile so the Magnus force direction, being dependent on the direction of the angle of attack, also alternates and tends to average to zero effect.

The lateral displacement of the trajectory is, in general, increased with increasing spin rate. Insufficient spin rate can be a stability factor as can excessive spin rate. Low values of angular momentum can allow the projectile to develop catastrophic yaw. High spin rates induce gyroscopic resistance to change in projectile orientation, allowing a positive angle of attack to build up as the trajectory progresses. A net lift is then developed which increases the time of flight of the projectile and, consequently, the cross range and downrange impact point.

A projectile released at zero angle of attack with no initial per-

turbations produces the least lateral displacement of the trajectory. If the projectile is released with an initial negative angle of attack, the lateral progression is increased only slightly. If the projectile is released with a rate rotational motion, as could be induced by the ejector mechanism or an initial positive angle of attack, the lateral progression is significantly increased. This increase is directly proportional to the amplitude of the projectile oscillations. The difference in lateral progression between the rate induced and displacement induced oscillation is less at higher airspeeds. Also, as oscillations increase the cross range impact point of the trajectory, there is, in general, a corresponding decrease in the downrange impact point. These results suggest the following conclusions:

1. Magnus force, as such, exerts no significant influence on the trajectory of a projectile such as the Mk-82 bomb. For most release airspeeds and altitudes, compensation for this specific effect in a weapons delivery system would not be cost effective.
2. The projectile should be designed to spin as slow as possible consistent with stability considerations.
3. Release mechanisms should be designed so no significant moment is applied. If assisted separation of the projectile from the delivery aircraft is desired, a slight negative angle of attack should be used instead of a moment.



Bibliography

1. Ausman, J.S. Theoretical Analysis and Experimental Measurements of Separation Disturbances in Weapon Delivery Systems. Aircraft/Stores Computability Symposium Proceedings, JTGG/MD WP No. 12:53-85 (September, 1975).
2. Cohen, C.J. and D. Werner. A Formulation of the Equations of Motion of a Four-Finned Missile. Defense Documentation Center Reference AD112006, September 1956.
3. Daniels, P. Minimization of Lock-In Roll Moment on Missiles via Slots. Defense Documentation Center Reference AD010130, January 1975.
4. Etkin, B. Dynamics of Flight. New York: John Wiley and Sons, Inc., 1959.
5. Ingram, C.W. A Computer Program for Integrating the Six Degree of Freedom Equations of Motion of a Symmetrical Missile. Unpublished notes, Aerospace Department, University of Notre Dame.
6. Likins, P.W. Elements of Engineering Mechanics. New York: McGraw-Hill Book Company, 1973.
7. Meirovitch, L. Methods of Analytical Dynamics. New York: McGraw-Hill Book Company, 1970.
8. Miklos, W. Analysis of the Stability and Flight Performance of the Candidate Replacement for the MK-82 Snakeye Bomb. Air Force Flight Dynamics Laboratory Report Number AFFDL-TR-77-108, June 1976.
9. Murphy, C.H. Free Flight Motion of Symmetric Missiles. Defense Documentation Center Reference AD442757, July 1963.
10. Naveh, B.Z.N. Untitled, unpublished notes, Aerospace Department, University of Notre Dame, 1974.
11. Nicolaides, J.D. Missile Flight and Astrodynamics. Defense Documentation Center Reference AD287400.
12. Vaughn, H.R. A Detailed Development of the Tricycle Theory. Sandia Laboratory Report SC-M-67-2933, February 1968.
13. Whittaker, E.T. A Treatise on the Analytical Dynamics of Particles and Rigid Bodies. Dover Publications, 1944.
14. Air Force Armament Laboratory Report. AFATL MK 82/84 Air Inflatable Retarder (Magnus Phase) in the Aerodynamic Wind Tunnel (4T) Off-Line Data, parts 6 through 153. F41C-86A, TC387 Arnold Air Force Station, Tennessee. (July 1975).

## Appendix A

Typical Wind Tunnel Data

The aerodynamic coefficients for a specific projectile model are normally obtained from wind tunnel tabulated data. Table A-I shows the spin-up data of a projectile model at a specific Mach and angle of attack. The data measurements were made as the projectile was progressively accelerated from a zero roll rate to the steady state spin rate ( $P_{ss}$ ). Table A-II shows the spin-down data taken as the projectile was progressively decelerated from a high spin rate down to  $P_{ss}$ . Both of these figures were obtained from reference 11, part 31.



TABLE A-1  
Spin-up Data

[illegible]

TABLE A-II

56



## Appendix B

Computer Program Data InputsCoefficient Arrays

A single 000005 card precedes all of the coefficient matrix input decks. This card designates the total number of aerodynamic coefficient arrays used in the program and must match the actual number of arrays that have been input. The last digit of the array designator integer must be in column 12. For example, if ten coefficients are used, the lead card is:

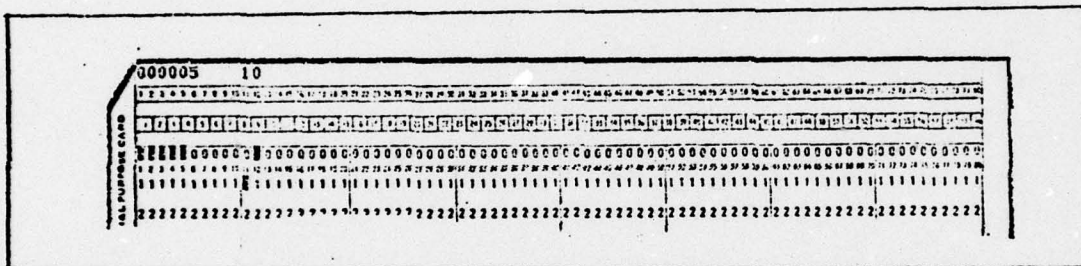


Fig. B-1a. Computer Input Card

Each individual coefficient array is then preceded by a card that specifies the desired coefficient symbol, the location of the array within the input deck in accordance with Table B-I, and the number of angle of attack columns and Mach number rows that will make up the array. A 20x20 matrix is the maximum size of the input array.

The first four spaces on the card shown in Fig. B-1b are available for the desired coefficient symbol. The last digit of the remaining three integers must lie on space 7, 9, and 11.





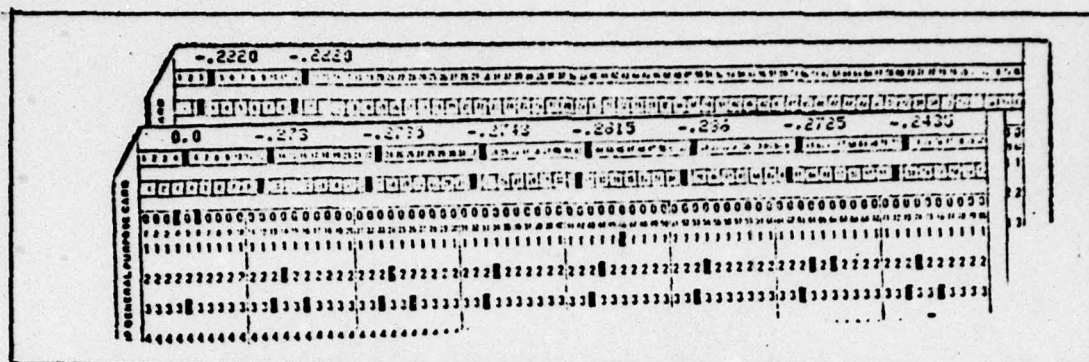


Fig. B-1d. Computer Input Card

The specific values of each element may be punched anywhere within successive ten-block segments of the card.

The remaining values of each element in the coefficient array are similarly entered until the matrix is complete (See Appendix G).

Each individual aerodynamic coefficient array used in the program is input in a similar manner. The sequence of these completed arrays must be in the order indicated in Table B-I. Only the desired aerodynamic coefficients need be input; zero entries are not required. The program will accept a maximum of thirty coefficient arrays.

#### Initial Conditions

The initial condition input deck is preceded with the desired title card. This title will appear as the heading of the computer output.

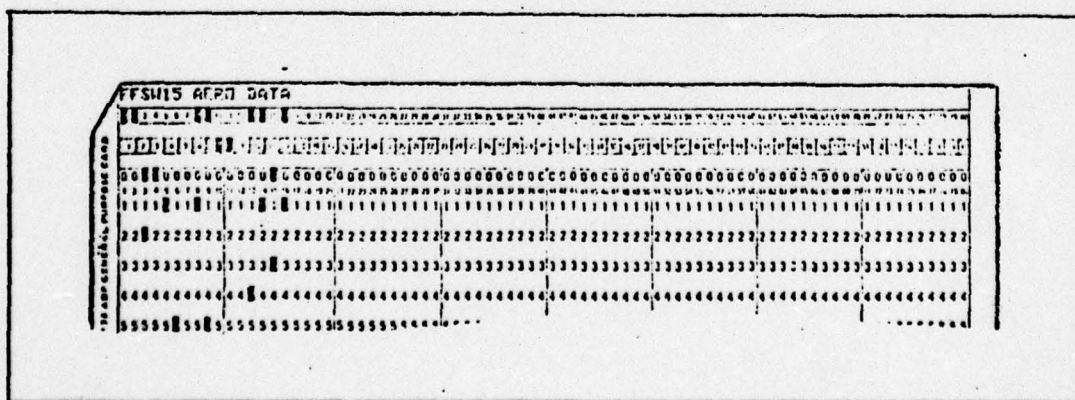


Fig. B-1e. Computer Input Card

The next card (Fig B-1f) identifies which of the option parameters available in the program are to be used. These parameters are (Ref 5:23):

NORC: Gravity designator

NORC=1 denotes constant gravity used.

NORC=0 denotes variable gravity will be input.

IPRN: Output time increment control

IPRN x  $\Delta t$  = output increment that will be printed.  $\Delta t$  is the A(20) value (Table B-2II).

NALL  $\equiv$  1 for this program.

IPUN: Punch option for angle of attack ( $\alpha$ ) and sideslip ( $\beta$ ) data

IPUN=1 implements the option.

IPUN=0 option is not used.

NBODY: Reference frame output designator

NBODY=1 output prints and/or punches  $\alpha$  &  $\beta$  in body axes.

NBODY=0 output prints and/or punches  $\alpha$  &  $\beta$  aeroballistic axes.

ISCALE: Coefficient scaling option.

ISCALE=1 implements option

ISCALE=0 option is not used

ITRST: Thrust option

ITRST=1 implements thrust equation into program (See Ref 5: 11, 12)

ITRST=0 for unpowered projectile

The last digit of these integers must fall on every tenth space.



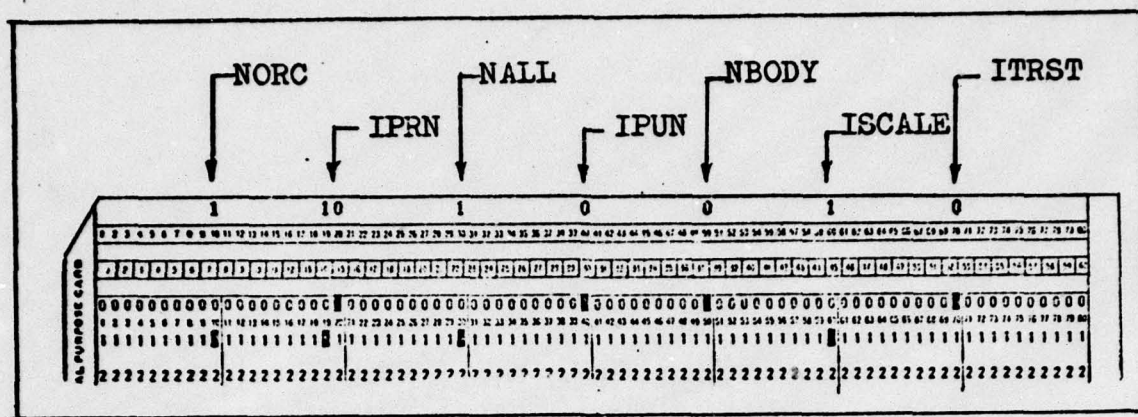


Fig. B-1f. Computer Input Card

The next three cards specify the desired initial conditions and projectile mass parameters in the sequence outlined by Table B-2II. All values are entered anywhere within successive ten-space segments.

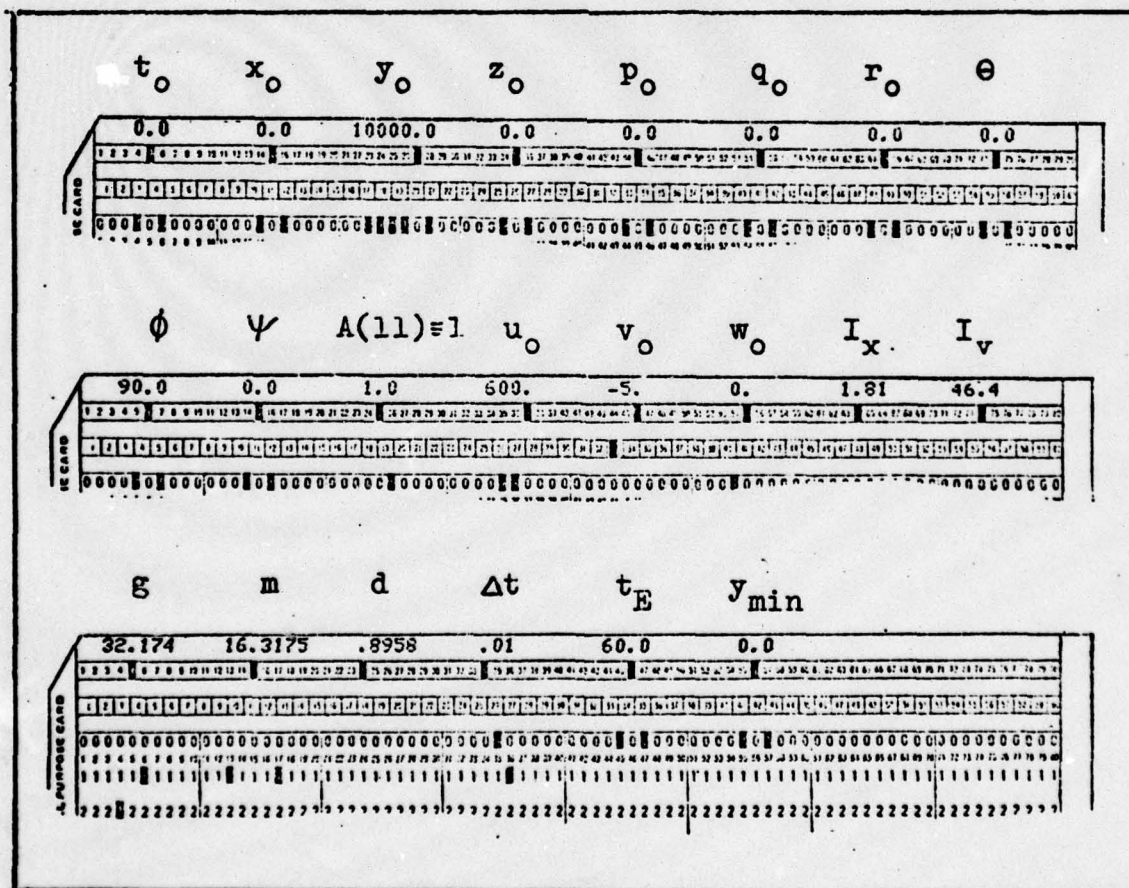


Fig. B-1g. Computer Input Cards

The units of the initial conditions are:

$t_0, \Delta t, t_E$	Sec
$x_0, y_0, z_0, d, y_{\min}$	Ft
$p_0, q_0, r_0$	Rad/Sec
$\theta, \phi, \psi$	Degrees
$u_0, v_0, w_0$	Ft/Sec
$I_x, I_y$	Lb-Ft-Sec <sup>2</sup>
$g$	Ft/Sec <sup>2</sup>
$m$	Slugs

The initial values of  $\theta$  and  $\alpha$  (which is input implicitly) as well as  $u_0$  &  $w_0$  are determined according to the following scheme:

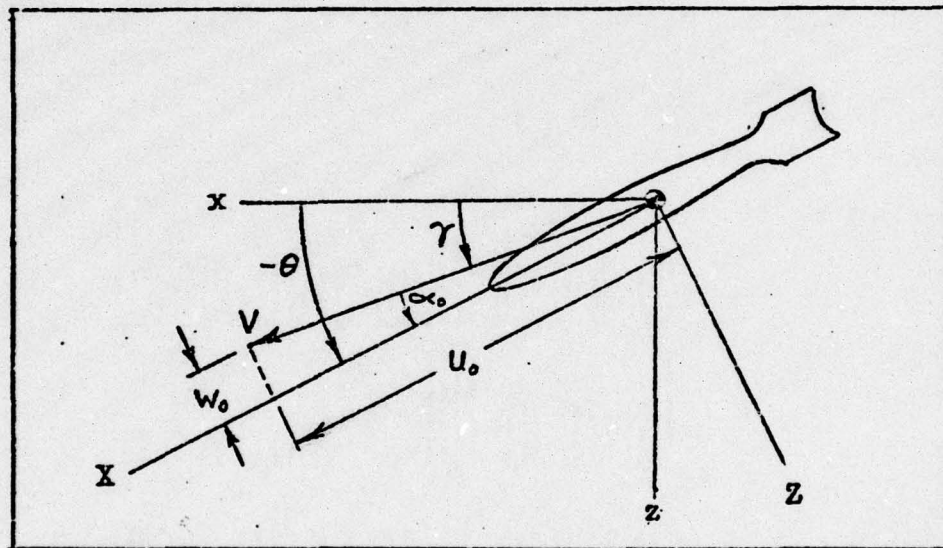


Fig. B-2. Flight Path/Perturbation Angle Input

where

$V$  = velocity vector of the center of gravity of the projectile.

$\theta$  = total angle between the body fixed and inertial frame.

$\gamma$  = flight path angle = angle between the inertial frame and velocity vector  $V$ .

$\alpha_0$  = initial perturbation angle from the initial flight path angle.

$w_0 = V \sin \alpha_0$  = projection of the velocity vector on the body  $Z$  axis.

$u_0 = V \cos \alpha_0$  = projection of the velocity vector on the body  $X$  axis.



For a projectile in a  $30^\circ$  initial dive angle at 800 ft/sec subjected to a  $5^\circ$  initial perturbation upon release, with no out-of-plane components, the following values would be input:

$$\begin{aligned}\theta &= -35.0, \phi = 90.0, \psi = 0.0 \\ u_0 &= 800 \cos 10^\circ = 787.846 \\ v_0 &= 0.0 \\ w_0 &= -800 \sin 10^\circ = -138.918\end{aligned}$$

Note:  $\theta \equiv 90^\circ$  to align the inertial frame with the body fixed frame (See Fig 1).

#### Scale Factors

The remaining four cards are for scale factors (applicable only if ISCALE was previously designated as 1). The scale factor changes the corresponding coefficient of Table B-I by the multiple of the scaling factor.

The only scaling factor used in this study was  $C_f(\delta w)$ .  $C_f(\delta w)$  is the coefficient for roll due to fin wedge angle. To scale the 15 degree wedge angle values of the coefficient array to, say, 10 degrees; the value .6666 is the appropriate scaling factor to enter in the ninth block of the scaling cards (Fig B-3).

The integer 1.0 is the required entry when no scaling of the corresponding coefficient array is desired.

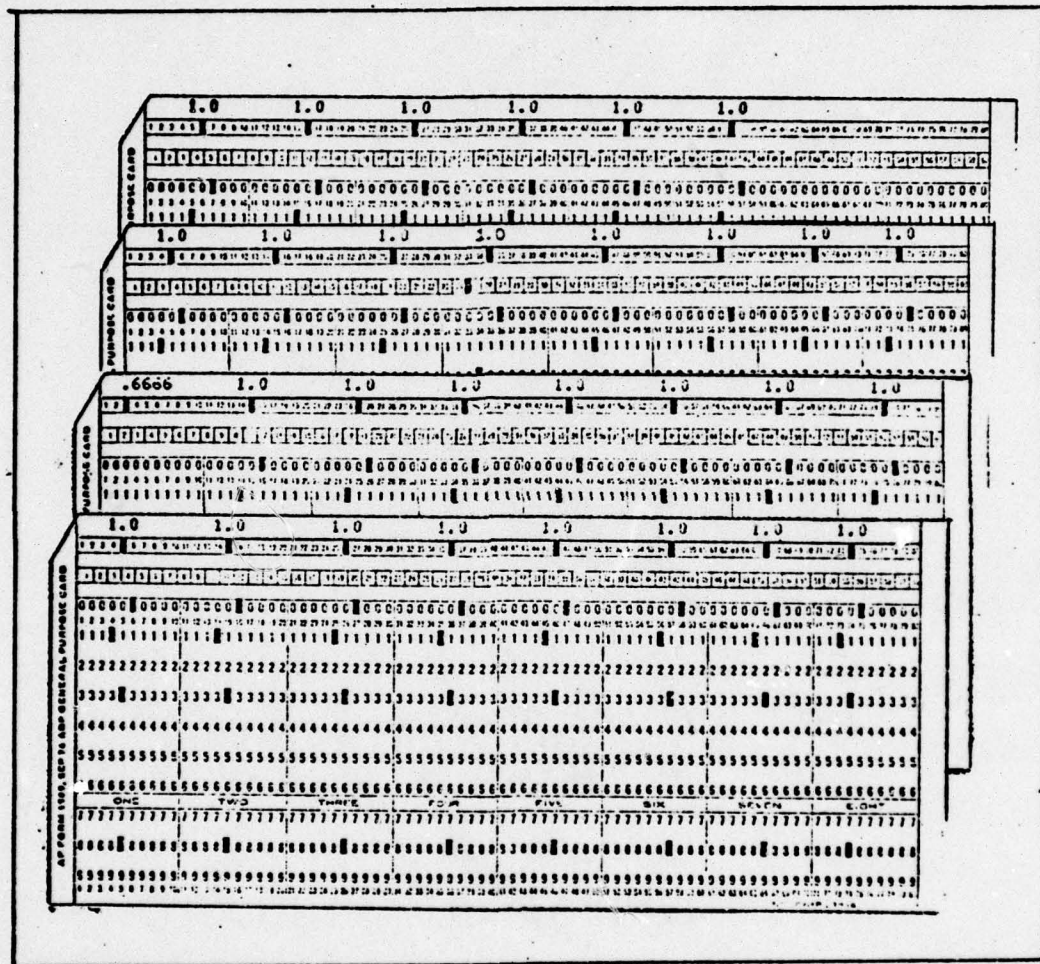


Fig. B-3. Scale Factor Inputs C(1) thru C(30)



TABLE B-I

Aerodynamic Coefficient Array  
(Adapted from Ref 5)

$C(I, J, K)$  Aerodynamic coefficient array

where: I Mach number array

J Angle of attack array

K Location of aerodynamic coefficient

$C(I, J, 1)$	$C_x$	$C(I, J, 2)$	$C_{y_0}$
$C(I, J, 3)$	$C_{y_7}$	$C(I, J, 4)$	$C_{y_8}$
$C(I, J, 5)$	$C_{yp}$	$C(I, J, 6)$	$C_{z_0}$
$C(I, J, 7)$	$C_{z_7}$	$C(I, J, 8)$	$C_{z_8}$
$C(I, J, 9)$	$C_{l_7}(\delta w)$	$C(I, J, 10)$	$C_{l_7}$
$C(I, J, 11)$	$C_{l_8}$	$C(I, J, 12)$	$C_{l_p}$
$C(I, J, 13)$	$C_{m_0}$	$C(I, J, 14)$	$C_{m_7}$
$C(I, J, 15)$	$C_{m_8}$	$C(I, J, 16)$	$C_{n_0}$
$C(I, J, 17)$	$C_{n_7}$	$C(I, J, 18)$	$C_{n_8}$
$C(I, J, 19)$	$C_{n_p}$	$C(I, J, 20)$	$C_{m_\epsilon}$
$C(I, J, 21)$	$C_{n_\epsilon}$	$C(I, J, 22)$	$C_{y_\epsilon}$
$C(I, J, 23)$	$C_{z_\epsilon}$	$C(I, J, 24)$	$C_{l_\epsilon \alpha_p}$
$C(I, J, 25)$	$C_{l_\epsilon \alpha_1}$	$C(I, J, 26)$	$C_{l_\epsilon \alpha_2}$
$C(I, J, 27)$	$C_{mq_0}$	$C(I, J, 28)$	$C_{mq_7}$
$C(I, J, 29)$	$C_{mq_8}$	$C(I, J, 30)$	$C_{l_0}$

TABLE B-II

Computer Input Array  
(Adapted from Ref 5)

A(1)	$t_o$	A(12)	$u_o$
A(2)	$x_o$	A(13)	$v_o$
A(3)	$y_o$	A(14)	$w_o$
A(4)	$z_o$	A(15)	$L_x$
A(5)	$p_o$	A(16)	$L_y$
A(6)	$q_o$	A(17)	$g$
A(7)	$r_o$	A(18)	$m$
A(8)	$\theta$	A(19)	$d$
A(9)	$\phi$	A(20)	$\Delta t$
A(10)	$\psi$	A(21)	$t_E$
A(11)	1.0	A(22)	$y_{min}$



## Appendix C

Computer Output Example

The computer output parameters are shown in Table C-I.

TIME is measured from release.

RANGE, ALT, Z correspond to x, y, z of the inertial reference frame.

V = total velocity of the projectile with respect to the air mass.

p = spin rate.

$\overline{\text{ALPHA}} = \sqrt{\alpha^2 + \beta^2}$  (where --- denotes vector).

M = mach number.

PHI = roll angle.

ALPHA = angle of attack.

BETA = yaw angle.

The next set of parameters are useful for stability analysis applications. The outputs are based on linearized equations for the tricyclic response of a projectile to an initial disturbance (Ref 12, 8 or 11):

L-N =  $\lambda_n$  = damping factor for nutation mode.

L-P =  $\lambda_p$  = damping factor for precession mode.

W-N =  $\omega_n$  = nutation frequency.

W-P =  $\omega_p$  = precession frequency.

S = s = stability factor.

TAU =  $\tau$  = dynamic weight factor.

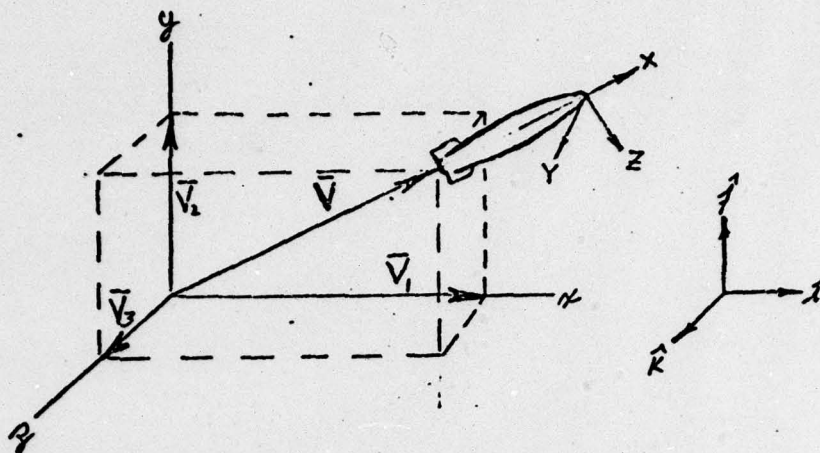
K-T =  $K_t$  = trim arm.

TABLE C-I  
Sample Computer Readout

FFSW15 AERO DATA																	PAGE 1	
TIME SEC	RANGE FEET	ALT FEET	Z FEET	V FT/SEC	P RA/SEC	--- ALPHA DEG	H	PHI DEG	ALPHA DEG	BETA DEG	L-N 1/SEC	L-P 1/SEC	M-N RA/SEC	M-P RA/SEC	S	TAU	K-T DEG	
0.1000	0.00	10000.00	0.00	500.02	0.0	.48	.56	90.00	.00	.44	0.00	0.00	0.0	0.0	0.000	0.00	0.000	
.1001	92.09	9999.84	.50	500.50	.4	.46	.55	73.51	.14	.44	-.22	-.22	4.0	4.0	-.000	-.000	-.00-22.744	
.2000	170.43	9999.36	.99	500.37	.7	.34	.56	104.96	-.07	.74	-.22	-.22	4.0	4.0	-.000	-.000	-.00-22.121	
.3000	249.85	9998.35	1.43	500.07	1.0	.50	.56	167.97	-.55	.21	-.22	-.22	4.0	4.0	-.000	-.000	-.01-2.203	
.4000	329.73	9997.42	1.97	500.79	1.6	1.25	.56	190.57	-1.75	.12	-.22	-.22	4.0	4.0	-.000	-.000	-.01-2.327	
.5000	409.73	9996.96	2.46	500.52	2.1	2.01	.56	201.95	-2.01	.10	-.22	-.23	4.0	4.0	-.000	-.000	-.01-2.500	
.6000	489.74	9996.16	2.96	500.27	2.4	2.71	.56	211.11	-2.71	.22	-.23	-.23	4.0	4.0	-.000	-.000	-.01-2.779	
.7000	569.16	9995.01	3.42	500.03	2.8	3.23	.56	219.72	-3.19	.51	-.23	-.23	4.0	4.0	-.000	-.000	-.01-3.185	
.8000	648.39	9993.51	3.90	500.80	3.1	3.49	.55	227.74	-3.36	.96	-.23	-.23	4.1	4.1	-.000	-.000	-.01-3.744	
.9000	727.59	9991.57	4.30	500.59	3.4	3.47	.55	234.47	-3.12	1.53	-.23	-.23	4.1	4.1	-.000	-.000	-.02-4.223	
1.0000	806.26	9989.49	4.62	500.40	3.7	3.25	.55	239.08	-2.45	2.13	-.23	-.23	4.1	4.1	-.000	-.000	-.02-4.761	
1.1000	884.48	9987.04	5.25	500.23	4.0	3.02	.55	236.52	-1.37	2.67	-.23	-.23	4.1	4.1	-.000	-.000	-.02-5.251	
1.2000	962.27	9984.07	5.56	500.09	4.3	3.47	.55	230.61	.03	3.02	-.23	-.23	4.1	4.1	-.001	-.001	-.02-5.774	
1.3000	1039.02	9980.79	6.05	500.95	4.6	4.19	.55	227.03	1.62	3.07	-.23	-.23	4.1	4.1	-.001	-.001	-.02-6.212	
1.4000	1115.84	9977.19	6.41	500.83	4.9	4.88	.55	230.49	3.20	2.70	-.23	-.23	4.1	4.1	-.001	-.001	-.02-6.560	
1.5000	1192.27	9973.55	6.74	500.71	5.1	5.31	.55	239.96	4.51	1.88	-.23	-.24	4.2	4.2	-.001	-.001	-.02-7.000	
1.6000	1268.49	9969.51	7.05	500.60	5.4	5.34	.55	251.10	5.27	.56	-.23	-.24	4.2	4.2	-.001	-.001	-.02-7.500	
1.7000	1344.27	9965.21	7.36	500.49	5.7	4.99	.55	267.52	5.28	-.78	-.23	-.24	4.2	4.2	-.001	-.001	-.02-8.000	
1.8000	1419.61	9960.72	7.67	500.41	6.1	4.55	.55	280.09	4.42	-2.33	-.23	-.24	4.2	4.2	-.001	-.001	-.02-8.500	
1.9000	1494.51	9956.54	8.00	500.34	6.4	4.50	.55	287.52	2.57	-3.68	-.23	-.24	4.2	4.2	-.001	-.001	-.02-9.000	
2.0000	1568.92	9952.54	8.37	500.20	6.8	5.07	.55	295.73	-2.52	-4.41	-.23	-.24	4.2	4.2	-.001	-.001	-.02-9.500	
2.1000	1642.83	9947.19	8.78	500.27	7.2	5.95	.55	300.84	-4.98	-3.26	-.23	-.24	4.2	4.2	-.001	-.001	-.02-10.000	
2.2000	1716.43	9941.93	9.22	500.25	7.6	6.53	.55	328.53	-6.51	-1.84	-.23	-.24	4.2	4.2	-.001	-.001	-.02-10.500	
2.3000	1789.51	9936.41	9.69	500.23	7.7	6.71	.55	352.77	-6.63	.97	-.23	-.24	4.2	4.2	-.001	-.001	-.02-11.000	
2.4000	1862.55	9930.66	10.17	500.21	8.0	6.05	.55	380.03	-5.86	2.84	-.23	-.24	4.2	4.2	-.001	-.001	-.02-11.500	
2.5000	1935.48	9924.56	10.65	500.27	8.4	4.98	.55	391.19	-2.95	4.02	-.23	-.24	4.2	4.2	-.002	-.002	-.02-12.000	
2.6000	2008.48	9918.05	11.10	500.28	8.9	4.19	.55	420.71	-1.15	4.19	-.23	-.24	4.2	4.2	-.002	-.002	-.02-12.500	
2.7000	2081.48	9911.50	11.51	500.37	9.5	4.14	.55	450.25	2.70	3.23	-.23	-.24	4.2	4.2	-.002	-.002	-.02-13.000	
2.8000	2154.48	9904.52	11.99	500.44	9.9	4.52	.55	480.97	3.03	.93	-.23	-.24	4.2	4.2	-.002	-.002	-.02-13.500	
2.9000	2227.48	9897.22	12.55	500.61	9.6	4.91	.55	512.74	4.72	-.23	-.23	-.24	4.2	4.2	-.002	-.002	-.02-14.000	
3.0000	2300.48	9889.72	13.07	500.74	9.7	4.87	.55	544.53	4.86	-.23	-.23	-.24	4.2	4.2	-.002	-.002	-.02-14.500	
3.1000	2373.48	9882.00	13.57	500.89	10.0	4.66	.55	576.39	4.80	-1.21	-.23	-.24	4.2	4.2	-.002	-.002	-.02-15.000	
3.2000	2446.48	9874.00	14.19	500.05	10.3	4.23	.55	608.25	3.62	-2.97	-.23	-.24	4.2	4.2	-.002	-.002	-.02-15.500	
3.3000	2519.48	9865.82	14.52	500.23	10.9	3.65	.55	640.17	2.42	-2.97	-.23	-.24	4.2	4.2	-.002	-.002	-.02-16.000	
3.4000	2592.48	9857.47	14.86	500.44	10.9	3.25	.55	672.07	1.04	-1.24	-.23	-.24	4.2	4.2	-.003	-.003	-.02-16.500	
3.5000	2665.48	9848.92	15.24	500.66	10.9	3.25	.55	704.07	-.04	-1.24	-.23	-.24	4.2	4.2	-.003	-.003	-.02-17.000	



## APPENDIX D

ROTATIONAL PARAMETER TRANSFORMATION (REF 10)

$x, y, z \equiv$  INERTIAL FRAME

$\hat{x}, \hat{y}, \hat{z} \equiv$  INERTIAL UNIT VECTORS

$X, Y, Z \equiv$  BODY FIXED FRAME

THE UNIT VECTOR  $\bar{V}$  IS MADE UP OF THE THREE COMPONENTS  $\bar{V}_1, \bar{V}_2, \bar{V}_3$  SO THAT

$$\bar{V} = \bar{V}_1 \hat{x} + \bar{V}_2 \hat{y} + \bar{V}_3 \hat{z} \quad (1)_D$$

NOW DEFINE  $\bar{V}_1 = \lambda_1 / \sin \alpha/2$

$$\bar{V}_2 = \lambda_2 / \sin \alpha/2 \quad (2)_D$$

$$\bar{V}_3 = \lambda_3 / \sin \alpha/2$$

WHERE  $\lambda_1, \lambda_2, \lambda_3$  AND  $\alpha$  ARE UNKNOWN PARAMETERS.

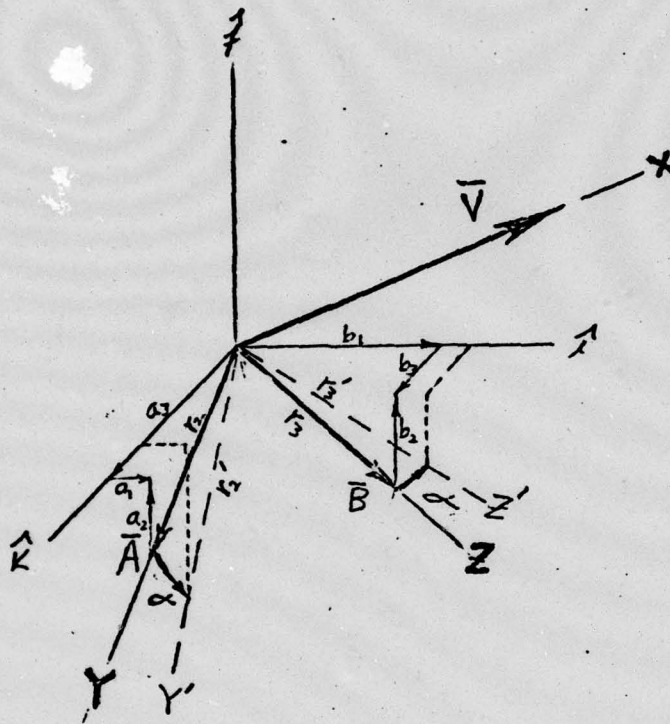
USING THE RELATION FOR DIRECTION COSINES THAT THE SUM OF THE SQUARES OF THE COMPONENTS OF A UNIT VECTOR MUST EQUAL ONE GIVES

$$\lambda_1^2 + \lambda_2^2 + \lambda_3^2 = \sin^2 \alpha/2 \quad (3)_D$$

NOW DEFINE ANOTHER PARAMETER  $\lambda_0^2 = \cos^2 \alpha/2$ . SO THE EXPRESSION CAN BE WRITTEN AS

$$\lambda_1^2 + \lambda_2^2 + \lambda_3^2 + \lambda_0^2 = 1 \quad (4)_D$$

THE BODY FIXED FRAME CAN BE RESOLVED INTO INERTIAL COMPONENTS AS FOLLOWS:



LET  $\bar{A}$  BE A UNIT VECTOR ALONG OY AND  $\bar{B}$  ALONG OZ SO THAT

$$\begin{aligned}\bar{A} &= a_1 \hat{x} + a_2 \hat{y} + a_3 \hat{z} \\ \bar{B} &= b_1 \hat{x} + b_2 \hat{y} + b_3 \hat{z}\end{aligned}\quad (5)_D$$

WHERE  $a_1, a_2, a_3, b_1, b_2, b_3$  ARE INERTIAL FRAME COMPONENTS. ALSO LET  $\alpha$  BE THE AMOUNT OF ROTATION OF THE PROJECTILE ABOUT THE OX AXIS WHERE  $r$  IS A VECTOR FIXED ON THE BODY BEFORE ROTATION AND  $r'$  IS THE POSITION AFTER ROTATION. THE DIRECTION COSINE MATRIX FOR



THIS ROTATION IS

$$\begin{bmatrix} r_1' \\ r_2' \\ r_3' \end{bmatrix} = \begin{bmatrix} 1 & 0 & 0 \\ 0 & C\alpha & -S\alpha \\ 0 & S\alpha & C\alpha \end{bmatrix} \begin{bmatrix} r_1 \\ r_2 \\ r_3 \end{bmatrix} \quad (6)_D$$

OR

$$\begin{aligned} r_2' &= r_2 C\alpha - r_3 S\alpha \\ r_3' &= r_2 S\alpha + r_3 C\alpha \end{aligned} \quad (7)_D$$

WHERE  $r_1, r_2, r_3$  ARE COMPONENTS OF  $\vec{r}$ ;

$C \equiv \cos$ ,  $S \equiv \sin$ ;

NEGATIVE ROTATION ABOUT X WAS USED  
SO EQN 12 SIMPLIFIES.

EXPRESSING  $\vec{r}$ 'S COMPONENTS IN THE INERTIAL FRAME:

$$r_1 \bar{V} = \frac{\lambda_1}{\sin \alpha/2} \hat{x} + \frac{\lambda_2}{\sin \alpha/2} \hat{y} + \frac{\lambda_3}{\sin \alpha/2} \hat{z}$$

$$r_2 \bar{A} = a_1 \hat{x} + a_2 \hat{y} + a_3 \hat{z} \quad (8)_D$$

$$r_3 \bar{B} = b_1 \hat{x} + b_2 \hat{y} + b_3 \hat{z}$$

COMBINING EQN 7 & 8 IN TERMS OF THE BODY FRAME:

$$r_1 \bar{V} = \frac{\lambda_1}{\sin \alpha/2} \hat{x} + \frac{\lambda_2}{\sin \alpha/2} \hat{y} + \frac{\lambda_3}{\sin \alpha/2} \hat{z} \quad (9)_D$$

$$r_2 \bar{A} = (a_1 \cos \alpha - b_1 \sin \alpha) \hat{x} + (a_2 \cos \alpha - b_2 \sin \alpha) \hat{y} + (a_3 \cos \alpha - b_3 \sin \alpha) \hat{z}$$

$$r_3 \bar{B} = (a_1 \sin \alpha + b_1 \cos \alpha) \hat{x} + (a_2 \sin \alpha + b_2 \cos \alpha) \hat{y} + (a_3 \sin \alpha + b_3 \cos \alpha) \hat{z}$$

DEFINING THE TRANSFORMATION MATRIX BY  $[C]$ , THE EXPRESSION THAT TRANSFORMS THE COMPONENTS OF THE MOVING BODY AXES SYSTEM TO INERTIAL REFERENCE IS:

$$\begin{bmatrix} C_{11} & C_{12} & C_{13} \\ C_{21} & C_{22} & C_{23} \\ C_{31} & C_{32} & C_{33} \end{bmatrix} \begin{bmatrix} \frac{\lambda_1}{\sin \alpha/2} & a_1 & b_1 \\ \frac{\lambda_2}{\sin \alpha/2} & a_2 & b_2 \\ \frac{\lambda_3}{\sin \alpha/2} & a_3 & b_3 \end{bmatrix} = \begin{bmatrix} \frac{\lambda_1}{\sin \alpha/2}, a_1 \cos \alpha - b_1 \sin \alpha, a_1 \sin \alpha + b_1 \cos \alpha \\ \frac{\lambda_2}{\sin \alpha/2}, a_2 \cos \alpha - b_2 \sin \alpha, a_2 \sin \alpha + b_2 \cos \alpha \\ \frac{\lambda_3}{\sin \alpha/2}, a_3 \cos \alpha - b_3 \sin \alpha, a_3 \sin \alpha + b_3 \cos \alpha \end{bmatrix} \quad \text{EQN (10)D}$$

POST MULTIPLYING BY THE INVERSE ( TRANSPOSE FOR THE ORTHOGONAL SYSTEM ):

$$\begin{bmatrix} C_{11} & C_{12} & C_{13} \\ C_{21} & C_{22} & C_{23} \\ C_{31} & C_{32} & C_{33} \end{bmatrix} = \begin{bmatrix} \frac{\lambda_1}{\sin \alpha/2}, a_1 \cos \alpha - b_1 \sin \alpha, a_1 \sin \alpha + b_1 \cos \alpha \\ \frac{\lambda_2}{\sin \alpha/2}, a_2 \cos \alpha - b_2 \sin \alpha, a_2 \sin \alpha + b_2 \cos \alpha \\ \frac{\lambda_3}{\sin \alpha/2}, a_3 \cos \alpha - b_3 \sin \alpha, a_3 \sin \alpha + b_3 \cos \alpha \end{bmatrix} \begin{bmatrix} \frac{\lambda_1}{\sin \alpha/2}, \frac{\lambda_2}{\sin \alpha/2}, \frac{\lambda_3}{\sin \alpha/2} \\ a_1 & a_2 & a_3 \\ b_1 & b_2 & b_3 \end{bmatrix} \quad \text{EQN (11)D}$$

MULTIPLYING IT OUT :

$$\begin{bmatrix} C_{11} & C_{12} & C_{13} \\ C_{21} & C_{22} & C_{23} \\ C_{31} & C_{32} & C_{33} \end{bmatrix} = \begin{bmatrix} \frac{\lambda_1^2}{\sin^2 \alpha/2} + (a_1^2 + b_1^2) \cos \alpha, \frac{\lambda_1 \lambda_2}{\sin^2 \alpha/2} + (a_1 b_2 - a_2 b_1) \sin \alpha + (a_1 a_2 + b_1 b_2) \cos \alpha, \\ \frac{\lambda_1 \lambda_3}{\sin^2 \alpha/2} + (a_1 b_3 - b_1 a_3) \sin \alpha + (b_1 b_3 + a_3 a_1) \cos \alpha \\ \frac{\lambda_2 \lambda_1}{\sin^2 \alpha/2} + (a_1 a_2 + b_1 b_2) \cos \alpha + (b_1 a_2 - a_1 b_2) \sin \alpha, \frac{\lambda_2^2}{\sin^2 \alpha/2} + (a_2^2 + b_2^2) \cos \alpha, \\ \frac{\lambda_2 \lambda_3}{\sin^2 \alpha/2} + (b_2 a_3 - b_3 a_2) \sin \alpha + (a_2 a_3 + b_2 b_3) \cos \alpha \\ \frac{\lambda_3 \lambda_1}{\sin^2 \alpha/2} + (a_1 a_3 + b_1 b_3) \cos \alpha + (b_1 a_3 - a_1 b_3) \sin \alpha, \\ \frac{\lambda_3 \lambda_2}{\sin^2 \alpha/2} + (a_3 a_2 + b_3 b_2) \cos \alpha + (b_2 a_3 - b_3 a_2) \sin \alpha, \frac{\lambda_3^2}{\sin^2 \alpha/2} + (a_3^2 + b_3^2) \cos \alpha \end{bmatrix} \quad \text{EQN (12)D}$$



THE FOLLOWING RELATIONSHIPS BETWEEN DIRECTION COSINES APPLY TO AN ORTHOGONAL, RIGHT-HAND SYSTEM :

$$a_1^2 + a_2^2 + a_3^2 = 1 \quad (13)_0$$

$$b_1^2 + b_2^2 + b_3^2 = 1 \quad (14)_0$$

$$a_1 \lambda_1 + a_2 \lambda_2 + a_3 \lambda_3 = 0 \quad (15)_0$$

$$b_1 \lambda_1 + b_2 \lambda_2 + b_3 \lambda_3 = 0 \quad (16)_0$$

$$a_1 b_1 + a_2 b_2 + a_3 b_3 = 0 \quad (17)_0$$

$$b_1 = \frac{1}{S^{1/2}} (\lambda_2 a_3 - \lambda_3 a_2) \quad (18)_0$$

$$b_2 = \frac{1}{S^{1/2}} (\lambda_3 a_1 - \lambda_1 a_3) \quad (19)_0$$

$$b_3 = \frac{1}{S^{1/2}} (\lambda_1 a_2 - \lambda_2 a_1) \quad (20)_0$$

$$\begin{vmatrix} \frac{\lambda_1}{S^{1/2}} & \frac{\lambda_2}{S^{1/2}} & \frac{\lambda_3}{S^{1/2}} \\ a_1 & a_2 & a_3 \\ b_1 & b_2 & b_3 \end{vmatrix} = 1 \quad (21)_0$$

EQUATIONS (15) AND (16) CAN BE WRITTEN AS:

$$a_2 = - \frac{1}{\lambda_2} (a_1 \lambda_1 + a_3 \lambda_3) \quad (22)_0$$

$$b_2 = - \frac{1}{\lambda_2} (b_1 \lambda_1 + b_3 \lambda_3) \quad (23)_0$$

SUBSTITUTING (22) & (23) INTO (17)

$$a_1 b_1 + \frac{1}{\lambda_2^2} (a_1 \lambda_1 + a_3 \lambda_3)(b_1 \lambda_1 + b_3 \lambda_3) + a_3 b_3 = 0 \quad (24)_0$$

$$a_1 b_1 (\lambda_1^2 + \lambda_2^2) + a_3 b_3 (\lambda_2^2 + \lambda_3^2) + (a_3 b_1 + b_3 a_1) \lambda_1 \lambda_3 = 0$$

SUBSTITUTING (22) INTO (13) AND (23) INTO (14)

$$a_1^2 (\lambda_1^2 + \lambda_2^2) + a_3^2 (\lambda_2^2 + \lambda_3^2) = \lambda_2^2 - 2 \lambda_1 \lambda_2 a_1 a_3 \quad (25)_D$$

$$b_1^2 (\lambda_1^2 + \lambda_2^2) + b_3^2 (\lambda_2^2 + \lambda_3^2) = \lambda_2^2 - 2 \lambda_1 \lambda_2 b_1 b_3 \quad (26)_D$$

EQUATIONS (22), (23) INTO (21)

$$\begin{aligned} & -\frac{\lambda_1 b_3}{\lambda_2} (a_1 \lambda_1 + a_3 \lambda_3) + \lambda_2 b_1 a_3 - \frac{\lambda_3 a_1}{\lambda_2} (b_1 \lambda_1 + b_3 \lambda_3) \\ & + \frac{\lambda_3 b_1}{\lambda_2} (a_1 \lambda_1 + a_3 \lambda_3) - \lambda_2 a_1 b_3 + \frac{\lambda_1 a_3}{\lambda_2} (b_1 \lambda_1 + b_3 \lambda_3) = S \approx \frac{\pi}{2} \end{aligned}$$

AFTER CANCELLATIONS AND REGROUPING

$$-b_3 a_1 [\lambda_1^2 + \lambda_2^2 + \lambda_3^2] + b_1 a_3 [\lambda_1^2 + \lambda_2^2 + \lambda_3^2] = \lambda_2 S \approx \frac{\pi}{2}$$

$$\text{AND SINCE } \lambda_1^2 + \lambda_2^2 + \lambda_3^2 = 1$$

$$b_3 = \frac{1}{a_1} [b_1 a_3 - \lambda_2 / S \approx \frac{\pi}{2}] \quad (27)_D$$

EQUATION (27) INTO (24)

$$\begin{aligned} & a_1 b_1 (\lambda_1^2 + \lambda_2^2) + \frac{a_3}{a_1} (\lambda_1^2 + \lambda_2^2 \lambda b_1 a_3 - \frac{\lambda_2^2}{S \approx \frac{\pi}{2}}) + \lambda_1 \lambda_3 [2 a_3 b_1 - \frac{\lambda_2}{S \approx \frac{\pi}{2}}] = 0 \\ & a_1^2 b_1 (\lambda_1^2 + \lambda_2^2) + b_1 a_3^2 (\lambda_2^2 + \lambda_3^2) + a_3 [2 \lambda_1 \lambda_3 a_1 b_1 - \frac{\lambda_2}{S \approx \frac{\pi}{2}} (\lambda_2^2 + \lambda_3^2)] = \frac{a_1}{S \approx \frac{\pi}{2}} \lambda_1 \lambda_2 \lambda_3 \quad (28)_D \end{aligned}$$

EQUATION (27) INTO (26)

$$\begin{aligned} & b_1^2 (\lambda_1^2 + \lambda_2^2) + \frac{1}{a_1^2} [b_1 a_3 - \frac{\lambda_2}{S \approx \frac{\pi}{2}}]^2 (\lambda_2^2 + \lambda_3^2) = \lambda_2^2 - 2 \frac{b_1}{a_1} (b_1 a_3 - \frac{\lambda_2}{S \approx \frac{\pi}{2}}) \lambda_1 \lambda_3 \\ & a_1^2 b_1^2 (\lambda_1^2 + \lambda_2^2) + a_3^2 b_1^2 (\lambda_2^2 + \lambda_3^2) + a_3 b_1 [2 \lambda_1 \lambda_3 a_1 b_1 - \frac{\lambda_2}{S \approx \frac{\pi}{2}} (\lambda_2^2 + \lambda_3^2)] = \\ & \lambda_2^2 a_1^2 + 2 b_1 a_1 \frac{\lambda_1 \lambda_2 \lambda_3}{S \approx \frac{\pi}{2}} - \frac{\lambda_2^2}{S \approx \frac{\pi}{2}} (\lambda_2^2 + \lambda_3^2) + a_3 b_1 \frac{\lambda_2}{S \approx \frac{\pi}{2}} (\lambda_2^2 + \lambda_3^2) \quad (29)_D \end{aligned}$$

LEFT SIDE OF (28)  $\times b_1$  = LEFT SIDE OF (29) THEREFORE



$$-\frac{a_1 b_1}{S^{1/2}} \lambda_1 \lambda_2 \lambda_3 = \lambda_2^2 a_1^2 + 2 b_1 a_1 \frac{\lambda_1 \lambda_2 \lambda_3}{S^{1/2}} + a_3 b_1 \frac{\lambda_1}{S^{1/2}} (\lambda_2^2 + \lambda_3^2) - \frac{\lambda_1^2}{S^{1/2}} (\lambda_2^2 + \lambda_3^2)$$

MULTIPLYING THRU BY  $\frac{S^{1/2}}{b_1}$

$$a_3 = \left\{ \left[ \frac{\lambda_2}{S^{1/2}} (\lambda_2^2 + \lambda_3^2) - S^{1/2} \lambda_2 a_1^2 \right] \frac{1}{b_1} - a_1 \lambda_1 \lambda_3 \right\} \frac{1}{\lambda_2^2 + \lambda_3^2} \quad (30)_D$$

EQUATION (18) AND (24)

$$b_1 = \frac{1}{S^{1/2}} \left[ \lambda_2 a_3 + \lambda_3 \frac{\lambda_1 a_1 + \lambda_3 a_3}{\lambda_2} \right] = \frac{\lambda_1 \lambda_3}{S^{1/2} \lambda_2} a_1 + \left( \frac{\lambda_2}{S^{1/2}} + \frac{\lambda_3^2}{S^{1/2} \lambda_2} \right) a_3 \quad (31)_D$$

EQUATION (30) INTO (33)

$$\begin{aligned} b_1 &= \frac{\lambda_1 \lambda_3}{S^{1/2} \lambda_2} a_1 + \left( \frac{\lambda_2}{S^{1/2}} + \frac{\lambda_3^2}{S^{1/2} \lambda_2} \right) \left\{ \left[ \frac{\lambda_2}{S^{1/2}} (\lambda_2^2 + \lambda_3^2) - a_1^2 \lambda_2 S^{1/2} \right] \frac{1}{b_1} - a_1 \lambda_1 \lambda_3 \right\} \\ &= \frac{\lambda_1 \lambda_3}{S^{1/2} \lambda_2} a_1 + \left( \frac{\lambda_2^2 + \lambda_3^2}{S^{1/2} \lambda_2} \right) \left\{ \left[ \frac{\lambda_2}{S^{1/2}} (\lambda_2^2 + \lambda_3^2) - (a_1^2 \lambda_2 S^{1/2}) \right] \frac{1}{b_1} - \lambda_1 \lambda_3 a_1 \right\} \\ &= \frac{\lambda_1 \lambda_3}{S^{1/2} \lambda_2} a_1 + \frac{1}{S^{1/2} \lambda_2} \left\{ \left[ \frac{\lambda_2}{S^{1/2}} (\lambda_2^2 + \lambda_3^2) - (a_1^2 \lambda_2 S^{1/2}) \right] \frac{1}{b_1} - \lambda_1 \lambda_3 a_1 \right\} \\ b_1 &= \frac{1}{S^{1/2} \lambda_2} \left[ \frac{\lambda_2}{S^{1/2}} (\lambda_2^2 + \lambda_3^2) - a_1^2 \lambda_2 S^{1/2} \right] \frac{1}{b_1} \end{aligned}$$

$$b_1^2 + a_1^2 = \frac{1}{S^{1/2}} (\lambda_2^2 + \lambda_3^2) \quad (32)_D$$

EQUATION (32) IS USED TO EVALUATE  $C_{11}$  IN (12)

$$C_{11} = \frac{\lambda_1^2}{S^{1/2}} + (a_1^2 + b_1^2) \cos \alpha$$

FROM THE DEFINITIONS  $\lambda_0^2 = \cos^2 \alpha/2$  AND  $\cos 2\alpha = 2 \cos^2 \alpha - 1$

$$\begin{aligned} C_{11} &= \frac{1}{S^{1/2}} \left[ \lambda_1^2 + (\lambda_2^2 + \lambda_3^2) (2 \lambda_0^2 - 1) \right] \\ &= \frac{1}{S^{1/2}} \left[ \lambda_1^2 + (1 - \lambda_0^2 - \lambda_1^2) (2 \lambda_0^2 - 1) \right] \\ &= \frac{1}{S^{1/2}} \left[ \lambda_1^2 + 2 \lambda_0^2 - 1 - 2 \lambda_0^2 + \lambda_0^2 - 2 \lambda_1^2 \lambda_0^2 + \lambda_1^2 \right] \\ &= \frac{1}{S^{1/2}} \left[ 2 (\lambda_1^2 + \lambda_2^2) - 2 (\lambda_0^2 + \lambda_1^2) \lambda_0^2 + \lambda_0^2 - 1 \right] \end{aligned}$$

$$= \frac{1}{S^{\alpha/2}} [2(\lambda_1^2 + \lambda_0^2)(1 - \lambda_0^2) - (1 - \lambda_0^2)]$$

$$= \frac{(1 - \lambda_0^2)}{S^{\alpha/2}} [2(\lambda_1^2 + \lambda_0^2) - 1]$$

$$\text{USING } S^{\alpha/2} = 1 - C^{\alpha/2} = 1 - \lambda_0^2$$

$$C_{11} = \frac{2(\lambda_1^2 + \lambda_0^2) - 1}{1} \quad (33)_D$$

SIMILARLY

$$C_{22} = \frac{\lambda_2^2}{S^{\alpha/2}} + (a_2^2 + b_2^2) \cos \alpha = \frac{2(\lambda_2^2 + \lambda_0^2) - 1}{1} \quad (34)_D$$

$$C_{33} = \frac{\lambda_3^2}{S^{\alpha/2}} + (a_3^2 + b_3^2) \cos \alpha = \frac{2(\lambda_3^2 + \lambda_0^2) - 1}{1} \quad (35)_D$$

FROM EQUATION (27)

$$b_1 a_3 - b_3 a_1 = \frac{\lambda_2}{S^{\alpha/2}} \quad (36)_D$$

BY ANALOGY AND WITH (21)

$$b_2 a_1 - b_1 a_2 = \frac{\lambda_3}{S^{\alpha/2}} \quad (37)_D$$

$$b_3 a_2 - b_2 a_3 = \frac{\lambda_1}{S^{\alpha/2}} \quad (38)_D$$

EVALUATE  $a_1 a_3 + b_1 b_3$  BY USING (27)

$$\begin{aligned} a_1 a_3 + b_1 b_3 &= a_1 a_3 + b_1 \frac{1}{a_1} (b_1 a_3 - \frac{\lambda_2}{S^{\alpha/2}}) \\ &= \frac{a_3}{a_1} (a_1^2 + b_1^2) - \frac{b_1}{a_1} \frac{\lambda_2}{S^{\alpha/2}} \end{aligned}$$

SUB EQUATION (32):

$$= \frac{a_3}{a_1} \frac{\lambda_2^2 + \lambda_3^2}{S^{\alpha/2}} - \frac{b_1}{a_1} \frac{\lambda_2}{S^{\alpha/2}}$$

SUB EQUATION (30):



$$\begin{aligned}
&= \frac{1}{S^{3/2} a_1} \left\{ \frac{1}{b_1} \left[ \frac{\lambda_2}{S^{1/2}} (\lambda_2^2 + \lambda_3^2) - S^{1/2} \lambda_2 a_1^2 \right] - a_1 \lambda_1 \lambda_3 \right\} - \frac{b_1 \lambda_2}{a_1 S^{1/2}} \\
&= \frac{\lambda_2}{S^{3/2} a_1 b_1} (\lambda_2^2 + \lambda_3^2) - \frac{\lambda_2 a_1^2}{S^{1/2} b_1 a_1} - \frac{\lambda_1 \lambda_3}{S^{1/2}} - \frac{b_1^2}{a_1} \frac{\lambda_2}{b_1 S^{1/2}} \\
&= \frac{\lambda_2}{S^{3/2} a_1 b_1} (\lambda_2^2 + \lambda_3^2) - \frac{\lambda_2}{S^{1/2} a_1 b_1} (a_1^2 + b_1^2) - \frac{\lambda_1 \lambda_3}{S^{1/2}}
\end{aligned}$$

SUB EQUATION (32)

$$a_1 a_3 + b_1 b_3 = - \frac{\lambda_1 \lambda_3}{S^{1/2}} \quad (39)_0$$

SIMILARLY

$$a_1 a_2 + b_1 b_2 = - \frac{\lambda_1 \lambda_2}{S^{1/2}} \quad (40)_0$$

$$a_2 a_3 + b_2 b_3 = - \frac{\lambda_2 \lambda_3}{S^{1/2}} \quad (41)_0$$

EVALUATING  $C_{12}$  FROM EQN (12) WITH (40) AND (37)

$$\begin{aligned}
C_{12} &= \frac{\lambda_1 \lambda_2}{S^{1/2}} + (a_1 a_2 + b_1 b_2) \cos \alpha + (a_1 b_2 - a_2 b_1) \sin \alpha \\
&= \frac{\lambda_1 \lambda_2}{S^{1/2}} - \frac{\lambda_1 \lambda_2 (2\lambda_0^2 - 1)}{S^{1/2}} + \frac{\lambda_3}{S^{1/2}} 2 S^{1/2} \lambda_0
\end{aligned}$$

$$\begin{aligned}
&\text{WHERE } \left. \begin{aligned} \cos 2(\alpha/2) &= 2(\cos^2 \alpha/2) - 1 \\ \sin 2(\alpha/2) &= 2(\sin \alpha/2)(\cos \alpha/2) \end{aligned} \right\} \cos \alpha/2 = \lambda_0
\end{aligned}$$

$$= \lambda_1 \lambda_2 \left[ \frac{2(1 - \lambda_0^2)}{S^{1/2}} \right] + 2 \lambda_0 \lambda_3$$

$$\underline{C_{12} = 2[\lambda_1 \lambda_2 + \lambda_0 \lambda_3]} \quad (42)_0$$

IN THE SAME MANNER, USING EQUATIONS  
(32) (37) (38) (39) (40) (41), THE

REMAINING COMPONENTS ARE

$$C_{21} = 2[\lambda_1 \lambda_2 - \lambda_0 \lambda_3] \quad (43)_D$$

$$C_{13} = 2[\lambda_1 \lambda_3 - \lambda_0 \lambda_2] \quad (44)_D$$

$$C_{31} = 2[\lambda_1 \lambda_3 - \lambda_0 \lambda_2] \quad (45)_D$$

$$C_{23} = 2[\lambda_2 \lambda_3 - \lambda_0 \lambda_1] \quad (46)_D$$

$$C_{32} = 2[\lambda_2 \lambda_3 - \lambda_0 \lambda_1] \quad (47)_D$$

SO THAT THE DIRECTION COSINE MATRIX  
BETWEEN THE INERTIAL AND BODY FIXED  
REFERENCE FRAMES AFTER ROTATION  $\alpha$  IS

$$\begin{bmatrix} C_{11} & C_{12} & C_{13} \\ C_{21} & C_{22} & C_{23} \\ C_{31} & C_{32} & C_{33} \end{bmatrix} = \begin{bmatrix} 2(\lambda_1^2 + \lambda_0^2) - 1 & 2(\lambda_1 \lambda_2 + \lambda_0 \lambda_3) & 2(\lambda_1 \lambda_3 - \lambda_0 \lambda_2) \\ 2(\lambda_1 \lambda_2 - \lambda_0 \lambda_3) & 2(\lambda_2^2 + \lambda_0^2) - 1 & 2(\lambda_2 \lambda_3 + \lambda_0 \lambda_1) \\ 2(\lambda_1 \lambda_3 + \lambda_0 \lambda_2) & 2(\lambda_2 \lambda_3 - \lambda_0 \lambda_1) & 2(\lambda_3^2 + \lambda_0^2) - 1 \end{bmatrix}$$

EQN (48)<sub>D</sub>

WHICH IS EQUIVALENT TO THE EULER ANGLE FORM  
OF THE DIRECTION COSINE MATRIX

$$\begin{bmatrix} C\theta C\psi & S\theta & S\psi C\theta \\ -S\psi S\phi - C\psi S\theta C\phi & C\theta C\phi & C\psi S\phi - S\psi S\theta C\phi \\ -S\psi C\phi + C\psi S\theta S\phi & -C\theta S\phi & C\psi C\phi + S\psi S\theta S\phi \end{bmatrix}$$

EQN (49)<sub>D</sub>



## COMPARING COEFFICIENTS

$$C_{11} = 2(\lambda_0^2 + \lambda_1^2) - 1 = C\psi C\theta \quad (50)_0$$

$$C_{22} = 2(\lambda_0^2 + \lambda_2^2) - 1 = C\phi C\theta \quad (51)_0$$

$$C_{33} = 2(\lambda_0^2 + \lambda_3^2) - 1 = C\psi C\phi + S\psi S\theta S\phi \quad (52)_0$$

FROM EQN (4)

$$\lambda_0^2 = 1 - (\lambda_1^2 + \lambda_2^2 + \lambda_3^2) \quad (53)_0$$

EQUATION (53) INTO (50)(51)(52)

$$1 - 2(\lambda_2^2 + \lambda_3^2) = C\psi C\theta \quad (54)_0$$

$$1 - 2(\lambda_1^2 + \lambda_3^2) = C\phi C\theta \quad (55)_0$$

$$1 - 2(\lambda_2^2 + \lambda_1^2) = C\psi C\phi + S\psi S\theta S\phi \quad (56)_0$$

EQN (56) - (55)

$$-2(\lambda_2^2 + \lambda_3^2) = C\psi C\phi + S\psi S\theta S\phi - C\phi C\theta \quad (57)_0$$

EQN (54) + (57)

$$1 - 4\lambda_2^2 = C\psi(C\theta + C\phi) + S\psi S\theta S\phi - C\phi C\theta$$

$$4\lambda_2^2 = 1 - C\psi(C\theta + C\phi) + C\phi C\theta - S\psi S\theta S\phi \quad (58)_0$$

USING THE IDENTITY  $C\theta + C\phi = 2C(\frac{\theta+\phi}{2})C(\frac{\theta-\phi}{2})$ 

$$4\lambda_2^2 = 1 - 2C\psi \left[ C\frac{\theta+\phi}{2} C\frac{\theta-\phi}{2} \right] + C\phi C\theta - S\psi S\theta S\phi$$

USING THE IDENTITY  $C2\psi = C^2\psi - S^2\psi$ 

$$4\lambda_2^2 = 1 - 2 \left( C^2\frac{\psi}{2} - S^2\frac{\psi}{2} \right) \left( C^2\frac{\theta}{2} C^2\frac{\phi}{2} - S^2\frac{\theta}{2} S^2\frac{\phi}{2} \right) + C\phi C\theta - S\psi S\theta S\phi$$

$$4\lambda_2^2 = 1 + 2 \left[ C^2\frac{\psi}{2} S^2\frac{\theta}{2} S^2\frac{\phi}{2} + S^2\frac{\psi}{2} C^2\frac{\theta}{2} C^2\frac{\phi}{2} \right] + C\phi C\theta - S\psi S\theta S\phi \\ - 2 \left[ C^2\frac{\psi}{2} C^2\frac{\theta}{2} C^2\frac{\phi}{2} + S^2\frac{\psi}{2} S^2\frac{\theta}{2} S^2\frac{\phi}{2} \right]$$

USING IDENTITIES  $C2\theta = 2C^2\theta - 1$  &  $C2\theta = 1 - 2S^2\theta$

$$4\lambda_1^2 = 2 \left[ C^2 \frac{\psi}{2} S^2 \frac{\theta}{2} S^2 \frac{\phi}{2} + S^2 \frac{\psi}{2} C^2 \frac{\theta}{2} C^2 \frac{\phi}{2} \right] + 1 + \\ - \frac{2}{8} \left[ (C\psi + 1)(C\theta + 1)(C\phi + 1) + (1 - C\psi)(1 - C\theta)(1 - C\phi) \right] + \\ + C\phi C\theta - S\psi S\theta S\phi$$

$$4\lambda_2^2 = 2 \left[ C^2 \frac{\psi}{2} S^2 \frac{\theta}{2} S^2 \frac{\phi}{2} + S^2 \frac{\psi}{2} C^2 \frac{\theta}{2} C^2 \frac{\phi}{2} \right] + 1 + \\ - \frac{1}{2} \left[ C\psi C\theta + C\psi C\phi + C\theta C\psi + 1 \right] + \\ + C\phi C\theta - S\psi S\theta S\phi$$

$$4\lambda_2^2 = 2 \left[ C^2 \frac{\psi}{2} S^2 \frac{\theta}{2} S^2 \frac{\psi}{2} + S^2 \frac{\psi}{2} C^2 \frac{\theta}{2} C^2 \frac{\psi}{2} \right] + \\ + \frac{1}{2} \left[ 1 - C\psi(C\theta + C\phi) + C\phi C\theta - S\psi S\theta S\phi \right] \\ - \frac{S\psi S\theta S\phi}{2}$$

$$4\lambda_2^2 = 2 \left[ C^2 \frac{\psi}{2} S^2 \frac{\theta}{2} S^2 \frac{\phi}{2} + S^2 \frac{\psi}{2} C^2 \frac{\theta}{2} C^2 \frac{\phi}{2} \right] + 2\lambda_2^2 - \frac{1}{2} S\psi S\theta S\phi$$

USING THE IDENTITY  $S 2\theta = 2S\theta C\theta$

$$\lambda_2^2 = C^2 \frac{\psi}{2} S^2 \frac{\theta}{2} S^2 \frac{\phi}{2} + S^2 \frac{\psi}{2} C^2 \frac{\theta}{2} C^2 \frac{\phi}{2} - 2C\frac{\psi}{2} S\frac{\psi}{2} C\frac{\theta}{2} S\frac{\theta}{2} C\frac{\phi}{2} S\frac{\phi}{2}$$

WHICH FACTORS INTO

$$\lambda_2^2 = \left( C\frac{\psi}{2} S\frac{\theta}{2} S\frac{\phi}{2} - S\frac{\psi}{2} C\frac{\theta}{2} C\frac{\phi}{2} \right)^2$$

$$\lambda_2 = \underline{C\frac{\psi}{2} S\frac{\theta}{2} S\frac{\phi}{2} - S\frac{\psi}{2} C\frac{\theta}{2} C\frac{\phi}{2}} \quad (59)_D$$

BY ANALOGY

$$\lambda_1 = \underline{-C\frac{\phi}{2} S\frac{\theta}{2} S\frac{\psi}{2} + S\frac{\phi}{2} C\frac{\theta}{2} C\frac{\psi}{2}} \quad (60)_D$$



EQN (57) - (54)

$$4\lambda_3^2 - 1 = C\psi C\phi + S\psi S\theta S\phi - C\phi C\theta - C\psi C\theta$$

$$4\lambda_3^2 = 1 - C\theta(C\psi + C\phi) + C\phi C\psi + S\psi S\theta S\phi$$

THE SOLN TO THIS EQN IS SIMILAR TO EQN 58:

$$\lambda_3 = \underline{C \frac{\theta}{2} S \frac{\psi}{2} S \frac{\phi}{2} + S \frac{\theta}{2} C \frac{\psi}{2} C \frac{\phi}{2}} \quad (61)_D$$

EQN (54) INTO (53)

$$\lambda_0^2 = 1 - [\lambda_1^2 + \frac{1}{2}(1 - C\psi C\theta)] = \frac{1}{2}(1 + C\psi C\theta) - \lambda_1^2$$

$$\lambda_0^2 = \frac{1}{2} + \frac{1}{2} C\psi C\theta - C^2 \frac{\phi}{2} S^2 \frac{\theta}{2} S^2 \frac{\psi}{2} - S \frac{\phi}{2} C \frac{\psi}{2} C \frac{\theta}{2} + \\ + 2C \frac{\phi}{2} S \frac{\phi}{2} C \frac{\psi}{2} S \frac{\psi}{2} C \frac{\theta}{2} S \frac{\theta}{2}$$

$$\lambda_0^2 = \frac{1}{2}(1 + C\psi C\theta) - (1 - S^2 \frac{\phi}{2}) S^2 \frac{\phi}{2} S^2 \frac{\psi}{2} - S^2 \frac{\phi}{2} C^2 \frac{\psi}{2} C^2 \frac{\theta}{2} + \\ + 2C \frac{\phi}{2} S \frac{\phi}{2} C \frac{\psi}{2} S \frac{\psi}{2} C \frac{\theta}{2} S \frac{\theta}{2}$$

$$\lambda_0^2 = \frac{1}{2} [1 + (2C^2 \frac{\psi}{2} - 1)(2C^2 \frac{\theta}{2} - 1)] + S^2 \frac{\phi}{2} S^2 \frac{\theta}{2} S^2 \frac{\psi}{2} + \\ - S^2 \frac{\theta}{2} S^2 \frac{\psi}{2} - S^2 \frac{\phi}{2} C^2 \frac{\psi}{2} C^2 \frac{\theta}{2} + 2C \frac{\phi}{2} S \frac{\phi}{2} C \frac{\psi}{2} S \frac{\psi}{2} C \frac{\theta}{2} S \frac{\theta}{2}$$

$$\lambda_0^2 = 1 + C^2 \frac{\psi}{2} C^2 \frac{\theta}{2} (1 - S^2 \frac{\phi}{2}) + S^2 \frac{\phi}{2} S^2 \frac{\theta}{2} S^2 \frac{\psi}{2} + C^2 \frac{\psi}{2} C^2 \frac{\theta}{2} + \\ - C^2 \frac{\psi}{2} - C^2 \frac{\theta}{2} - S^2 \frac{\theta}{2} S^2 \frac{\psi}{2} + 2C \frac{\phi}{2} S \frac{\phi}{2} C \frac{\psi}{2} S \frac{\psi}{2} C \frac{\theta}{2} S \frac{\theta}{2}$$

NOTE THAT

$$1 + C^2 \frac{\psi}{2} C^2 \frac{\theta}{2} - C^2 \frac{\psi}{2} - C^2 \frac{\theta}{2} - S^2 \frac{\theta}{2} S^2 \frac{\psi}{2} =$$

$$1 + C^2 \frac{\theta}{2} (1 - S^2 \frac{\psi}{2}) - C^2 \frac{\psi}{2} - S^2 \frac{\theta}{2} S^2 \frac{\psi}{2} =$$

$$1 - S^2 \frac{\psi}{2} - C^2 \frac{\psi}{2} = 0$$

THEREFORE

$$\lambda_0^2 = C^2 \frac{\psi}{2} C^2 \frac{\theta}{2} C^2 \frac{\phi}{2} + S^2 \frac{\phi}{2} S^2 \frac{\theta}{2} S^2 \frac{\psi}{2} + 2C \frac{\phi}{2} S \frac{\phi}{2} C \frac{\psi}{2} S \frac{\psi}{2} C \frac{\theta}{2} S \frac{\theta}{2}$$

$$\lambda_0 = \underline{C \frac{\psi}{2} C \frac{\phi}{2} C \frac{\theta}{2} + S \frac{\psi}{2} S \frac{\phi}{2} S \frac{\theta}{2}} \quad (62)_D$$

THE SET OF ROTATIONAL PARAMETERS ARE

$$\lambda_0 = C_{\frac{\psi}{2}} C_{\frac{\phi}{2}} C_{\frac{\theta}{2}} + S_{\frac{\psi}{2}} S_{\frac{\phi}{2}} S_{\frac{\theta}{2}}$$

$$\lambda_1 = -C_{\frac{\phi}{2}} S_{\frac{\theta}{2}} S_{\frac{\psi}{2}} + S_{\frac{\phi}{2}} C_{\frac{\theta}{2}} C_{\frac{\psi}{2}}$$

$$\lambda_2 = C_{\frac{\psi}{2}} S_{\frac{\theta}{2}} S_{\frac{\phi}{2}} - S_{\frac{\psi}{2}} C_{\frac{\theta}{2}} C_{\frac{\phi}{2}}$$

$$\lambda_3 = C_{\frac{\theta}{2}} S_{\frac{\psi}{2}} S_{\frac{\phi}{2}} + S_{\frac{\theta}{2}} C_{\frac{\psi}{2}} C_{\frac{\phi}{2}}$$



## Appendix E

Coriolis

From the kinematical expression for motion in terms of moving reference frames (Ref 7:111):

$$\ddot{\mathbf{r}}^i = \ddot{\mathbf{r}}^e + 2\boldsymbol{\omega}^e \times \dot{\mathbf{r}}^e + \dot{\boldsymbol{\omega}} \times \mathbf{r}^e + \boldsymbol{\omega}^e \times (\boldsymbol{\omega}^e \times \mathbf{r}^e) \quad (1)E$$

where the superscripts denote the applicable frame of reference.

The term  $2\boldsymbol{\omega}^e \times \dot{\mathbf{r}}$  is the coriolis acceleration and, for the application of a projectile moving with a velocity ( $V$ ) over the earth rotating at rate ( $\Omega$ ), the coriolis expression becomes

$$2\Omega \times V \quad (2)E$$

Define the body frame ( $XYZ$ ) moving globally with respect to a north-east-down reference frame ( $NED$ ):

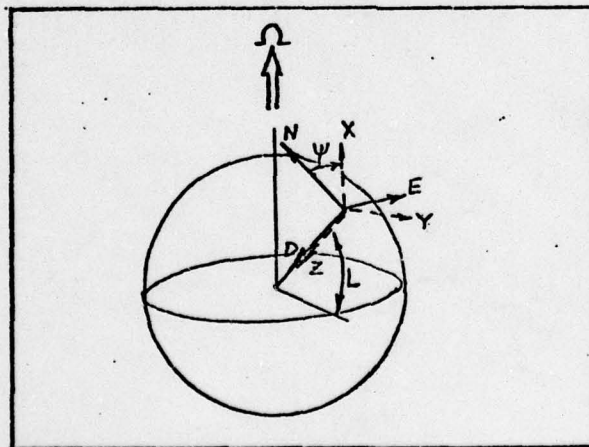


Fig. E-1. Local Level Reference Frame

where  $\psi$  is the heading with respect to north and  $L$  denotes latitude.

The transformation between the body frame and north frame is

$$C_N^b = \begin{bmatrix} \cos \psi & \sin \psi & 0 \\ -\sin \psi & \cos \psi & 0 \\ 0 & 0 & 1 \end{bmatrix} \quad (3)E$$

The earth rate component as seen by the body frame is then

$$\begin{aligned} \Omega^b &= C_N^b \Omega^N = \begin{bmatrix} \cos \psi & \sin \psi & 0 \\ -\sin \psi & \cos \psi & 0 \\ 0 & 0 & 1 \end{bmatrix} \begin{bmatrix} \Omega \cos L \\ 0 \\ -\Omega \sin L \end{bmatrix} \\ &= \begin{bmatrix} \Omega \cos L \cos \psi \\ -\Omega \cos L \sin \psi \\ -\Omega \sin L \end{bmatrix} \end{aligned} \quad (4)E$$

so that the coriolis expression becomes

$$2\Omega \times V = 2 \begin{bmatrix} \hat{\lambda} & \hat{\tau} & \hat{r} \\ \Omega \cos L \cos \psi & -\Omega \cos L \sin \psi & -\Omega \sin L \\ V_N & V_E & V_D \end{bmatrix} \quad (5)E$$

where  $V_N$ ,  $V_E$ ,  $V_D$  are the N, E, D velocity components. The scalar components of coriolis acceleration then, are

$$\begin{aligned} (2\Omega \times V)_x &= -2V_D \Omega \cos L \sin \psi + 2V_E \Omega \sin L \\ (2\Omega \times V)_y &= -2V_D \Omega \cos L \cos \psi - 2V_N \Omega \sin L \\ (2\Omega \times V)_z &= 2V_E \Omega \cos L \cos \psi + 2V_N \Omega \cos L \sin \psi \end{aligned} \quad (6)E$$



AD-A048 966

AIR FORCE INST OF TECH WRIGHT-PATTERSON AFB OHIO SCH--ETC F/G 19/4  
MAGNUS EFFECTS ON BALLISTIC TRAJECTORIES.(U)

DEC 77 J D SCHNEIDER

AFIT/GA/AA-77D-8

UNCLASSIFIED

NL

242

ADAO48 966



END  
DATE  
FILMED  
2-78  
DDC

Appendix F

Six Degree of Freedom Computer Program

PROGRAM SIXDOF 74/74 OPT=1

FTN 4.5+414

09/12/77 17.09.00

```
1      PROGRAM SIXDOF (INPUT,OUTPUT,TAPES=INPUT)
      EXTERNAL ARDCHA
      CALL CFRO
      CALL INIT6
5      CALL SIXDEG (ARDCHA)
      STOP
      END
```

BEST AVAILABLE COPY



SUBROUTINE AROCHA 74/74 OPT=1

FTN 4.5+414

09/12/77 17.09.

```

1      SUBROUTINE AROCHA(M)
C      NARR_E 250  R. S. EIKENBERRY, AERO-SPACE ENGR.
C      UNIVERSITY OF NOTRE DAME, NOTRE DAME, IND.
5      C AROC 1959 MODEL ATMOSPHERE SUBROUTINE
C
C      COMMON /AIRBLK/ T,P,R,VK,VS
C      DIMENSION A(3),H(3),C(3),J(3)
C      DIMENSION H9(12),W1(11),W2(11),W3(11),T8(11),P9(11),Q9(11)
10     C
C      DATA H9/0.,11000.,25000.,47000.,53000.,79000.,90000.,105000.,16000
$9.,170000.,200000.,700000./
C      DATA W1/-.225567E-4,0.,.134456E-4,0.,-.159202E-4,0.,.241459E-4,
$8.895283E-4,.7543,1E-5,.350715E-5,.222129E-5/
15     C      DATA W2/-.525612E-1,0.,.117837E2,0.,-.759218E1,0.,.854120E1,
$1.70124E1,.341643E1,.687235E1,.376137E1/
C      DATA W3/0.,.157649E-3,0.,.120949E-3,0.,.236236E-3,0.,0.,0.,0.,0./
C      DATA T8/51868.8E3,.389989E3,.349989E3,.509788E3,.508788E3,
$2.98184E3,.298184E3,.405184E3,.248618E4,.256618E4,.293618E4/
20     C      DATA P9/211621E4,.4727E3,.5197E2,.25155E1,.12181E1,.2108E-1,
$2.1809E-2,.15562E-3,.7578E-5,.58954E-5,.29759E-5/
C      DATA R9/237632E-2,.7062E-3,.7765E-4,.28304E-5,.139468E-5,
$4.1149E-7,.4261E-9,.2212E-9,.1945E-11,.1338E-11,.6113E-12/
25     C      DATA CON1,CON2,CON3,CON4,CON5,CON6/.3049,5356766.,49.020576,0.0226H3L01279
$388E-05,198.72,91000./
C      DATA A/1.,.759511,.375787/
C      DATA B/0.,.17416.,.273966/
C      DATA C/0.,.22E6,.19E6/
C      DATA D/0.,.25E5,.14E6/
30     C
C      HGP=CON1*H/(1.+(CON1*H/CON2))
C      IF(HGP.LT.0.) HGP=0.
C      DO 1002 M=1,11
C      IF(M*P-H9(M)) 1003,1004,1002
35     1002 CONTINUE
C      IF ((HGP-H9(12)).GT.0.) GO TO 1052
C      M=12
1003 M=M-1
1004 TM=T8(M)*(1.+W1(M)*(HGP-H9(M)))
40     IF ((HGP-90000.).GT.0.) GO TO 1006
C      T=TM
C      GO TO 1070
1006 IF ((HGP-160000.).GT.0.) GO TO 1009
C      I=2
C      GO TO 1007
45     1009 I=3
1007 T=TM*(A(I)-B(I))*ATAN((HGP-C(I))/C(I))

1070 IF (W2(M)) 1011,1020,1011
50     1011 TEMP=1.+W1(M)*(HGP-H9(M))
C      P=P9(M)/TEMP**W2(M)
C      R=P9(M)/TEMP** (1.+W2(M))
C      GO TO 1030
1020 TEMP=EXP(-W3(M)*(HGP-H9(M)))
55     P=P9(M)*TEMP
C      R=P9(M)*TEMP
1030 IF ((HGP-CON6).GT.0.) GO TO 1032
C      VS=CON3*SQR(TM)
C      VK=CON4*(T**1.5/(1.+CON5)*P)
60     RETURN
1052 T=0.
C      P=0.
C      R=0.
1032 VS=0.
65     VK=0.
C      RETURN
C      END

```

BEST AVAILABLE COPY

SUBROUTINE CFRD

74/74 OPT=1

FTN 4.5+414

09/12/77 17.09.

```

1      SUBROUTINE CFRD                                00000070
C                                                    00000080
C SIXDEG 50 C. W. INGRAM, AERO-SPACE ENGR.          00000090
C UNIVERSITY OF NOTRE DAME, NOTRE DAME, IND.          00000100
5      C                                                    00000110
C READS COEFFICIENTS IN TABULAR FORM AS A FUNCTION OF ANGLE OF
C ATTACK AND MACH NUMBER                             00000120
C MAXIMUM NUMBER OF ANGLES OF ATTACK = 20, MAXIMUM NUMBER OF MACH
C NUMBERS = 20                                       00000130
10     C                                                    00000150
1001  FORMAT(A4,1X,3I2)                               00000160
1002  FORMAT(//14X,*ALPHA*, 2X,10F10.4/21X,10F10.4)
1003  FORMAT(/5X,*MACH*,1F10.4,2X,10F10.4/21X,10F10.4)
1004  FORMAT(/1XA6,3X24C(I2,1H))                      00000190
15     C                                                    00000200
1006  FORMAT(8F10.4)
1007  FORMAT(8F10.4)
COMMON /COEF/ AMCH(20,30),ALPHA(20,10),C(20,20,30),NOA(30),NOM(30) 00000210
COMMON /COEP1/ NPLY
COMMON /POL/ CE(30), ALPHAR,CMA,CMPA,CZA
COMMON /BLK1/ RUN
20     DIMENSION AMC(600),ALP(600),CC(12000)          00000230
EQUIVALENCE (AMC,AMCH),(ALP,ALPHA),(CC,C)            00000240
C                                                    00000250
C SET ARRAY TABLE TO ZERO                          00000260
25     NPLY=0
DO 110 I=1,600
AMC(I)=0.
110  ALP(I)=0.
DO 111 I=1,12000
30     CC(I)=0.
DO 112 I=1,30
NOA(I)=0
NOM(I)=0
112  CONTINUE
35     CZA=0.0
CMA=0.0
CMPA=0.0
C                                                    00000400
40     C READ NUMBER OF AERODYNAMIC COEFFICIENTS      00000410
READ(5,1005) RUN,NC
1005  FORMAT(A6,4X,I2)
PRINT 1005,RUN,NC
1006  FORMAT(1H1,2X,A6,2X,I2 // )
45     C FOR CONSTANT ANGLE OF ATTACK NO ANGLE OF ATTACK TABLES ARE READ 00000430
C FOR CONSTANT MACH NUMBER ONE TABLE OF MACH NUMBER IS READ 00000440
DO 120 M=1,NC
READ(5,1001) NAME,K,NOA(K),NOM(K)
50     PRINT 1004, NAME,K
NM=NOM(K)
IF(NM.EQ.0) NM=1
NA=NOA(K)
IF(NA.EQ.0) NA=1
IF(NA.EQ.1) GO TO 119
55     READ(5,1006) (ALPHA(I,K),I=1,NA)
PRINT 1002, (ALPHA(I,K),I=1,NA)
119  DO 120 I=1,NM
120  READ(5,1007) AMCH(I,K),(C(I,J,K),J=1,NA)
DO 125 I=1,NM
60     125 PRINT 1003,AMCH(I,K),(C(I,J,K),J=1,NA)
130  CONTINUE
RETURN
END
00000560
00000570
00000580
00000590

```

BEST AVAILABLE COPY



SUBROUTINE EO

74/74 OPT=1

FTN 4,5+414

09/12/77 17.09.

```

1      SUBROUTINE EO                                00004560
      REAL MASS,IX,IY,L
      INTEGER PG                                00004590
      COMMON /AIRBLK/ TEM,PRFS,RMD,KVIS,VA      00004600
      COMMON /COEF/ AMOM(20,30),ALPHA(20,30),C(20,20,30),NOA(30),NOM(30) 00004610
      COMMON /INDBLK/ IDEN,IMND,ITCO,IPRN,IALL,NORC,IPUN,NRODY,ITRST,NT0000-320 00004630
      3RST                                         00004640
      COMMON /INIT/ TITLE(12),SCALE(30),A(22)    00004650
      COMMON /THRUST/TIM(15),TOST(15),MASS(15),CG(15),IX(15),IY(15),CGP(15) 00004660
10     33)                                         00004670
      COMMON /TSTOAT/EPS,TTCO,ETA,L,RL           00004680
      COMMON /WINBLK/ NOM,YM(120),M(120,3)        00004690
      COMMON /COEP1/ NPLY                         00004700
      COMMON /POL/ CE(30),ALPHA0,CMA,CMPA,C7A      00004710
15     COMMON /EDBK2/D1(14),D2(14),D3(14),D4(14),MIN(3),DAL(10),DRE(10) 00004720
      COMMON /EDBK2/V,D,S,CP,ALPHAN,AYC4N,PG,LN    00004730
      COMMON /EDBK3/AXX,AXY,AXZ,AYX,AYY,AYZ,AZX,AZY,AZZ
      COMMON /EDBK4/ LGOUNT
      COMMON /RLK1/ RUN
20     DATA COMD/57.295779/
1000    FORMAT(56X, '----')
1001    FORMAT(1X,T4,'TIME',5X,'RANGE',5X,'ALT',7X,'Z',9X,'V',7X,'D',3X,
      1*ALPHA',3X,'M',5X,'PHI',2X,'ALPHA',2X,'BETA',2X,'L-N',3X,'L-P',
      24X,'W-N',4X,'W-P',5X,'S',5X,'TAU',3X,'K-T')
25     1002 FORMAT(1X,T4,'SEC',7X,'FEET',5X,'FEET',5X,'FEET',4X,'FT/SEC',2X,
      1*RA/SEC',2X,'DEG',10X,'DEG',1X,'DEG',4X,'DEG',1X,'1/SEC',1X,
      2*1/SEC',1X,'RA/SEC',1X,'RA/SEC',15X,'DEG')
1003    FORMAT(1X,1F6.4,2F10.2,2F9.2,1F7.1,2F6.2,1F7.2,4F6.2,2F7.1,
      11F4.3,1F6.2,1F7.3)
30     1010 FORMAT(1H11244,31X4PAGFI4)
      1090 FORMAT(10F7.3,2X,1HA)
      1091 FORMAT(10F7.3,2X,1HR)
      IF (MRODY.EQ.1) GO TO 821
      3P=V*(2.*AXZ*D2(3)-2.*AXX*D2(4))
35     AP=2.*AXY*V-D2(3)*D1(12)
      XI=ACOTAN(AP,AP)
      BETA=-ALPHAN*SIN(XI)
      ALPH=ALPHAN*COS(XI)
      GO TO 841
40     821 ALPH=ATAN(D1(14)/D1(12))*CONV
      BETA=ATAN(D1(13)/D1(12))*CONV
      841 PP=JPCONV
      IF (MND(LN,50).NE.0) GO TO 2
      PG=PG+1
45     PRINT 1010,TITLE,PG
      PRINT 1000
      PRINT 1001
      PRINT 1002
      2 P=D1(5)
50     IF (P.EQ.0.) GO TO 4752
      SSNC=(D1(5)*D1(5)*A(15)*A(15))/(10*S*A(19)*CMA*A(16)*4.)
      TAU = 1./SQRT(1. - 1./SSNC)
      J24= A(19)*A(19)*A(15)
      CLAMP = (2*S)/(2.*A(14)*V)*(C7A*(1.-TAU)+ D24/(2.*A(15))* (CF(27)
55     1*(1.-TAU)) - D24/A(15)*CMPA*TAU)
      CLAMP = (2*S)/(2.*A(15)*V)*(C7A*(1.-TAU)+ D24/(2.*A(16))* (CF(27)

```

BEST AVAILABLE COPY

SUBROUTINE	ED	74/74	OPT=1	FTN 4.5+414	09/12/77 17.09.00
					00005110
					00005120
60					00005130
					00005140
					00005150
					00005160
65	4762				00005170
					00005180
					00005190
					00005200
					00005210
70					00005220
					00005230
	4763				00005250
					00005260
75					00005270
					00005280
					00005290
					00005300
80					00005310
					00005320
					00005330
	1112				00005340
					00005350
					00005360
85	1113				00005370
					00005380
					00005390
					00005400
					00005410

BEST AVAILABLE COPY



SUBROUTINE INIT6

74/74 OPT=1

FTN 4.5+414

09/12/77 17.09.0

```

1      SUBROUTINE INIT6
C
C SIXDEG 100 C. W. INGRAM, AERO-SPACE ENGR.
C UNIVERSITY OF NOTRE DAME, NOTRE DAME, IND.
C
C INITIALIZATION PROGRAM FOR N-DEGREE OF FREEDOM MOTION (3+N*6)
C
      REAL MASS,IX,IY,L
1001  FORMAT(12A4)
1002  FORMAT(////1X,23#ECHO OF INITIALIZATION INPUT'//)
1003  FORMAT(4(6(1X,2HA(I2,4H) = ,F11.4)/))
1004  FORMAT(1X,7HNORC = ,I1,3X,7HTPRV = ,I2,3X,7HNALL = ,I1,3X,
      $7HIPIN = ,I1,3X,7HN9DDY = ,I1,3X,9HISCAL = ,I1,3X,8HITRST = ,I1,/,0000773)
      $/)
1005  FORMAT(//5(6(1X,64SCALE(I2,4H) = ,E8.2)/))
1006  FORMAT(1,5X,4HTIME,5X,8HTHRUST,7X,4HMASS,5X,11HCG POSITION,7X,5HCG0000760
      $-AC,2HIX,7X,2HIY,/)
1007  FORMAT(4X,F5.2,5X,F5.0,5X,F5.3,6X,F8.2,8X,F6.2,4XF6.3,4X,F6.3)
1008  FORMAT(5X,13HTHRUST DATA ',3X,6HEPS = ,F5.2,3X,9HTHETAC = ,F5.2,3X,0000790
      $,6HETA = ,F5.2,3X,4HL = ,F5.2,/)
1009  FORMAT(//,5X,14H3DDY LENGTH = ,F4.2,/)
1010  FORMAT(7I10)
1011  FORMAT(I10,3E10.4,I10,E10.4)
1012  FORMAT(8E10.4 / 5E10.4 / 5E10.4)
1013  FORMAT(6E10.4)
1014  FORMAT(2E10.4)
1015  FORMAT(3(8E10.4 /), 5E10.4)
      LOGICAL LSCALE,IALL,LTRST
      COMMON /WINGBLK/ NOW,YH(128),W(128,3)
      COMMON /AIRBLK/ TE4,PRES,RHO,KVIS,VA
      COMMON /DENBLK/ NOD,YO(128),DEN(128),TEMP(128)
      COMMON /COEP1/ NPLY
      COMMON /POL/ CE(30),ALPHA8,CMA,CHPA,C7A
      COMMON /INOBK/ IDEN,IWIND,ITER,IPRN,IALL,NORC,IPUN,NBODY,ITRST,NT
35      $RST
      COMMON /INIT/TITLE(12),SCALE(30),A(22)
      COMMON /THRUST/TI4(15),TPST(15),MASS(15),CG(15),IX(15),IY(15),CGP(15)
      $)
      COMMON /TSTDAT/ EPS,THTC,ETA,L ,RL
      READ(5,1001) TITLE
C
      DO 10 I=1,15
      TIM(I)=0.0
      TRST(I)=0.0
      MASS(I)=0.0
      CG(I)=0.0
      IX(I)=0.0
      IY(I)=0.0
      CGP(I)=0.0
50      10 CONTINUE
      IDEN=0
      IWIND=0
      DO 11 J=1,3
      DO 11 I=1,128
      W(I,J)=0.0
      V(I,J)=0.0
55

```

BEST AVAILABLE COPY

SUBROUTINE INIT6

76/74 OPT=1

FTN 4,5+414

09/12/77 17.09

```

      VD(I)=0.0
      DEN(I)=0.0
      TEMP(I)=0.0
60      11 CONTINUE
      C
      C READ CONTROL PARAMETERS
65      READ(5,1010) NORC,IPRN,NALL,IPUN,NRODY,ISCALE,ITRST
      LSCALE=ISCALE.EQ.1
      IALL=NALL.EQ.1
      LTRST=ITRST.EQ.0
      C
70      C READ INITIAL CONDITIONS
      IF(LTRST) GO TO 4
      READ(5,1011) NTRST,EPS,THTC,ETA,L,BL
      EPS=EPS/57.295779
      THTC=THTC/57.295779
75      GO TO 7
      4 CONTINUE
      NTRST=1
      7 CONTINUE

80      READ(5,1012) (A(I),I=1,22)
      IF(LSCALE) GO TO 1
      DO 2 I=1,30
      2 SCALE(I)=1.
      GO TO 3
85      1 READ(5,1015) (SCALE(I),I=1,30)
      3 CONTINUE
      IF(LTPST) GO TO 5
      READ(5,1013) TIM(1),MASS(1),CG(1),IX(1),IY(1),CGP(1)
      READ(5,1013) TIM(ID),MASS(ID),CG(ID),IX(ID),IY(ID),CGP(ID)
90      READ(5,1014) (TIM(I),TRST(I),I=1,NTRST)
      5 CONTINUE

      C
      C ECHO OUTPUT
95      PRINT 1002
      PRINT 1004, NORC,IPRN,NALL,IPUN,NRODY,ISCALE,ITRST
      PRINT 1003, (I,A(I),I=1,22)
      PRINT 1005, (I,SCALE(I),I=1,30)
      IF(LTPST) GO TO 5
      EEPS=EPS*57.295779
      TTHTC=THTC*57.295779
100      PRINT 1006,EEPS,TTHTC,ETA,L
      PRINT 1009 ,BL
      PRINT 1006
      PRINT 1007, (TIM(I),TRST(I),MASS(I),CGP(I),CG(I),IX(I),IY(I),I=1,NTRST)
105      $RST)
      6 CONTINUE
      RETURN
      END

```

BEST AVAILABLE COPY



SUBROUTINE SIXDEC 74/74 OPT=1 PTN 4.5+414 09/12/77 17.09.

```

1      SUBROUTINE SIXDEC(ATTMOS)
C      UNIVERSITY OF NOTRE DAME, NOTRE DAME, IND.
1004 FORMAT(12H ALPHA ERROR2XE14.5)
1005 FORMAT(11H WIND ERROR2)
5      1006 FORMAT(11H MACH ERROR2XE14.8)

1157 FORMAT (1X, F20.5)
0989 FORMAT(/// 5X, *-----ALPHA *, F10.4, * DEGREES EXCEEDS MAXIMUM*,
1* ALPHA IN ARRAY-----*)
10 1666 FORMAT(/// 5X, *-----MACH *, F10.4, * EXCEEDS MAXIMUM MACH *,
1* NUMBER IN ARRAY-----*)
      REAL MASS, IX, IY, MTX, MTY, MTZ, L, MYJD, MZJD
      REAL MDOT
      INTEGER PG
15     LOGICAL LCZA, LCMA, LCMPA
      LOGICAL LTRST
      COMMON /AIRPLK/ TEM, PRES, RHO, KVIS, VA
      COMMON /COEF/ ANCH(20, 30), ALPHA(20, 30), C(20, 20, 30), NOA(30), NOM(30)
      COMMON /INDBLK/ IDEN, IMIND, ITER, IPRN, IALL, NORC, IPUN, NRODY, ITRST, NT
20     SRST
      COMMON /INIT/ TITLE(12), SCALE(30), A(22)
      COMMON /THRUST/ TI(15), TRST(15), MASS(15), CG(15), IX(15), IY(15), CGP(15)
      COMMON /TSTOAT/ EPS, THTC, CTA, L, RL
25     COMMON /WINBLK/ NOW, YW(128), W(128, 3)
      COMMON /COEP1/ NP, Y
      COMMON /POL/ CE(10), ALPHA, CMA, CMPA, CTA
      COMMON /DENBLK/ YOD, YD(128), DEN(128), TEMP(128)
      COMMON /ED9K/D1(14), D2(14), D3(14), DE2(14), WIN(3), DAL(10), DRE(10)
30     COMMON /ED9K2/V, Q, S, OP, ALPHAN, ANCHN, PG, LN
      COMMON /ED9K3/AXX, AXY, AXZ, AYY, AYZ, AZX, AZY, AZZ
      COMMON /ED9K4/ LCOUNT
      DATA COND, RAD/57.295779, .017453233/
      LTRST=ITRST.EQ.0
35     ITER=0
      LN=0
      PG=0
      KOUNT=0
      LCOUNT=0
40     M4=1
      D2(1)=1.
      S=3.1415927*A(19)**2/4.
      DO 20 I=1, 14
45     20 D1(I)=A(I)

      RAD2=RAD/2.
      D=D1(8)*RAD2
      E=D1(9)*RAD2
      F=D1(10)*RAD2
50     CP=COS(E)
      SP=SIN(E)
      CT=COS(D)
      ST=SIN(D)
      CS=COS(F)
      SS=SIN(F)
55     C VEPSOR COMPONENTS (54)
      J1(I)=-CP*ST*SS*SP*CT*CS

```

BEST AVAILABLE COPY

SUBROUTINE SIXDES

74/74 OPT=1

FTN 4.5+414

09/12/77 17.09.0

```

        D1(9)=-CP*CT*SS+SP*ST*CS      00002080
        D1(10)=CP*ST*CS+SP*CT*SS      00002090
        D1(11)=CP*CT*CS+SP*ST*SS      00002100
        AMP=A(18)                      00002110
        M = A(20)                      00002120
25      IF(A(20)*(D1(11)-A(21)).GT.0.)GO TO 597 00002130
        M1=1                          00002140
65      55 Y=D1(3)                    00002150
        IF(LTRST) GO TO 56             00002160
        X=D1(1)                       00002170
        IF(X.GT.TIM(NTRST)) GO TO 56   00002180
        I=1                           00002190
70      58 IF(X.LT.TIM(I+1)) GO TO 57   00002200
        I=I+1                         00002210
        GO TO 58                      00002220
57      CONTINUE                     00002230
        V1=TRST(I)                    00002240
75      V2=TRST(I+1)                  00002250
        V=Y1+(X-TIM(I))*((Y2-V1)/(TIM(I+1)-TIM(I))) 00002260
        ATRST=Y                       00002270

        V1=MASS(1)                    00002280
60      V2=MASS(NTRST)                00002290
        Y=Y1+(X-TIM(1))*((Y2-V1)/(TIM(NTRST)-TIM(1))) 00002300
        A(18)=Y                       00002310
        MDOT=(AMP-A(18))/A(20)        00002320
        AMP=A(18)                     00002330
85      V1=CG(1)                      00002340
        V2=CG(NTRST)                  00002350
        Y=Y1+(X-TIM(1))*((Y2-V1)/(TIM(NTRST)-TIM(1))) 00002360
        ACS=Y                         00002370
        V1=IX(1)                      00002380
90      V2=IX(NTRST)                  00002390
        Y=Y1+(X-TIM(1))*((Y2-V1)/(TIM(NTRST)-TIM(1))) 00002400
        A(15)=Y                       00002410
        V1=IY(1)                      00002420
        V2=IY(NTRST)                  00002430
95      Y=Y1+(X-TIM(1))*((Y2-V1)/(TIM(NTRST)-TIM(1))) 00002440
        A(16)=Y                       00002450
        V1=CGP(1)                     00002460
        V2=CGP(NTRST)                  00002470
        Y=Y1+(X-TIM(1))*((Y2-V1)/(TIM(NTRST)-TIM(1))) 00002480
100     CGL=Y                         00002490
56      CONTINUE                     00002500
        IF(X.GT.TIM(NTRST)) MDOT=0.    00002510
        SCL=1./SQRT(D1(8)**2+D1(9)**2+D1(10)**2+D1(11)**2) 00002520
105     D1(8)=SCL*D1(8)                00002530
        D1(9)=SCL*D1(9)                00002540
        D1(10)=SCL*D1(10)              00002550
        D1(11)=SCL*D1(11)              00002560
        CALL ATMOS(Y)                  00002570
110     C MATRIX OF DIRECTION COSINES 00002580
        AX=D1(8)**2+D1(11)**2-.5      00002590

        AXV=D1(8)*D1(9)+D1(10)*D1(11) 00002600
        AXZ=D1(8)*D1(10)-D1(11)*D1(9) 00002610
        AYX=D1(8)*D1(9)-D1(11)*D1(10) 00002620

```

BEST AVAILABLE COPY



SURROTIME SIXDEC

76/76

OPT=1

FTN 4.5+416

09/12/77 17.09.0

```

115      QVY=Q1(9)**2+Q1(11)**2-.5      00002670
      QVZ=Q1(9)*Q1(10)+Q1(11)*Q1(9)      00002640
      QZX=Q1(8)*Q1(10)+Q1(11)*Q1(9)      00002650
      QZY=Q1(9)*Q1(10)-Q1(11)*Q1(9)      00002660
      QZZ=Q1(10)**2+Q1(11)**2-.5      00002670
120      IF(IWIND.EQ.0) GO TO 2104      00002680
      C COMPUTE WIND      00002690
      IF(Y.LT.YW(1)) GO TO 101      00002690
      I=2      00002700
125      100 IF(YW(I).GE.Y) GO TO 210      00002710
      I=I+1      00002720
      GO TO 100      00002730
      101 PRINT 1005      00002740
      RETURN      00002750
      210 FASE=(Y-YW(I-1))/(YW(I)-YW(I-1))      00002760
130      DO 220 K=1,3      00002770
      220 WIN(K)=W(I-1,K)+FASE*(W(I,K)-W(I-1,K))      00002780
      C WIND COMPONENTS      00002790
      WX=2.*(WIN(1)*AXX+WIN(2)*AXY+WIN(3)*AXZ)      00002800
      WY=2.*(WIN(1)*AYX+WIN(2)*AYY+WIN(3)*AYZ)      00002810
      WZ=2.*(WIN(1)*AZX+WIN(2)*AZY+WIN(3)*AZZ)      00002820
135      C VELOCITY VECTOR      00002830
      D1(12)=D1(12)-WX      00002840
      D1(13)=D1(13)-WY      00002850
      D1(14)=D1(14)-WZ      00002860
140      C SPEED      00002870
      2104 V=SQRT(D1(12)**2+D1(13)**2+D1(14)**2)      00002880
      C ALPHA PRIME - YAW - ARCTAN(SQRT(V*V+W*W)/U)      00002890
      ALPHA=ARCTAN(SQRT(D1(13)**2+D1(14)**2),D1(12))      00002900
145      ALPHA=ALPHA*CONV      00002910
      C DYNAMIC PRESSURE      00002920
      Q=.5*RH0*V*V      00002930
      C CROSS-SPIN      00002940
      QPP=SQRT(D1(6)**2+D1(7)**2)      00002950
150      C ROLL ANGLES      00002960
      QP=ARCTAN(D1(13),D1(14))      00002970
      QPP=ARCTAN(-D1(7),D1(6))      00002980
      C PD/2V AND QD/2V      00002990
      IF(V.GT.0.) GO TO 2214      00003000
155      2 CONTINUE      00003010
      PD=0.      00003020
      QD=0.      00003030
      QMCHN=0.      00003040
      GO TO 2215      00003050
160      2214 PD=(D1(5)*A(19))/(2.*V)      00003060
      QD=(QPP*A(19))/(2.*V)      00003070
      QMCHN=V/VA      00003080
      2215 QSD=Q*S*A(19)      00003090
      QSM=(Q*S)*1./A(19)      00003100
165      C INTERPOLATE COEFFICIENT TABLES      00003110
      DO 150 K=1,30      00003120
      IF((NOA(K).EQ.0).AND.(NM(K).EQ.3)) GO TO 145      00003130
      I=1      00003140
      J=1      00003150
170      IF(NOA(K).EQ.0) GO TO 120      00003160
      IF(ALPHA.LT.ALPHA(1,K)) GO TO 111      00003170
      00003180

```

BEST AVAILABLE COPY

SUBROUTINE SIXDES

74/74 OPT=1

FTN 4,5+414

09/12/77 17.09.

	N=NOA(K)	00003200
	IF(ALPHA.GT.ALPHA(N,K)) GO TO 8888	
	J=2	00003210
175	110 IF(ALPHA(J,K).GE.ALPHA(N)) GO TO 115	00003220
	J=J+1	00003230
	GO TO 110	00003240
	111 PRINT 1004,ALPHA	00003250
	RETURN	00003260
180	8888 PRINT 8889, ALPHA	
	RETURN	
	115 FRA=(ALPHA-ALPHA(J-1,K))/(ALPHA(J,K)-ALPHA(J-1,K))	00003270
	120 IF(NOM(K).EQ.0) GO TO 140	00003280
185	IF(AMCHN.LT.AMCH(1,K)) GO TO 131	00003290
	N=NOM(K)	00003300
	IF(AMCHN.GT.AMCH(N,K)) GO TO 1131	
	I=2	00003310
190	130 IF(AMCH(I,K).GE.AMCHN) GO TO 135	00003320
	I=I+1	00003330
	GO TO 130	
	131 PRINT 1006,AMCHN	00003340
	RETURN	00003350
195	1131 PRINT 1665, AMCHN	00003360
	RETURN	
	135 FRA=(AMCHN-AMCH(I-1,K))/(AMCH(I,K)-AMCH(I-1,K))	00003370
	CE(K)=C(I-1,J,K)+FRA*(C(I,J,K)-C(I-1,J,K))	00003380
	IF(NOA(K).EQ.0) GO TO 150	00003390
200	T1=C(I-1,J-1,K)+FRA*(C(I,J-1,K)-C(I-1,J-1,K))	00003400
	LCZA=K.EQ.6	00003410
	LCMA=K.EQ.13	00003420
	LCMPA=K.EQ.19	00003430
205	IF(LCZA) CZA=(CE(K)-T1)/(ALPHA(J,K)-ALPHA(J-1,K))*COND*	00003440
	SSCALE(K)	00003450
	IF(LCMA) CMA=(CE(K)-T1)/(ALPHA(J,K)-ALPHA(J-1,K))*COND*	00003460
	SSCALF(K)	00003470
	IF(LCMPA) CMPA=(CE(K)-T1)/(ALPHA(J,K)-ALPHA(J-1,K))*COND*	00003480
	SSCALF(K)	00003490
210	CE(K)=T1+FRA*(CE(K)-T1)	00003500
	GO TO 150	00003510
	140 CE(K)=C(I,J-1,K)+FRA*(C(I,J,K)-C(I,J-1,K))	00003520
	GO TO 150	00003530
	145 CE(K)=C(1,1,K)	00003540
215	150 CE(K)=CE(K)*SCALE(K)	00003550
	C COMPUTE COEFFICIENTS CX, CY, CZ, CL, CM, CN (TABLE 3)	00003560
	1511 CONTINUE	00003570
	IF(AMPL.NE.1) GO TO 1512	00003580
	DO 1513 KK=1,30	00003590
220	1513 CE(KK)=CE(KK)*SCALE(KK)	00003600
	1512 CONTINUE	00003610
	SP=SIN(OP)	00003620
	CP=COS(OP)	00003630
	SP4=SIN(4.*OP)	00003640
225	CP4=COS(4.*OP)	00003650
	SPP4=SIN(4.*OPP)	00003660
	CPP4=COS(4.*OPP)	00003670
	CX=CE(1)	00003680

BEST AVAILABLE COPY



76/76 OPT=1

09/12/77 17.09.

BEST AVAILABLE COPY

SUBROUTINE SIXDFG 74/74 OPT=1

FTN 4.5+414

09/12/77 17.09.0

	C RUNGE-KUTTA CONSTANTS	00004240
	DO 298 I=1,14	00004250
	GO TO (294,295,296,297,70),41	00004260
290	294 DE1(I)=D1(I)	00004270
	DE2(I)=D2(I)*H	00004280
	E1=DE2(I)*.5	00004290
	GO TO 298	00004300
	295 E1=DE2(I)*.5*H	00004310
	DE2(I)=DE2(I)+4.*E1	00004320
295	GO TO 298	00004330
	296 E1=DE2(I)*H	00004340
	DE2(I)=DE2(I)+E1+E1	00004350
	GO TO 298	00004360
	297 E1=(DE2(I)+D2(I)*H)/5.	00004370
300	298 D1(I)=DE1(I)+E1	00004380
	41=M1+1	00004390
	GO TO 55	00004400
	70 GO TO (540,550),44	00004410
	540 KOUNT=KOUNT+1	00004420
305	IF(D1(3)-A(22)) 550,597,580	00004430
	550 IF(ABS(D1(3)-A(22)).LT..01) GO TO 597	00004440
	44=-(D1(3)-A(22))/D2(3)	00004450
	44=2	00004460
	41=1	00004470
310	C NEXT TIME LINE	00004480
	GO TO 55	00004490
	380 IF(MOD(KOUNT,IPRN).NE.0) GO TO 25	00004500
	CALL FD	00004510
	GO TO 25	00004520
315	597 CALL FD	00004530
	RETURN	00004540
	END	00004550

BEST AVAILABLE COPY



FUNCTION ARCTAN 74/74 OPT=1

FTN 4.5+414

09/12/77 17.09.

1	FUNCTION ARCTAN(P1,P2)	ARC00000
	IF(P2) 2,1,2	ARC00010
	1 IF(P1) 3,8,4	ARC00020
	3 ARCTAN=4.7123890	ARC00030
5	RETURN	ARC00040
	4 ARCTAN=1.5707963	ARC00050
	RETURN	ARC00060
	2 IF(P1) 5,6,5	ARC00070
	6 IF(P2.GT.0.) GO TO 8	ARC00080
10	ARCTAN=3.1415927	ARC00090
	RETURN	ARC00100
	8 ARCTAN=.0	ARC00110
	RETURN	ARC00120
15	5 ARC=ATAN(P1/P2)	ARC00130
	IF(P2) 10,9,9	ARC00140
	10 ARCTAN=ARC+3.1415927	ARC00150
	RETURN	ARC00160
	9 IF(ARC) 11,12,12	ARC00170
20	11 ARCTAN=ARC+6.2831853	ARC00180
	RETURN	ARC00190
	12 ARCTAN=ARC	ARC00200
	RETURN	ARC00210
	END	ARC00220

BEST AVAILABLE COPY

## Appendix G

Coefficient Arrays Input

000005 12

CX C ( 1 )

	ALPHA	0.0000	2.0000	5.0000	10.0000	15.0000	20.0000	25.0000	27.0000	50.0000
MACM	0.0100	-.2730	-.2735	-.2748	-.2915	-.2860	-.2725	-.2435	-.2220	-.2220
MACM	.4100	-.2730	-.2735	-.2748	-.2915	-.2860	-.2725	-.2435	-.2220	-.2220
MACM	.8100	-.2918	-.2930	-.3010	-.3225	-.3175	-.3110	-.2993	-.2630	-.2630
MACM	.9100	-.3090	-.3110	-.3200	-.3450	-.3409	-.3430	-.3250	-.2910	-.2910
MACM	1.0100	-.3890	-.3965	-.4200	-.4520	-.4610	-.4550	-.4150	-.3750	-.3750
MACM	1.1100	-.5050	-.5055	-.5120	-.5420	-.5700	-.5660	-.5290	-.5110	-.5110
MACM	1.2100	-.5210	-.5218	-.5260	-.5560	-.5840	-.5790	-.5470	-.5430	-.5430
MACM	2.0100	-.5210	-.5218	-.5260	-.5560	-.5840	-.5790	-.5470	-.5430	-.5430

CY7 C ( 3 )

	ALPHA	0.0000	2.0000	4.0100	8.0000	10.0000	15.0000	20.0000	25.0000	50.0000
MACM	0.0100	-.0213	-.0043	-.0208	-.0441	-.0631	-.1343	-.2663	-.1906	-.2000
MACM	.4100	-.0213	-.0043	-.0208	-.0441	-.0631	-.1343	-.2663	-.1994	-.2000
MACM	.8100	-.0612	-.0013	-.0033	-.0190	-.0670	-.1652	-.1945	-.2000	-.2000
MACM	.9100	-.0009	-.0036	-.0025	-.0529	-.0987	-.1914	-.2227	-.3940	-.1000
MACM	1.0100	-.0009	-.0012	-.0013	-.0641	-.1129	-.2410	-.2903	-.1543	-.2000
MACM	1.1100	-.0050	-.0051	-.0109	-.0570	-.1141	-.2395	-.2807	-.0965	-.1000
MACM	1.2100	-.0056	-.0023	-.0076	-.0585	-.1031	-.2235	-.2170	-.0319	-.1000
MACM	2.0100	-.0056	-.0023	-.0076	-.0585	-.1031	-.2235	-.2170	-.0319	-.1000

BEST AVAILABLE COPY



	ALPHA	0.0000	2.0000	4.0000	6.0000	8.0000	10.0000	15.0000	20.0000	25.0000	50.0000
WACW	0.7700	0.0000	-0.0300	-0.1350	-0.5350	-0.7750	-2.4830	-5.9180	-12.5000	-12.5000	-12.5000
WACW	0.4700	0.0000	-0.0300	-0.1350	-0.5350	-0.7750	-2.4830	-5.9180	-12.5000	-12.5000	-12.5000
WACW	0.3700	0.0000	-0.0300	-0.1750	-0.4100	-0.6600	-1.1650	-2.8900	-6.1500	-6.1500	-6.1500
WACW	0.2700	0.0000	-0.1050	-0.1850	-0.3500	-0.6400	-1.1000	-2.8000	-5.0000	-5.0000	-5.0000
WACW	1.0700	0.0000	-0.0700	-0.1650	-0.2950	-0.3300	-0.7800	-2.3720	-3.4500	-3.4500	-3.4500
WACW	1.1700	0.0000	-0.0900	-0.1800	-0.3120	-0.2540	-0.6000	-2.4630	-3.4000	-3.4000	-3.4000
WACW	1.2700	0.0000	-0.0800	-0.1800	-0.3100	-0.2650	-0.6750	-1.7700	-2.3300	-2.3300	-2.3300
WACW	2.0700	0.0000	-0.0800	-0.1800	-0.3100	-0.2650	-0.6750	-1.7700	-2.3300	-2.3300	-2.3300

	ALPHA	5.0000	10.0000	15.0000	20.0000	25.0000	27.0000	50.0000
WICH	0.0700	-0.3600	-0.7500	-1.1900	-1.7100	-2.4600	-2.7800	-2.7800
WICH	.6700	-0.0000	-0.7600	-1.1300	-1.7100	-2.4600	-2.7700	-2.7300
WICH	.9700	-0.0000	-0.6100	-1.2900	-1.8750	-2.5400	-2.9150	-2.9150
WICH	.9700	-0.0000	-0.7800	-1.3800	-1.9600	-2.6700	-3.0900	-3.0900
WICH	1.0700	-0.0000	-0.8100	-1.4600	-2.1600	-3.0600	-3.6600	-3.6600
WICH	1.1700	-0.0000	-0.8100	-1.4600	-2.1600	-3.3160	-3.9100	-3.9100
WICH	1.2700	0.0000	-0.8100	-1.5270	-2.4000	-3.6800	-4.2600	-4.2600
WICH	2.0700	0.0000	-0.8100	-1.5270	-2.4000	-3.6800	-4.2600	-4.2600

CLOW 5 (9)

	0.0000	2.0000	4.0000	6.0000	8.0000	10.0000	15.0000	20.0000	25.0000	30.0000
ALPHA	0.0000	0.0000	0.0000	0.0000	0.0000	0.0000	0.0000	0.0000	0.0000	0.0000
WACH 0.7700	.0470	.0470	.0460	.0460	.0495	.0504	.0490	.0471	.0415	.0415
WACH .6700	.0470	.0470	.0460	.0460	.0495	.0504	.0490	.0471	.0415	.0415
WACH .5700	.0533	.0627	.0634	.0634	.0665	.0690	.0704	.0677	.0596	.0596
WACH .4700	.0567	.0562	.0561	.0561	.0585	.0606	.0610	.0582	.0361	.0361
WACH 1.0700	.0520	.0522	.0542	.0542	.0574	.0593	.0622	.0560	.0409	.0409
WACH 1.1700	.0536	.0540	.0541	.0541	.0555	.0565	.0604	.0576	.0500	.0500
WACH 1.2700	.0546	.0543	.0547	.0547	.0552	.0567	.0582	.0530	.0444	.0444
WACH 2.0700	.0545	.0543	.0547	.0547	.0552	.0567	.0582	.0530	.0444	.0444

CLGA 5 (10)

	0.0000	2.0000	4.0000	6.0000	8.0000	10.0000	15.0000	20.0000	25.0000	27.0000	30.0000
ALPHA	0.0000	0.0000	0.0000	0.0000	0.0000	0.0000	0.0000	0.0000	0.0000	0.0000	0.0000
WACH 0.0700	0.0000	0.0000	0.0000	0.0000	.0123	.0251	.0343	.0311	.0534	.0620	.0620
WACH .4700	0.0000	0.0000	0.0000	0.0000	.0123	.0251	.0343	.0311	.0534	.0620	.0620
WACH .5700	0.0000	.0031	.0055	.0055	.0147	.0246	.0544	.0962	.1406	.1406	.1406
WACH .9700	0.0000	.0031	.0068	.0068	.0166	.0346	.0543	.1043	.1725	.1725	.1725
WACH 1.0700	0.0000	.0042	.0099	.0099	.0187	.0274	.0494	.0886	.1459	.1459	.1459
WACH 1.1700	0.0000	.0040	.0084	.0084	.0217	.0285	.0574	.0907	.1060	.1060	.1060
WACH 1.2700	0.0000	.0050	.0059	.0059	.0160	.0259	.0543	.0860	.0940	.0940	.0940
WACH 2.0700	0.0000	.0050	.0059	.0059	.0160	.0259	.0543	.0860	.0940	.0940	.0940



CLP C(12)

ALPHA	0.0000	2.0000	4.0000	6.0000	8.0000	10.0000	15.0000	20.0000	25.0000	50.0000
WICH	0.0700	-1.0769	-1.0500	-1.0415	-1.0518	-1.0014	-0.6497	-1.0173	-0.9332	-0.9332
WICH	.4700	-1.0789	-1.0500	-1.0415	-1.0518	-1.0014	-0.8497	-1.0173	-0.9332	-0.9332
WICH	.8700	-1.0916	-1.0426	-1.0569	-1.0987	-1.0394	-1.0569	-1.0088	-0.9868	-0.9868
WICH	.9700	-1.0964	-1.0694	-1.0738	-1.1036	-1.1083	-1.1149	-1.0869	-0.9498	-0.9498
WICH	1.0700	-1.0413	-1.0893	-1.0978	-1.1634	-1.1900	-1.2546	-1.2537	-1.4388	-1.4388
WICH	1.1700	-1.1042	-1.1130	-1.1261	-1.1723	-1.1878	-1.2629	-1.2605	-1.3954	-1.3954
WICH	1.2700	-1.1117	-1.1008	-1.1316	-1.2086	-1.2152	-1.2192	-1.4101	-1.4405	-1.4405
WICH	2.0700	-1.1117	-1.1008	-1.1316	-1.2086	-1.2152	-1.2192	-1.4101	-1.4405	-1.4405

CLP C(13)

ALPHA	0.0000	5.0000	7.0000	10.0000	15.0000	20.0000	22.0000	25.0000	27.0000	50.0000
WICH	0.0700	0.0000	-0.3450	-0.4850	-1.2500	-1.7450	-1.9600	-2.3190	-2.4930	-2.4930
WICH	.4700	0.0000	-0.3450	-0.4850	-1.2500	-1.7450	-1.9600	-2.3190	-2.4930	-2.4930
WICH	.8700	0.0000	-0.3590	-0.5700	-1.4000	-1.9820	-2.2280	-2.5800	-2.8200	-5.5500
WICH	.9700	0.0000	-0.4400	-0.6400	-1.5190	-2.0900	-2.2600	-2.4850	-2.6700	-2.6700
WICH	1.0700	0.0000	-0.4850	-0.6750	-1.5900	-2.1600	-2.1650	-2.1700	-2.1900	-2.1900
WICH	1.1700	0.0000	-0.4160	-0.6050	-1.4500	-1.9000	-1.9050	-1.9100	-1.9500	-1.9500
WICH	1.2700	0.0000	-0.3950	-0.5700	-1.3700	-1.8200	-1.9000	-2.0500	-2.1400	-2.1400
WICH	2.0700	0.0000	-0.3950	-0.5780	-1.3700	-1.8200	-1.9000	-2.0500	-2.1400	-2.1400

BEST AVAILABLE COPY

CNGA C(17)

ALPHA	0.0000	2.0000	4.0000	6.0000	8.0000	10.0000	15.0000	20.0000	25.0000	27.0000	50.0000
WACH	0.0000	.0025	.0249	.1364	.2148	.5009	.9434	.9261	1.0609	1.0609	1.0609
WACH	0.0000	.0025	.0249	.1364	.2148	.5009	.9434	.9261	1.0609	1.0609	1.0609
WACH	0.0000	.0035	.0037	.1727	.3312	.7229	.9509	.5038	.2629	.2629	.2629
WACH	0.0000	.0031	.0057	.2021	.3780	.8345	1.0400	.6287	.3916	.3916	.3916
WACH	0.0000	.0009	.0073	.2511	.4548	1.0030	1.2680	.4800	.3099	.3099	.3099
WACH	0.0000	.0261	.0450	.2755	.4570	1.0010	1.2840	.8332	.6044	.6044	.6044
WACH	0.0000	.0008	.0176	.2233	.3931	.9091	1.0051	.5373	.6214	.6214	.6214
WACH	0.0000	.0008	.0176	.2233	.3931	.9091	1.0051	.5373	.6214	.6214	.6214

CNGA C(19)

ALPHA	0.0000	5.0000	10.0000	12.0000	14.0000	16.0000	20.0000	22.0000	25.0000	25.0000
WACH	0.0000	.2300	.5300	.9200	1.5200	2.6000	4.6000	12.5000	19.5000	35.8000
WACH	0.0000	.2300	.5300	.9200	1.5200	2.6000	4.6000	12.5000	19.5000	35.8000
WACH	0.0000	.4700	.5900	.5800	.9300	1.5500	2.7000	6.6400	9.5000	15.4000
WACH	0.0000	.5500	.4200	.2400	.5000	1.1400	2.2000	5.6000	8.0000	12.0000
WACH	0.0000	.1400	.1100	0.0000	0.0000	.4600	1.3500	5.0000	6.0000	6.7000
WACH	0.0000	.3800	.3300	-.3200	-.5000	-.3000	.6900	4.1500	5.4100	6.7100
WACH	0.0000	.4500	.3200	-.5000	-.5000	0.0000	.8000	3.3000	4.1000	4.7400
WACH	0.0000	.4500	.3200	-.5000	-.6000	0.0000	.8000	3.3000	4.1000	4.7400

BEST AVAILABLE COPY



CHRE 5 (20)

	ALPHA	0.0000	50.0000
WACH	0.0100	.0714	.0714
WACH	.4700	.0714	.0714
WACH	.9700	.0616	.0616
WACH	.0100	.0900	.0900
WACH	1.0100	.0973	.0973
WACH	1.1700	.0800	.0800
WACH	1.2700	.0727	.0727
WACH	2.0700	.0727	.0727

CMO 5 (27)

	ALPHA	0.0000	2.0000	4.0000	8.0000	15.0000	25.0000	50.0000
WACH	0.0100	-111.3300	-115.0000	-119.0000	-124.0000	-130.5000	-154.0000	-154.0000
WACH	.4700	-111.3300	-115.0000	-119.0000	-126.0000	-135.5000	-154.0000	-154.0000
WACH	.9700	-136.0200	-141.0000	-145.4000	-152.5000	-164.0000	-178.3000	-178.3000
WACH	.0100	-135.6200	-145.0000	-154.5000	-163.5000	-167.5000	-210.0000	-210.0000
WACH	1.0100	-105.7500	-130.0000	-147.0000	-163.5000	-192.0000	-215.0000	-215.0000
WACH	1.1700	-121.1000	-126.0000	-134.0000	-144.4000	-156.4000	-175.0000	-175.0000
WACH	1.2700	-143.7600	-131.0000	-123.0000	-111.0000	-97.0000	-83.5000	-83.5000
WACH	2.0700	-143.7600	-131.0000	-123.0000	-111.4000	-97.4000	-83.5000	-83.5000

BEST AVAILABLE COPY

Vita

James D. Schneider graduated from Oklahoma State University in 1962 with a Bachelor of Science degree in Mechanical Engineering. He entered pilot training, after receiving his commission through Officer Training School, and earned his aeronautical rating in February 1964. He accumulated twelve years of flying experience including instructor pilot in both the T-37 and T-38 trainers, aircraft commander in the F-4D, and operations pilot in the T-39. After completing an assignment to Headquarters Air Training Command as Operations Center Staff Officer, Major Schneider entered the Air Force Institute of Technology for study in Astronautical Engineering.

Permanent address: Fargo, Oklahoma 73840



REPORT DOCUMENTATION PAGE		READ INSTRUCTIONS BEFORE COMPLETING FORM
1. REPORT NUMBER AFIT/GA/AA77D-8 ✓	2. GOVT ACCESSION NO.	3. RECIPIENT'S CATALOG NUMBER
4. TITLE (and Subtitle) MAGNUS EFFECT ON A BALLISTIC TRAJECTORY		5. TYPE OF REPORT & PERIOD COVERED AFIT Thesis
7. AUTHOR(s) James D. Schneider Major USAF		6. PERFORMING ORG. REPORT NUMBER
9. PERFORMING ORGANIZATION NAME AND ADDRESS Air Force Institute of Technology (AU) ✓ Wright-Patterson AFB, Ohio 45433		8. CONTRACT OR GRANT NUMBER(s)
11. CONTROLLING OFFICE NAME AND ADDRESS		10. PROGRAM ELEMENT, PROJECT, TASK AREA & WORK UNIT NUMBERS
12. REPORT DATE December, 1977		13. NUMBER OF PAGES
14. MONITORING AGENCY NAME & ADDRESS (if different from Controlling Office) Air Force Institute of Technology (AU) Wright-Patterson AFB, Ohio 45433		15. SECURITY CLASS. (of this report) Unclassified
16. DISTRIBUTION STATEMENT (of this Report)  Approved for public release; IAW AFR/190-17  Approved for public release, distribution unlimited.		15a. DECLASSIFICATION/DOWNGRADING SCHEDULE
17. DISTRIBUTION STATEMENT (of the abstract entered in Block 20, if different from Report)		
18. SUPPLEMENTARY NOTES  Approved for public release; IAW AFR/190-17  JERRAL F. GUESS, CAPT, USAF Director of Information		
19. KEY WORDS (Continue on reverse side if necessary and identify by block number)  Ballistic Trajectory Magnus Lift Trajectory Simulation		
20. ABSTRACT (Continue on reverse side if necessary and identify by block number)  → The effect of Magnus coefficients, projectile spin rate, and pitching motion on lateral displacement of a ballistic trajectory is investigated by use of a six degree of freedom simulation. The coefficients had no significant effect. Increased spin rate extends the projectile impact point both down range and cross range. Oscillations induced by rate motion increased the lateral deviation but oscillations induced by an initial displacement did not. ←		